FEDERAL SERVICE FOR HYDROMETEOROLOGY AND ENVIRONMENTAL MONITORING

Arctic and Antarctic Research Institute

*As a manuscript*

**Lis Natalia Andreevna**

# LONG-TERM VARIABILITY IN THE ICE COVERAGE AND SEA SURFACE TEMPERATURE OF THE NORTH EUROPEAN BASIN'S SEAS

Scientific specialty 1.6.17. Oceanology

**Dissertation**

for the academic degree of

candidate of geographical sciences

Translation from Russian

**Scientific supervisor:**

D. Sc. in Physics and Math's, Professor

Timokhov L. A.

Saint-Petersburg – 2023

# TABLE OF CONTENTS

# INTRODUCTION

***Relevance of the research topic***

The North European basin (SEB) includes the main seas Greenland, Barents and Norwegian, the boundaries are represented in Figure 1.1. The White Sea, officially there is part of the North European basin (Atlas of the Oceans, 1980), it is small and isolated, therefore, the work is not studied.

Norwegian, Barents and Greenland Seas play a key role in the processes of interaction between the North Atlantic and the North European basin with an Arctic basin, are an important part of the Arctic climatic system. Through them, the warm and salty waters of the North-Atlantic current enter the Arctic seas and the Arctic basin, and in the opposite direction the East Greenland flow transports sea ice and cold and relatively spread waters to the North Atlantic (Nikiforov and Shpayher, 1980). This area is one of the key in the system of the conveyor of heat flows in the Arctic. In the North European basin there is one of the most powerful foci of the “overheating” of the atmosphere, the so-called “Norwegian Energy Activities” (Alekseev et al., 1985; Malinin and Shmakova, 2018). According to Shuleykin (Shuleikin, 1933), the North European basin occupies an important place in the system of “thermal machines” on the globe and is not only one of the grandiose “refrigerators”, the operating mode of which significantly affects the functioning of the rest of the planetary “heat machines” system, But even due to the known symmetry of the development of processes regarding the equator and its relatively small size, a unique “landfill” for the study of the interconnection of atmospheric and oceanic processes in the polar regions of the Earth and, in particular, the mechanism of fluctuations in these processes. Norwegian, Greenland and, especially, the Barents Sea are waters of year-round shipping, as well as regions of intensive fishing and oil and gas production. Therefore, the study of the ice and thermal regime of the seas is an urgent task, both for science and practice in terms of the prediction of the ice conditions and the temperature of the seas.

***The level of knowledge of long-term fluctuations in the ice coverage and sea surface temperature of the seas North European basin***

Studies of the surface temperature of the water have been underway for a long time, the first works were published at the beginning of the XIX (Helland-Hansen and Nansen, 1909). Some time later, the main ideas about the state of ice in V.Yu. Vise were also obtained (Vize 1923, 1924, 1925, 1930), which considered the possible causes of the variability of the ice ice coverage and abnormal. The main studies of that time were aimed at studying the hydrological and ice regime, abnormalities of the Arcticity, the main ideas about the state of ice and thermal processes (Berezkin, 1939; visa 1940, 1944; teeth 1935, 1945) were formed. Since the study of long-term variability of ice and hydrological characteristics requires long-term observations, the first work on their intersection of their variability was published only by the end of the 1950s (Izhevsky 1957, 1961; Karakash, 1950, 1957; Urals, 1961a, b). During this period, the first methods of long-term forecasts of the adolescence and the sea surface temperature (SST) of the seas of the North European basin with an advance of 1 to 6 months were developed for the first time. The spectral analysis of cyclic vibrations of the variability of the surface temperature was successfully used by many authors and helped to advance in long-term forecasting (Bochkov 1964a, B, C; Smirnov and others, 1967; Smirnov, 1968, Seryakov, 1979). The identified cycles of fluctuations in water temperature (according to the Kola Meridian section for the period 1922-1961) (Bochkov, 1964) made it possible to develop a long-term forecast of water temperature, based on the use of significant fluctuations on the context of the Kola Meridian (data were used for period 1964-1985). When constructing a prognosis models, taking into account astrogeophysical characteristics and parameters allowed (Bochkov, 1978, 1979) with a fairly high time to predict the tendency of long-term fluctuations in water temperature Barents Sea.

Further, on the data of more modern and long-term observations (1959-1995), the new forecast model was created, it indirectly took into account the flow of heat from the Norwegian Sea (September and others, 1997). The direction of research on water temperature is carried out not only in the “classical” form (Seryakov, 1979; Otteersen et al., 1994), but also using the models of modern mathematical methods, taking into account the identified laws of significant periods of oscillations (Bohokov, 1979). The result of many years of study of water temperature and methods for its forecasting was the monograph (Malinin and Gordeeva, 2003). In which the combined method of physical and statistical modeling is used using the example of the Norwegian Sea.

Currently, a number of different methods are used for the long forecast of water temperature in the context of the Kola Meridian (Bulaeva 1987; Gvozdeva et al., 1970, Golubev et al., 1980; Karakash, 1976; Karsakov and others, 2000; Averkiev et al., 1997; Methodological recommendations, 1979; Fuchs, 1980). However, for us, the greatest interest, of course, is represented by a physico-statistical method proposed by Yu.V. Joint (Joints, 1978, 1985). It is based on the equation of the variability of the temperature of the sea water in a spectral form. The physical substantiation of these models is the well -known fact that the transfer of heat anomalies in the Gulf Stream system, by which we understand the entire set of warm currents directly related to the golfstim and its sequels, up to the Arctic Central Basin, is one of the most important determining factors of the formation of large -scale inter -day variability The TPO fields in the North Atlantic (Baranov, 1988; Smirnov, 1998; Ugryumov, 1981).

In the same period, the study of the long-term variability of the ice coverage of the North European basin, as well as the features of the influence on them of the tributary of warm Atlantic waters (Lebedev and Urals, 1972, 1976; Kirillov and Khromtsev, 1970; Kirillov, 1973). Based on the analysis of the ice balance of the seas, methods were developed for long -term forecasts of ice conditions (Lebedev and Urals, 1977).

By the beginning of the 1980s, in connection with the accumulation of relatively long-term data, the first results were obtained on the large-scale variability of the ice conditions of the North European basin (Vinje, 1979; Santsevich and Khromtsev, 1980; Lebedev and Uralov, 1981; Zakharov, 1981; VINJE, 1984; Potanin, 1987, Dementiev and Zubakin, 1987). At this time, G. K. Zubakin published a monograph, which was a generalization of the results of the study of the Murmansk branch of AARI on the basis of the new data of the hydrometeorological and ice conditions of the Barents Sea, obtained according to the results of expeditions (Zubakin, 1987). In 1990, a reference publication was published edited by Teriziev and others. On the basic characteristics of the hydrometeorological and ice conditions of the Barents Sea (Hydrometeorology and hydrochemistry of the seas, 1990). A. A. Lebedev paid special attention to the study of large abnormalities of the ice coverage (Lebedev, 1993). After long research (Mironov, 1979, 1994; Mironov et al., 1997; Frolov et al., 1997; Lebedev and Mironov, 1997; Mironov and Babko, 1997; Mironov et al., 1998; Mironov and Turyakov, 1998) E) E. Mironov (Mironov, 2004) summarized the existing data on the main elements of the ice regime of the seas of the North European basin, and also proposed new methods for forecasts for changing the ice regime in time for one to six months. He identified the following factors affecting the ice coverage of both seas: air temperature, atmospheric circulation, water and current temperature, i.e. those basic processes in the variability of which are distinguished by quasi-cyclic fluctuations of various sizes.

Currently, with the active development of satellite altimetry, due to the sufficiently long time series of data changes in the area of the ice coverage Greenland and the Barents Seas, both seasonal and interannual variability of the ice coverage (Zubakin et al., 2006; Levitus et al., 2009a,b; Buzin, 2008; Buzin and Gudkovich, 2011; Zolotkorlin et al., 2014; Titkova et al., 2014; Tregobova et al., 2015; Prokofiev et al., 2015). For foreign authors, special attention is paid to the relationship of the ice coverage with the variability of atmospheric circulation (Vinje, 2001; Wu et al., 2004; Sorteber and Kvings, 2006; Deser and Teng, 2008; Zhang et al., 2008; Lind et al., 2018).

The monograph (Frolov et al., 2007) gives the results of successful thermohydrodynamic modeling of synoptic, seasonal processes and interannual. But interannual and climatic changes are so far reproduced by climatic models unsatisfactory. An extreme reduction in the area of the ice coverage at the beginning of the current century, accompanied by abnormal fluctuations in the thermocal structure (Timokhov et al., 2012) and rapid climate change in the Arctic (Alekseev, 2015), turned out to be faster than climatic models. Existing mathematical climatic models predict a further decrease in the area of the ice coverage in the summer. So in the article (Aksenov et al., 2017), which shows the results of the calculations according to the RCP8.5 NEMO model, it is indicated that by 2030-2039. The concentration of ice in the navigation period can be significantly reduced by opening the route from Europe to Asia through the North Pole. At the same time, in the monograph (Frolov et al., 2007), based on the analysis of the actual interannual changes in the area of ice coverage and the empirical model, it was obtained that in the 21st century it was expected to preserve the oscillatory (and not a single -controlled) background of changes in the area of ice in the Arctic seas. According to this forecast, in the 2020-2040s. Probably an increase in the area of ice with the maximum around 2030 in the eastern Arctic seas and about 2035 in the Western Seas will increase. This indicates that at present there is no unequivocal answer to the question of which scenario will develop changes in the northern Arctic Ocean, and the question of the causes and genesis of long-term and climatic changes in the area of the ice coverage is still at the stage of research and search.

We note the importance of the development of numerical modeling, we state that at the present stage, a numerical forecast of climate changes, including the ice coverage and sea surface temperature, has not yet reached the level of realistic reproduction of climatic changes. Therefore, the relevance of the description of long-term and climatic variability of the state was especially increased not only by improving hydrodynamic models, but also by developing physico and statistical models (Nikiforov and Shpayher, 1980; Mironov, 2004; Alekseev et al., 2016, 2017; Malinin and Gordeeva 2003; Timokhov et al., 2019a,b; Vyazigina et al., 2021).

The **object** of the study is the water area of the seas of the North European basin, which includes the Barents, Greenland and Norwegian seas. The **subject** of the study is the long-term variability of the ice coverage and the seas surface temperature.

***The main goal and tasks of research***

The main goal of the work is the study of the structure of long-term variability sea surface temperature and the ice coverage, the establishment of the causes of long-term variability, and the development of statistical models of long-term changes in the thermal and ice state of the seas of the North European basin.

To achieve this goal, the following **tasks** were set:

– the creation of a working electronic archive of hydrometeorological climatic indices and astrogeophysical parameters;

– the study of the statistical structure of the interannual variability of the sea surface temperature and the ice coverage;

– the study of the physical connections of response functions (studied process) with determining factors;

– the establishment of the conjugation of long-term variability in the sea surface temperature and ice coverage in seas of the North European basin with hydrometeorological and astrogeophysical parameters;

– analysis of the information content of various hydrometeorological and astrogeophysical factors in the task of describing long-term variability in the sea surface temperature and ice coverage in seas of the North European basin;

– the construction of physico-statistical models of long-term variability in the sea surface temperature and the ice coverage of the seas of the North European basin.

***The theoretical and methodological basis*** of the dissertation is the research and development of domestic and foreign scientists in the field of studying the climatic variability of the ice coverage and sea surface temperature. The information base consists of time series of hydrometeorological climatic indices and astrogeophysical characteristics, monographic works, materials of scientific and technical conferences, intellectual property objects, articles in periodicals and scientific collections on the problem under study.

***When conducting research, we used:***

– basic statistical analysis, including the analysis of statistical estimates;

– cluster analysis using Euclidean distance;

– spectral analysis (expansion in a Fourier series);

– correlation analysis (mutual correlations, cross-correlations, autocorrelations);

– multiple linear regression.

***Research novelty***:

– expanded knowledge about the structure of long-term variability in sea surface temperature and ice coverage of the seas of the North European basin,

– an original technique was developed based on physical and statistical modeling, which made it possible to obtain equations that more accurately describe long-term variability in sea surface temperature and ice coverage in the seas of the North European basin. At the same time, for the first time, a set of data sets was used as predictors, both for hydrometeorological and astrogeophysical parameters;

– estimates of the contribution of hydrometeorological and astrogeophysical factors to the climatic variability of the sea surface temperature and ice coverage of the seas of the North European Basin were obtained;

– estimates of the accuracy of reproduction by equations of long-term variability in sea surface temperature and ice coverage of the seas of the North European basin were made;

– time extrapolation for 2-3 years ahead according to the known data of predictors showed the stability of calculations by equations and allows us to conclude that it is possible to use the proposed physical-statistical approach for the development of methods for predicting long-term variability in ice coverage and sea surface temperature.

***The main points for defense:***

- statistical models of long-term variability of sea surface temperature and ice coverage of the North European Basin depending on variations in hydrometeorological and astrogeophysical factors, which describe a high percentage of the total dispersion of long-term variability in ice coverage (up to 87%) and sea surface temperature (up to 80%) in the seas of the North the European basin, and the justification is up to 100%;
- assessment of the contribution of hydrometeorological and astrogeophysical factors to the climatic variability of the sea surface temperature and ice coverage of the seas of the North European Basin; the contribution to the total dispersion of sea surface temperature and ice coverage of hydrometeorological factors (atmospheric temperature, inflow of Atlantic waters and variability of atmospheric circulation) for various model options is up to 70%, and astrogeophysical factors (nutation parameters and the change in the position of the Earth's pole, solar activity) - up to 50%;
- an effective method for calculating long-term variability in ice coverage and sea surface temperature of the ocean of the North European Basin is proposed based on physical and statistical modeling using both hydrometeorological and astrogeophysical indices and variables as predictors.

***Practical significance***

The obtained estimates of the statistical structure of long-term variability in sea surface temperature and ice coverage in the North European Basin can be used as information on the long-term behavior of the state of the seas. The developed statistical models of ice coverage and sea surface temperature in the seas of the North European Basin can be used as methods for diagnosing the thermal and ice state of the North European Basin. The developed technique can be used in the study of long-term changes (interannual and climatic) of ice coverage and sea surface temperature in other Arctic seas.

**Approbation of work.** *The dissertation results were presented on:*

1. IV all-Russian scientific conference of young scientists "Comprehensive studies of the World Ocean" CSWO -2019 "Long-term changes in ice coverage and sea surface temperature of the North European Basin and their statistical models", Sevastopol, April 22-26, 2019.
2. IV all-Russian scientific conference of young scientists "Comprehensive studies of the World Ocean" CSWO-2019 "Interannual changes in the ice cover of the Greenland Sea and their causes", Sevastopol, April 22-26, 2019.
3. The General Assembly 2019 of the European Geosciences Union (EGU-2019) «The structure of long-term ice cover variability in the Western Arctic and its statistical models» Austria Center Vienna (ACV) in Vienna, Austria, 2019, from 7–12 April.
4. International Conference on Russian-German projects "Variability of the Arctic Transpolar System" / "Quantitative Assessment of Rapid Climate Changes in the Russian Arctic" (CATS/QUARCCS) "Climatic fluctuations of sea surface temperature and ice coverage in the Nordic Seas" St. Petersburg, "AARI", December 3-5, 2019.
5. Arctic Science Summit Week (ASSW-2020) «Climatic fluctuations of sea ice cover anomalies and anomalies ocean surface temperature in the Nordic Seas and Barents sea, it structure and statistical models», Akureyri, Iceland, 2020, 27 March to 2 April.
6. V all-Russian Scientific Conference of Young Scientists "Integrated Studies of the World Ocean" (CSWO-2020) "Physico-statistical models of ice coverage and sea surface anomalies in the North European Basin", Kaliningrad, May 18-22, 2020;
7. Students in polar and alpine research, SPARC «The possibility of using astroogeophysical parameters as predictors for statistical equations for interannual variability of sea ice extent in the Greenland Sea», Brno, Czechia, 2021, 3-4 May.

8. VI All-Russian Scientific Conference of Young Scientists "Integrated Studies of the World Ocean" (CSWO -2021) "Informativeness of various hydrometeorological and astrogeophysical factors on the example of describing long-term variability in the ice coverage of the Greenland Sea", Moscow, April 18-24, 2021.
9. All-Russian scientific conference "Russian Seas: Challenges of Russian Science" "Statistical models of climatic variability of sea surface temperature and ice coverage in certain areas of the Barents Sea", Sevastopol, September 24-30, 2022.
10. VI All-Russian conference with international participation "Hydrometeorology and ecology: achievements and development prospects": MGO 2022 named after L. N. Karlin "Assessment of the information content of various factors that form long-term variability in the ice coverage of the Barents Sea over the past 90 years", St. Petersburg, December 14-15 2022.
11. XXX International Scientific Conference of Students, graduate students and young scientists of Lomonosov “Statistical models of the long-term variability of the Arcticity of individual regions of the Barents Sea”, Moscow: MSU, 10-21-April 2023.

**Published results**. *On the topic of the dissertation, 13 works were published, 5 of them in journals recommended by the by the HAC system, 3 – indexed in Scopus, 7 - abstracts.*

***List of papers published on the topic of the dissertation:***

1. Timokhov L.A., **Vyazigina N.A.**, Mironov E.U., Popov A.V. Seasonal and inter-annual variability of the ice cover in the Greenland Sea //Ice and Snow. – 2018. – T.58. – №1. – C.127-134. – RSCI, HAC, Scopus.
2. Timokhov L.A., **Vyazigina N.A.**, Mironov E.U., Yulin A.V. Climatic changes of seasonal and inter-annual variability of the ice coverage of the Greenland and

Barents seas //Arctic and Antarctic Research. – 2019. – T.65. – №2. – C.148-168. – RSCI, HAC.

3. Timokhov L.A., Borodachev V.E., Borodachev I.V., **Vyazigina N.A.**, Mironov E.U., Janout M. Role of hydrometeorological factors and solar activity in interannual variability of ice coverage in the East Siberian Sea //Ice and Snow. – 2019. – T.59. – №2. – C.222-232. (In Russian). – RSCI, HAC, Scopus.
4. Yulin A.V., **Vyazigina N.A.**, Egorova E.S. Interannual and seasonal variability of Arctic sea ice extent according to satellite observations //Russian Arctic. – 2019. – №7. – C. 28-40. – RSCI.
5. **Vyazigina N.A.** Timokhov L.A. Long-term changes in ice coverage and sea surface temperature in the North European Basin and their statistical models. Interannual changes in the ice cover of the Greenland Sea and their causes //Integrated research of the World Ocean: Materials of the IV All-Russian scientific conference of young scientists, Sevastopol. – 2019. – C. 43-44. – RSCI.
6. Egorova E.S., **Vyazigina N.A.** Interannual changes in the ice coverage of the Greenland Sea and their causes //Integrated research of the World Ocean: Materials of the IV All-Russian scientific conference of young scientists, Sevastopol. – 2019. – C.54-55. – RSCI.
7. **Viazigina N.,** Timokhov L. Mironov E. The structure of long-term ice cover variability in the Western Arctic and its statistical models. Geophysical Research AbstractsVol. 21, EGU 2019-1435, 2019EGU General Assembly 2019.
8. **Vyazigina N.A.** Timokhov L.A. Physico-statistical models of ice coverage and sea surface temperature anomalies in the North European Basin //Research of the World Ocean: Materials of the V All-Russian scientific conference of young scientists, Kaliningrad. – 2020. – C.54-55. – RSCI.

9. **Viazigina N.,** Timokhov L. The possibility of using astroogeophysical parameters as predictors for statistical equations for interannual variability of sea ice extent in the Greenland Sea. Students in polar and alpine research Abstracts Vol. 21. SPARC 2021 – 57 p.
10. **Vyazigina N.A.** Timokhov L.A., Egorova E.S., Yulin A.V. Informativeness of various hydrometeorological and astrogeophysical factors on the example of the description of long-term variability in the ice coverage of the Greenland Sea. //Comprehensive studies of the World Ocean. Materials of the VI All-Russian scientific conference of young scientists, Moscow. – 2021. – C.51-52. – RSCI.
11. **Viazigina N.A.**, Timokhov L.A., Egorova E.S., Yulin A.V. Informativeness (information-bearing) of hydrometeorological and astrogeophysical factors in the problem of describing interannual fluctuations of the Greenland Sea ice coverage //Ice and Snow. – 2021. – T.61. –№3. – C.431-444. (In Russian). – RSCI, HAC, Scopus.
12. **Lis N.A.**, Egorova E.S. Climatic variability of the ice extent of the Barents Sea and its individual areas //Arctic and Antarctic Research. – 2022. – T.68. – №3. – C.234-247. (In Russian). – RSCI, HAC.
13. **Lis N.A.**, Timokhov L.A. Statistical models of climatic variability of surface water temperature and ice cover in certain areas of the Barents Sea //All-Russian Scientific Conference "Russian Seas: Challenges of National Science", Sevastopol. 111–112 . – RSCI.

***The reliability of the results of the work*** is ensured by providing estimates of the quality of models, such as coefficients of multiple correlation and determination, justification and error of model data. A confirmation of the stability of the obtained equations is provided by checking for 20 years (the period 2001–2021 for ice coverage and the period 2000–2019 for SST).

***The structure and scope of the thesis***

The thesis consists of an introduction, four chapters, main conclusions, a conclusion an application and a bibliography with a total volume of 145 titles, 18 tables and 26 figures. The bibliography includes 192 titles.

***Personal contribution of the author***

The author independently obtained an electronic archive of data, analyzed the research results, identified the patterns of the statistical structure of the characteristics under consideration, developed physical and statistical models, analyzed the contribution and information content of the parameters of the equations obtained for the studied areas, developed a methodology for calculating the interannual variability of ice coverage and sea surface temperature.

***Compliance with the passport of the specialty*** of the Higher Attestation Commission***:***

The work touches upon the following sections of the specialty passport 1.6.17. – Oceanology:

- External forces acting on the ocean and flows of matter and energy;
- Properties and processes of sea ice formation, their distribution and movement in the World Ocean;
- Interaction in the system lithosphere – hydrosphere – atmosphere;
- Methods of research, modeling and forecasting of processes and phenomena in the oceans and seas;
- Methods for the analysis of water masses, their classification, zoning of water areas and the search for patterns in the formation of the structure of the waters of the World Ocean.

***The structure and scope of the thesis***

*In the introduction* substantiates the relevance of the problem solved in the dissertation, formulates the purpose and objectives of the research, and outlines the main provisions submitted for defense.

*Chapter 1* provides basic information about the geographical position of the seas, the characteristics of the region, and the ice and hydrological regimes. The main structures of the bottom relief and the systems of surface currents associated with them are considered. The basic principles of the statistical approach to solving the problem of analyzing long-term oscillations are outlined. Data sources are described, and research methods are given.

*Chapter 2* the results of the analysis of the statistical structure of interannual variability of sea surface temperature in the seas of the North European basin are presented. A division into homogeneous regions is proposed. A cluster analysis has been performed and periods of high, medium and low sea surface temperatures have been identified. The analysis of the trend component was performed, the presence of a positive trend for sea surface temperature was confirmed. The periods of cyclic fluctuations (up to 22 years inclusive) of the studied characteristics were determined using spectral analysis and analyzed, an autocorrelation analysis was performed, and the inertia of the processes was studied.

*Chapter 3* the results of the analysis of the statistical structure of interannual variability in the ice coverage of the seas of the North European basin are presented. The analysis of the trend component was performed, the presence of a negative trend for ice coverage was confirmed. The time periods of small, medium and large ice coverage are determined. The periods of cyclic fluctuations (up to 22 years inclusive) of the studied characteristics were determined using spectral analysis and analyzed, an autocorrelation analysis was performed and the inertia of the processes was studied.

*Chapter 4* the results of studies of the conjugation of ice coverage and sea surface temperature with hydrometeorological and astrogeophysical characteristics are presented. The results of the analysis of cyclic fluctuations of global climate indices, as well as astrogeophysical parameters, are presented. The comparison of coinciding periods of selected cyclic oscillations is analyzed.

The results of studying the information content of various hydrometeorological and astrogeophysical characteristics in the problem of describing interannual fluctuations in ice coverage and sea surface temperature in the seas of the North European basin are analyzed. Estimates of the contribution of the obtained predictors are given. The developed equations for describing the interannual fluctuations of the studied characteristics are presented with an analysis of the quality indicators of the models. The stability of the developed models was checked for 20 years.

*The conclusion* contains a description of the main results of the dissertation research.

***Acknowledgments***

I express my deep gratitude and gratitude to my supervisor, Doctor of Physical and Mathematical Sciences ***L.A. Timokhov*** and scientific consultant Doctor of Geographical Sciences ***E.U. Mironov*** for sensitive guidance, advice, and valuable comments in the work on the dissertation. I also express my gratitude for advice, critical remarks, joint work and support to the candidate of geographical sciences ***A.V. Yulin*** and candidate of geographical sciences ***T.K. Karandasheva***.

# CHAPTER 1 CHARACTERISTICS OF THE OBJECTS, DATA AND METHODS RESEARCH'S

## 1.1 Geographical characteristic of the region

The North European Basin (NEB), which includes the Norwegian, Greenland and Barents Seas according to the nomenclature of the bottom relief from 1967 (Treshnikov et al., 1967), is part of the Arctic Ocean (AO). The location of the boundaries of the seas is schematically presented in the diagram (Figure 1.1.) in accordance with the established boundaries in the Atlas of the Oceans in 1980 (Atlas of the Oceans, 1980). The North European Basin connects the North Atlantic with the Arctic Basin of the Arctic Ocean.

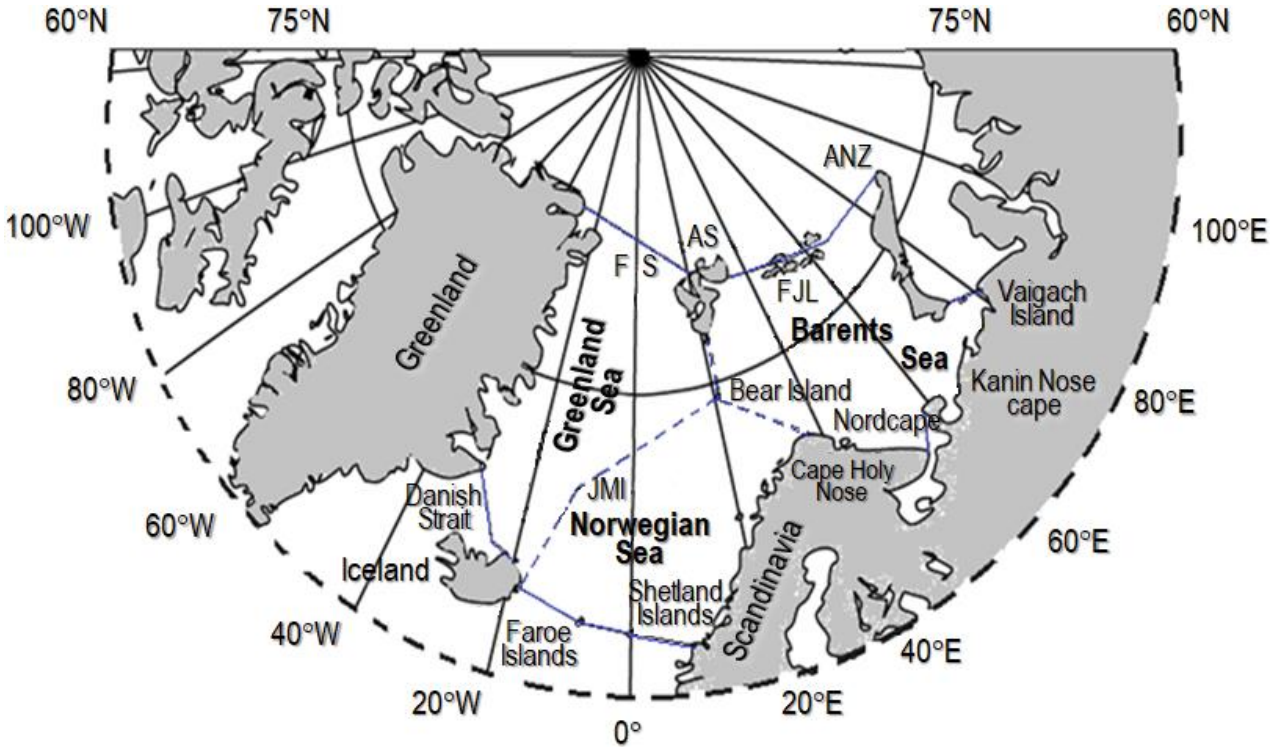


Figure 1.1. Scheme of the borders of the seas of the North European basin: the Greenland, Norwegian and Barents seas. The blue color indicates the boundaries of the water area of the North European basin, the dotted line - the boundaries between the seas.

*Note*. Designations: FS – Fram Strait; FJL – Franz Josef Land; AS – Spitsbergen archipelago; ANZ – Novaya Zemlya archipelago; JMI – Jan-Mayen Island.

*Borders of the Norwegian Sea:*

From the East it is limited by the shores of Norway, from Cape North Cape (25 ° E) to about. Bear, following to the southern part of about. Western Svalbard. From the West, the boundary line runs from Svalbard to about. Jan Mayen, to Cape Gernir in Iceland (65°N, 13°W). The boundary in the South extends from Cape Gerpir to the Faroe Islands (Fuglö, 62°N, 6°W), after which it follows to a latitude of 61°N at 0,5° W (to the north of the Shetland Islands) and continues along this latitude to the coast of Norway a little south of the Sognefjord.

*Borders of the Greenland Sea:*

From the South, the boundary passes through the line: NW Iceland to Cape Nansen (Greenland, 68°N, 29°W) The north of the sea is bounded by a line that connects the ends of North Greenland and Svalbard, the boundary in the east runs along a line that connects the south of Western Svalbard, about. Jan Mayen and Eastern Iceland (65°N, 13°W).

*Borders of the Barents Sea:*

In the West, the boundary of the sea is a line running from Cape Yuzhny to about. Bear and following to m. North Cape. In the South, the sea is limited by the coastline of Eurasia and the line Cape Svyatoy Nos - Cape Kanin Nos, which separates it from the White Sea. The eastern border is limited by the islands of Vaygach and Novaya Zemlya. The northern boundary of the sea is limited by the server part of the islands of Franz Josef Land and the line that goes through such islands as Bely and Victoria to the island of North-East Land.

The Greenland, Barents and Norwegian Seas occupy approximately the same areas in the North European Basin (Table 1.1.) and account for 30%, 36% and 34% respectively. At the same time, the Greenland and Norwegian Seas have significantly greater depths, exceeding the depths of the Barents Sea by several times. Accordingly, the volume of the Barents Sea is less than the other seas of the North European basin by

more than 6 times (see Table 1.1.). The change in the ice coverage is a fundamental parameter not only of the climate of the Arctic region, but also an indicator of climate change in the entire Northern Hemisphere. In the context of climate change, ice coverage is a particularly useful indicator of recent changes in the Arctic.

Table 1.1. Main Statistical Characteristics of the North European Basin

| Characteristic | Greenland Sea | Barents Sea | Norwegian Seas |
|---|---|---|---|
| Area, n·$10^3$ km $^2$ | 1195 | 1424 | 1340 |
| % of the area of NEB | 30% | 36% | 34% |
| Medium depth, m | 1641 | 222 | 1735 |
| Max depth, m | 5527 | 600 | 3970 |
| Volume, n·$10^3$ km$^3$ | 1961 | 316 | 2325 |
| Medium SST in the north, °C | –1 | –1 | +2,5 |
| Medium SST in the south, °C | +1,5 | +6 | +6,5 |
| Max FSS, °C | +9 | +9 | +13 |
| Min FSS, °C | –1,9 | –1,9 | –1 |
| Medium STA in August in the South, °C | +5 | +9 | +11 |
| Medium STA in August in the north, °C | ±0 | +0,5 | +9 |
| Medium STA in February in the south, °C | –10 | –4 | +4 |
| Medium STA February in the north, °C | –26 | –22 | –4 |
| Min STA, °C | –49 | –25 | –9 |
| Max STA, °C | +3 | +6 | +12 |
| Medium ice coverage, n·$10^3$ km $^2$ | 489 | 499 | 0 |
| Max ice coverage, n·$10^3$ km $^2$ | 1052 | 1235 | 0 |
| Min ice coverage, n·$10^3$ km $^2$ | 36 | 0 | 0 |
| % from max ice coverage NEB | 33% | 39% | 0 |
| % from min ice coverage NEB | 100% | 0% | 0 |

*Note:* STA – surface temperature of the atmosphere; SST is the sea surface temperature; NEB – North European Basin (Hydrometeorology and hydrochemistry of the seas, 1990; Mironov, 2004; CDAS-1 Reanalysis database of the International Climate Research Institute and Columbia University Society in New York (USA http://iridl.ldeo.columbia.edu/).

The climate of the Greenland Sea is arctic and varies to a large extent throughout the sea. The minimum values of PTA are –49°C in the Svalbard region in winter, and the highest PTA up to +3°C are distributed near the coastline of Greenland in the summer season. On average, STA are –10°C in the south and –26°C in the north. Similarly, the average temperatures for the summer season are +5°C in the south and 0°C in the north. The summer season in the Greenland Sea lasts for a very short period: per year, the number of days with temperatures above ±0°C ranges from 225 (north) to 334 (south).

A similar situation is observed in the northern part of the Barents Sea, where the influence of the inflow of warm waters from the North Atlantic is much less. Here, the STA drops below –22°C (see Table 1.1.), and in summer it only slightly exceeds zero on average +5°C. The southwestern region of the Barents Sea is under a fairly strong influence of cyclonic circulation and the inflow of warm and saline waters of the North Cape Current.

The region is characterized by strong winds, most often SW direction, increased cloudiness and precipitation. The southeastern region is characterized by the alternating influence of warm Atlantic air masses and cold air masses coming from the Eurasian continent. In this regard, high temperature gradients are observed in this area of the Barents Sea. The temperature of the atmosphere decreases sharply towards the east and southeast. Where the influence of the influx of cold waters of the Kara Sea, entering through the straits of Yugorsky Shar and the Kara Gates, is great. The northwestern region of the Barents Sea occupies the water area to the north of about. Bearish, and is under a fairly strong influence from the Arctic basin. This part is characterized by especially cold surface temperatures of the atmosphere and sea surface temperatures, the presence of ice and icebergs, and northeasterly winds. Warm Atlantic waters enter the central and northeastern regions of the Barents Sea from the Kolguyevo-Novaya Zemlya branch of the North Cape Current.

In the winter season, the surface temperature of the atmosphere of the Norwegian Sea is -4°C in the north and +4°C in the south. The isotherm of zero value is located on the line from Iceland towards about. Bearish. At the same time, in the summer season, when the Icelandic low is weakening, and the Azores high is intensifying, the winds are significantly weakened, the temperature rises to +12°C. At the same time, when the atmosphere warms up, cyclone activity weakens.

The Barents and Greenland Seas are similar in temperature regime. Thus, the average ocean surface temperature in the north of both seas is –1°C, while in the Norwegian Sea it is +2,5°C (see Table 1.1.). The distribution of maximum/minimum ocean surface temperatures looks similar: the lowest ocean surface temperature in the Greenland (–1,9°C) and Barents (–1,9°C) seas is much lower than in the Norwegian Sea (–1,0°C ). Such low temperatures are observed only in the northern part of the sea. The Greenland and Barents Seas are located outside the Arctic Circle and, unlike the Norwegian Sea, are affected by warm Atlantic waters to a much lesser extent. Which leads to quite severe weather conditions. Even in summer, the SST does not always and not in the entire water area of these seas reach positive temperatures.

Through the southern straits of the basin, waters of Atlantic origin invade the Arctic Ocean. In the opposite direction, through the North European Basin, cold and desalinated surface water and ice enter the North Atlantic, sometimes reaching 43 °N and forming a "cold wall" along the western edge of the Gulf Stream. Cold and relatively desalinated bottom waters of the ocean, overflowing through its southern sills into the North Atlantic, form here intermediate layers reaching the Gulf Stream front and determine the intensity of flows of the Gulf Stream and all its branches in the northwest Atlantic (Nikiforov, 2006; Blindheim and Osterhus, 2005). These features of the hydrology of the area are associated primarily with the morphometry of its bottom (Figure 1.2).

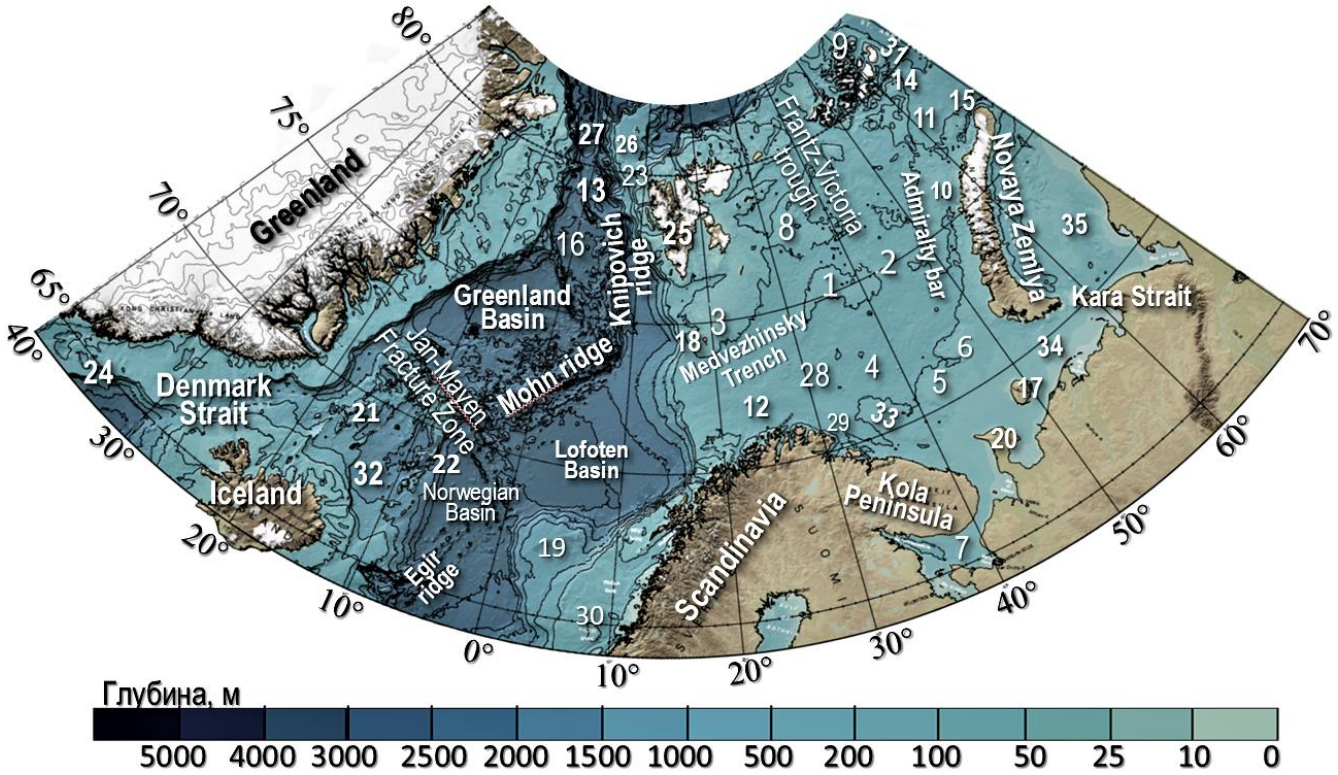


Figure 1.2. Scheme of the relief of the bottom of the North European basin. Adapted (Jakobsson, 2008).

*Note. Designations:* 1. Central Upland 2. North Barents Sea Depression 3. Svalbard Bank 4. South Barents Sea Depression 5. North Kaninskaya Bank 6. Goose Bank 7. White Sea 8. Perseus Hill 9. Franz-Josef Land 10. West Novaya Zemlya Trench 11. East Barents Sea depression 12. North Cape Bank 13. Fram Strait 14. North-Eastern Plateau 15. Litke Plateau 16. Borea Basin 17. Kolguev 18. Bear 19. Vöring Plateau 20. Kanin Nos Peninsula 21. Icelandic Ridge 22. Jan Mayen Ridge 23. Svalbard Valley 24. Greenland-Icelandic Threshold 25. Svalbard Archipelago 26. Ermak Plateau 27. Molloy Ridge 28. Central Plateau 29. North Cape-Murman Trench 30 Bank Halten 31. St. Anne's Trough. 32. Icelandic Plateau 33. Murmansk bar 34. Pechora Sea 35. Kara sea.

The relief of the bottom of the seas of the North European basin has significant differences from sea to sea. Unlike the deeper Norwegian and Greenland Seas, the Barents Sea belongs to the Shelf Seas of the Russian Arctic and has average depths of 190–230 m (Lisitsyn, 2021). The bottom of this sea is a plain cut with troughs in different directions. Thus, the Medvezhinsky Trench is located on the border with the Norwegian Sea, the Franz Victoria Trench is located between the archipelagos of Franz Josef Land and Svalbard on the border with the Arctic Basin, and the St. Anna Trench is on the northeastern border with the Kara Sea.

The location of such large gutters (with depths of 300-600 m) at the boundaries of the Barents Sea contributes to increased water exchange in these areas with neighboring water areas. The basis of the southern and central parts of the Barents Sea are extensive depressions and small elevations: the North, South and East Barents Sea depressions, surrounded by banks (the largest of which are Central and Perseus - in the north and south; Murmansky swell, Kaninskaya and Gusinaya banks - on south). More complex topography is represented by the waters of the Greenland and Norwegian Seas. Their basins are separated by a system of oceanic ridges, the largest of which are the Mona ridge (to the north of the Jan Mayen fault) and the meridional Knipovich ridge. Between the ranges and the Scandinavian peninsula in the Norwegian Sea, there are two large basins - Norwegian and Lofoten (Zalogin and Kosarev, 1999; Blindheim and Osterhus, 2005). The Norwegian basin is the largest and deepest basin of the sea (average depths are 3200-3600m). Its borders extend north from the Aegir range, east to the Icelandic plateau to the Vøring plateau up to the continental slope from the coast of Scandinavia. The Lofoten basin is somewhat smaller and, relative to the Norwegian one, shallower (average depths are about 3200m). It extends north of the Norwegian Basin and the Vøring Plateau, southeast of the Mona Range, borders the Barents Sea to the northeast and Scandinavia to the southeast (Blindheim and Osterhus, 2005). Topographically, the Greenland Sea also

has two main basins: the Greenland and Borea basins (with average depths of 3400-3600m and 3200m, respectively). The Greenland Basin is located from the west and east between the Mona and Knipovich oceanic ridges and Greenland, from the south - the Jan Mayen Fault area, from the north in the Greenland Fault zone - with a much smaller Borea basin.

Despite the noted differences, all seas belong to the same basin, and the Norwegian Sea is a kind of link between the Greenland and Barents Seas.

Sources and sinks of fresh water, phase transitions during ice melting and growth, as well as advection of Atlantic waters through the Fram Strait (and partly through the Barents Sea) are the main generators of the thermohaline structure of the Arctic Ocean and largely affect the formation of the density and circulation fields of water and ice drift in the Arctic Ocean (Nikiforov and Speicher, 1980). In the North European Basin there is a zone of "anomalous overheating" of the atmosphere, due to the strong release of heat from the ocean (Alekseev et. al., 1985).

The North European basin is complex, both in terms of bathymetry and in terms of hydrological, meteorological and ice regimes. The hydrological, atmospheric and ice processes taking place in this region extend their influence not only to the Arctic, but also reach about. Baikal (Nikiforov, 2006). Therefore, the study of the North European Basin is assigned a key role in the formation of the thermohaline structure of the Arctic Ocean and the influence of the Arctic Ocean on the North Atlantic.

## 1.2 Data and methods

The data on the average monthly ice coverage of the Greenland and Barents Seas used in the work were provided by the Department of Ice Regime and Forecasts of the Federal State Budgetary Institution "AARI" from 1950 to 2021 (Mironov, 2004; Atlas

of the Oceans, 1980). Ice cover - the area of the sea occupied by ice of any concentration within the boundaries of the sea (WMO sea-ice nomenclature, 2017).

The initial average monthly ice coverage values were averaged over the seasons of the year in accordance with the following gradations (Mironov, 2004): winter corresponds to the months from December to April, spring - from May to June, summer - from July to September; and finally, autumn - from October to November. As a result, a working database of seasonal ice coverage values for the period 1950-2021 was obtained.

Monthly mean ocean surface temperature (SST) data for the Barents, Greenland and Norwegian seas were obtained from the CDAS-1 Reanalysis database site of the International Climate Research Institute and Columbia University Society in New York (USA), located at http://iridl.ldeo.columbia.edu/. Monthly average SST values were selected from January 1949 to December 2019 at 2°x2° grid points (Figure 1.3).

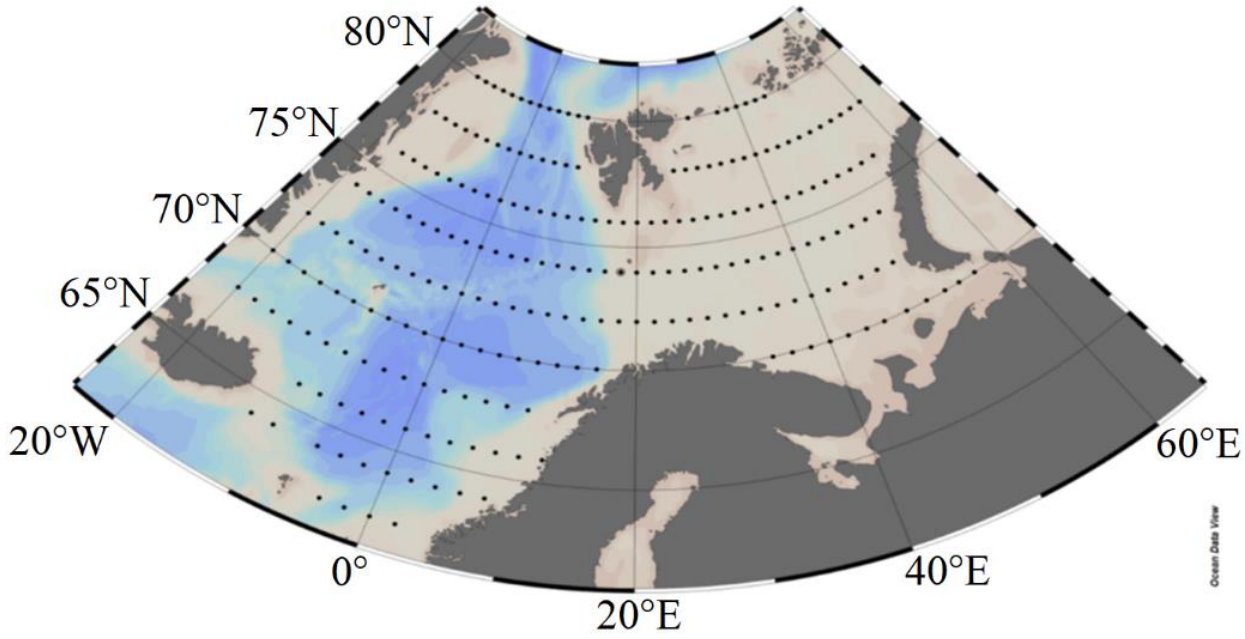


Figure 1.3. Schematic map of data sampling points for the seas of the North European Basin.

The resulting SST fields were averaged for each sea and then averaged over the seasons, similar to those for ice coverage. As a result, a working database of seasonal SST fields in the North European Basin was formed for the period 1950–2019.

As characteristics of atmospheric processes, we have chosen the average annual and average seasonal indices of large-scale atmospheric circulation: the Arctic Oscillation Index AO, the Arctic Dipole Index AD, the Pacific-North American Index PNA, the North Atlantic Oscillation NAO, and the surface temperature of the atmosphere PTA. Time series of indices AO, AD, PNA kindly provided M. A. Janout (Janout et al., 2017). They represent the first three modes of decomposition of surface atmospheric pressure from 60ºN to the pole by empirical orthogonal functions (EOF). AO index (Arctic Oscillation) reproduces situations of increase/decrease in atmospheric pressure over the Arctic, reflecting the intensification of latitudinal exchange; index AD (Arctic Dipole), reflects the intensification of the meridional exchange; the third mode of EOF3 is a dipole with an axis perpendicular to the AD axis and is traditionally called Pacific North American Oscillation (PNA). NAO index data (North Atlantic Oscillation), is the difference in surface height of 500 hPa between locations in Iceland (64° N, 24° W) and near the Azores (39° N, 24° W), were taken from the site (https://www.cpc.ncep.noaa.gov/products/precip/CWlink/). The listed indices reflect the nature of air transfers that induce wind drift of ice, and also change the topography of the sea surface, especially near the coast (surge phenomena), and through the level gradient affect the drift of the ice cover.

In the database of hydrometeorological factors were introduced Atlantic Multidecadal Oscillation (AMO, http://www.esrl.noaa.gov/psd/data/timeseries/AMO/) and surface air temperature STA (from the database website CDAS-1 Reanalysis International Climate Research Institute and Society of Columbia University in New York City (USA), located at http://iridl.ldeo.columbia.edu/). Monthly average STA values were selected from January 1949 to December 2021 at 2°x2° grid points (Figure

1.3). These parameters refer to thermodynamic characteristics: the FTA temperature affects the intensity of phase transitions (ice melting in spring and summer and its growth in autumn and winter), and the AMO index reflects the effect on the ice cover of the Greenland and Barents Seas of the warm waters of the North Atlantic, which enter through the Ferrero-Shetland strait.

Scientific publications publish information on the statistical relationship between sea level, water temperature, and ice coverage with astrogeophysical parameters (Boitsov, 2007, 2009; Gudkovich et al., 2008; Loginov, 2020; Shapkin et al., 2021). The monograph (Frolov et al., 2007) provides an overview of the results of empirical studies of the influence of the long-term “pole tide”, the nineteen-year declination tide, and the Earth's rotation rate on the ocean level and on the ice coverage of individual Arctic seas. This became the basis for including astrogeophysical factors as predictors in the study. Thus, in the regulation of solar radiation inflow to the Earth (excluding the atmosphere) and its distribution over the earth’s surface (solar climate), two mechanisms are distinguished that have different physical nature (Fedorov et al., 2016; Fedorov, 2017, 2018, 2019). One mechanism is determined by celestial-mechanical processes that change the elements of the Earth's orbit (the Earth-Sun distance, the duration of the tropical year, etc.), the tilt of the rotation axis, and the associated changes in the Earth's insolation. To take into account this mechanism, we used the anomalies of the distances between the Earth and the Sun for the winter (October-March) $C_W$ and summer (April-September) $C_S$ half-years, calculated according to the website (https://soft-ok.net/226-astroprocessor-zet-9-lite.html).

Another mechanism is associated with a change in solar activity, Wolf numbers are traditionally used as an indicator Wolf

(https://solarscience.msfc.nasa.gov/greenwch/SN_m_tot_V2.0.txt).

A review of studies of the relationship between sea ice coverage and SST of the seas and solar activity indicates, on the one hand, the presence of little-studied natural mechanisms that determine the identified dependencies, and, on the other hand, the complex nature of these mechanisms. However, the annual average Wolf number W was included in the number of variables in the database of tested predictors.

The long-term gravitational forces of the Moon and the Sun and fluctuations in the Earth's rotation rate were taken into account by variations in the average annual coordinates X, Y of the Earth's pole (ftp://hpiers.obspm.fr/iers/series/opa/eopc04) and average annual nutation parameters of the Earth's axis $\Delta\varepsilon$ and $\Delta\psi$ (https://datacenter.iers.org/eop.php). The average annual fluctuation of day length was used as an index of the Earth's rotation speed lod (length of day; https://astro.ukho.gov.uk/nao/lvm/#tabs-d3) (Egorov, 2003; Abdusamatov, 2019). This subgroup of variables produces effects through a partial change in the gravitational field, which forms a long-term forced wave of a tidal nutation type and the emergence of a partial geostrophic current.

The time series of data considered in this paper are more than 70 years. In the study of various parameters of long-term variability, its structure and features, in order to reduce the influence of high-frequency fluctuations, which may be due, among other things, to errors in the calculation of ice cover and SST, as well as fluctuations in hydrometeorological factors on a scale of up to a year, all available data were averaged either by seasons either for a year or six months.

As shown (Gudkovich and Nikolaeva, 1963), when the drift velocity is averaged over a month, half a year or more, the contribution of the wind component decreases,

and the role of constant (actually slowly changing) currents increases - up to 40% according to the authors. Those. In addition to atmospheric circulation, the long-term dynamics of the ice cover is also largely influenced by the ocean level and currents.

There is another feature of hydrometeorological characteristics averaged over a season, half a year, a year, etc. When averaging, additional effects of interaction with other factors are included in the hydrometeorological parameter. For example, the ice coverage of the Barents Sea in late autumn and early winter is influenced by current regional atmospheric processes. However, starting from February, the distribution of ice begins to influence local atmospheric processes (Mironov, 2004). As a result, the atmospheric pressure field averaged over the winter period also includes the effect of interaction with the ice cover. It is important to keep this in mind when constructing statistical models and explaining the role of predictors included in the model.

*Research methods*

Processing of time series included correlation, spectral, cross-correlation and multi-regression analyzes performed using the Statistics software package (statsoft.ru).

Correlation analysis was used to establish the relationship between the ice cover and SST of the seas of the North European Basin with hydrological, meteorological, and astrogeophysical factors. With the help of cross-correlation analysis, the time delay (in years) of ice coverage and SST fluctuations with respect to the predictor was determined. The correlation coefficient was calculated:

$$r = \frac{\sum_{i-1}^{N}[(x_{1i}-\overline{x_1})(x_{2i}-\overline{x_2})]}{\mathrm{N}\sigma_1\sigma_2}, \quad (1)$$

« $x_{i1}$ and $x_{i2}$– are the values of the first and second variables, respectively; $\overline{x_1}$ and $\overline{x_2}$ – are the mean values of the first and second variables, respectively; $\sigma_1$ and $\sigma_2$ – re the standard deviations of the first and second variables, respectively; N – is the length of the series of the first and second variables» (Gordeeva, 2013).

The significance of the correlation coefficients and its particular value, such as the autocorrelation coefficient, in the analysis of the ACF (autocorrelation function), was tested by Student's t-test at a significance level of 0,05 and the number of degrees of freedom N-2.

To check the series for stationarity and to identify fluctuations with a period exceeding the length of the series, a linear trend was calculated and analyzed. Linear trend equation:

$$y = a_1 t + a_0 + \varepsilon, \quad (2)$$

t – time, $a_1$ – linear trend coefficient, $\varepsilon$ – remnants (noise), $a_0$ – dimensionless coefficient. The first part of the equation $a_1 t + a_0$ is actually a linear trend. The trend value shows how much the studied characteristic changes over a selected period of time (Gordeeva, 2013). Before calculating the correlation and autocorrelation coefficients, the linear trend was removed from the series under study.

The method of spectral analysis was used to obtain the composition of cyclicities of both ice coverage and SST and predictors, in the analysis of contingency of the studied characteristics. The Fourier expansion was calculated using the program of the Statistica analysis package. A periodogram (spectrum) was constructed from the frequency and dispersion of the harmonics of the studied series. The spectrum identified peaks corresponding to the main harmonics, which were subsequently checked for significance, and the contribution $V_k$ of each significant harmonic to the total variance of the series was calculated.

$$V_k = \frac{D_k}{D_y}, \quad (3)$$

$D_k$ – dispersion of the k-th harmonic, $D_y$ – dispersion of the original series.

Cluster analysis (automatic classification method) was used both to identify homogeneous periods and to combine them into homogeneous regions. Clusters of high, medium and low SST and large, medium and low ice cover were identified by time periods. According to the SST fields, zoning was carried out. Using the Statistica analysis package program, a tree-like dendrogram was built (Vainovsky and Malinin, 1992; Smirnov et.al., 1992; Belov et al., 2008), which was used to visually select the most adequate number of clusters. Further, using the K-means method (Belov et al., 2008), the data were combined into a number of groups determined by the dendrogram. The Euclidean distance was used as a proximity measure in both methods. To obtain a better result on the zoning of the North European Basin, in order to “avoid noise”, before clustering, decomposition in natural orthogonal functions (principal component method, PC) was performed (Vainovsky and Malinin, 1992). The decomposition was performed without rotation; the first three modes were used in the classification.

To obtain statistical equations, we used the apparatus of multi-regression analysis (MRA) from the "Statistics" software package. A description of the MPA is given in the application of the programs "Statistics", and is also described in the monograph (Malinin and Gordeeva, 2003). Since our database contained a large number of variables, we chose the procedure for eliminating variables to obtain statistical equations using the multiregression method. First, a complete multiple regression model (MLR) was built, while in STATISTICS the initial version contains no more than 20 variables.

Then, the least significant variables according to the p-level criterion were excluded from it, which either weakly correlate with ice coverage or are collinear with other variables (the latter is automatically estimated by the program). After that, the next most important factor is excluded from the model. This continued until the most significant factors remained. In the process of building a statistical model, the program "STATISTICS" produces a table (bulletin) in which the criteria for the adequacy of the p-level of each variable are given. Thus, from a large number of tested variables (predictors), by enumerating them, variables (no more than 7–10) with sufficient statistical significance are found. The construction of a statistical model ends with the highest overall coefficient of multiple linear correlation, and the p-level criterion for the adequacy (significance) of the entire model is equal to or less than 0,01.

## Conclusions for Chapter 1

The features of the geographical location of the study area, which largely form the climate of the North European basin, are revealed. In this case, the relief has a great influence on the formation of a system of surface currents.

An analysis of works on the use of statistical analysis in hydrometeorology shows the productivity of the multiple regression method for obtaining statistical models of the variability of hydrometeorological processes, which makes it possible to choose it for modeling temporal changes in both ice coverage and sea surface temperature.

# CHAPTER 2 SEA SURFACE TEMPERATURE OF THE NORTH EUROPEAN BASIN'S SEAS

## 2.1 Characteristics of the thermal state of the surface of the seas North European Basin

From the point of view of the hydrological regime, the North European Basin seems to be a very interesting object for research (Figure 2.1.). The water area of the Greenland Sea is subject to permanent northerly winds. Which significantly affect the cooling of the surface layer of water, and also contribute to the drift of ice from the Arctic basin to the North Atlantic. Warm and saline waters entering with the North Atlantic Current cool in the surface layer, moving northward towards Svalbard and flowing through the western border of the Barents Sea into the Barents Sea and through the Fram Strait into the Central Arctic Basin (Ivanov and Repina, 2018; Ivanov et al. , 2020; Ivanov, 2021). As part of the Atlantic Conveyor, these waters return from the north with the waters of the cold East Greenland Current. To the east of the Greenland Sea is the warm Svalbard Current, which is an offshoot of the North Atlantic Current of the Gulf Stream system. This combination of countercurrents contributes to the creation of various cyclonic whirlpools in the center of the Greenland Sea (Nikiforov and Speicher, 1980).

At the same time, the Norwegian Sea is one of the zones in which there is a significant overheating of the atmosphere, due to the influx of a large amount of warm and saline water from the Atlantic Ocean (Lappo et al., 1990; Alekseev and Korablev, 1994; Malinin and Shmakova, 2018). These waters enter the Norwegian Sea with the Norwegian current, they are also a continuation of the warm North Atlantic current of the Gulf Stream system. At the same time, in the south of the Norwegian Sea, this current branches into two parts.

The coastal eastern part of the current, fed by the fresh waters of the continental runoff, moving along the coast of the Scandinavian Peninsula, goes to the Barents Sea. Some of these waters recirculate after some time and return in a transformed form to the Norwegian Sea (Walczowski, 2014). In the winter season, this current is observed at greater depths and the flow is narrower. At the same time, in the summer season, it expands to a large area, but at the same time becomes smaller, forming a kind of wedge over the Atlantic waters.

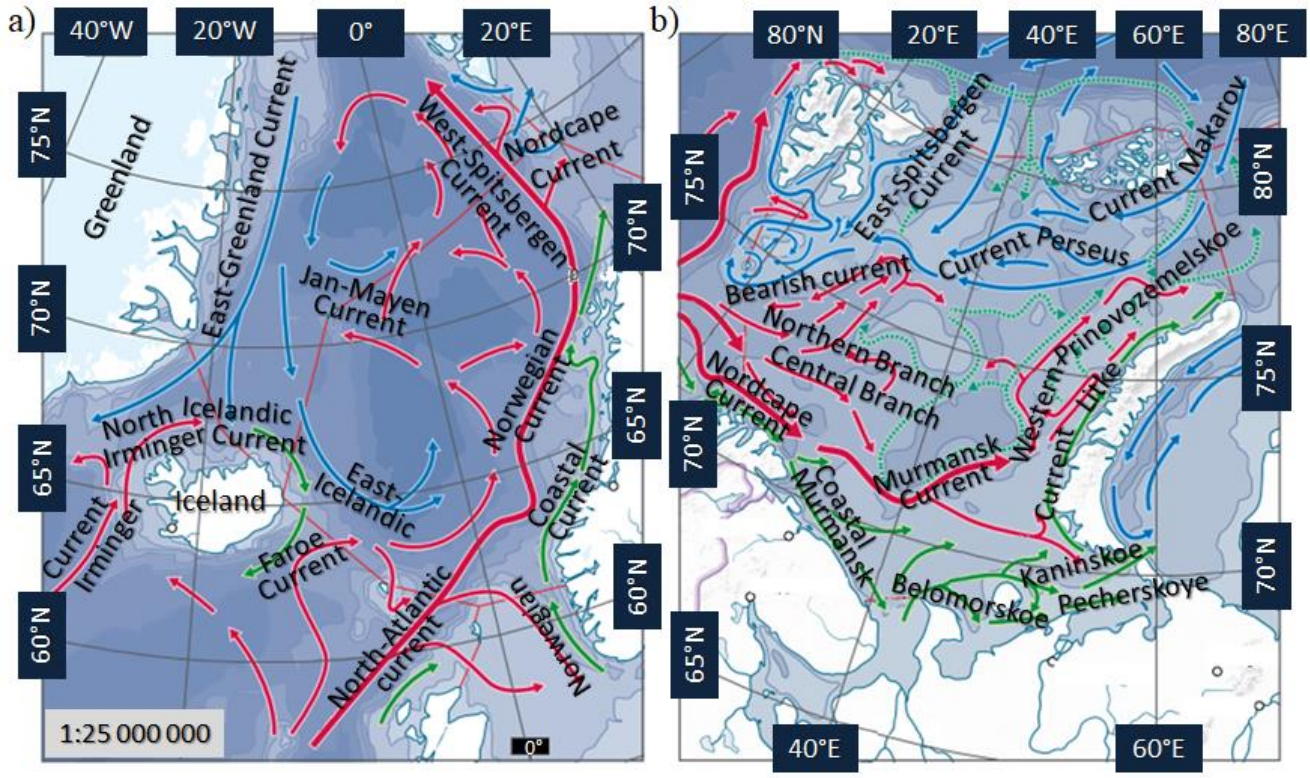


Figure 2.1. Scheme of surface currents of the North European basin. Adapted (Ecological Atlas, 2020).

The North Cape Current, entering the Barents Sea, is the most powerful current affecting the hydrological regime of the sea. Moving deep into the sea from west to east, it is divided into branches. One of them is Coastal, narrow enough (no more than 40 miles) and Northern, wider - about 60 miles. In the area of the Kola Bay, a branch of the waters of the North Cape Current of the Coastal Branch deviates to the southeast,

moving along the coast to the White Sea. Another stream of the Coastal current is directed to the northeast, transforming into the Murmansk current, which also has a branch of a small part of the water flow to the east, and with the Kolguyevo-Pechora current it is directed to the Pechora Sea. At the same time, a certain part of this flow moves towards the cyclonic circulation. The main flow of waters of the North Cape current in the north turns in the opposite direction: to the west and southwest. As mentioned earlier, the most important feature of the North European Basin is the presence of strong temperature contrasts in the surface layer. It is in this region that the warm waters of the North Atlantic, which enter the region with the Irminger Current and the Norwegian Current, and the cold waters from the Arctic Basin, which enter with the East Greenland Current, come into contact. The described conditions form sufficiently powerful and stable hydrofronts (Nikiforov and Speicher, 1980).

The long-term average sea surface temperature has a pronounced zonal distribution in the Norwegian and Barents Seas in all seasons (Figure 2.2 a, b, c, d).

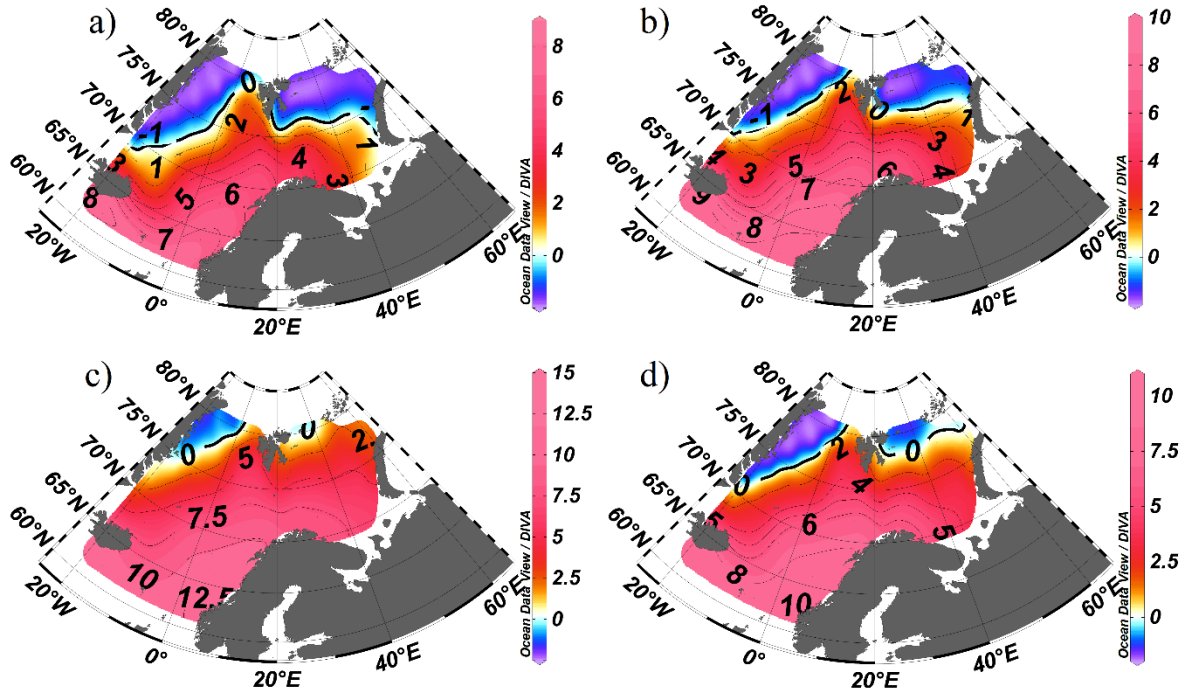


Figure 2.2. Average long-term distribution of sea surface temperature in the seas of the North European basin by seasons for the period 1950–2019: a) winter (December-April), b) spring (May-June), c) summer (July-September), d) autumn (October November).

The zonality structure in the distribution of SST in all seasons of the year in the Greenland Sea is “disturbed” by the outflow of cold Arctic waters along with the drift of old ice. Which contributes to the stretching of the tongue of cold waters from the Fram Strait towards the Denmark Strait. At the same time, areas of inflow of warm Atlantic waters through the Faroe-Shetland Strait are clearly distinguished. The zero isotherm is located depending on the season from 68°N. up to 75°N in the Greenland Sea and from 75°N up to 80°N in the Barents Sea, with negative temperatures only off the northeastern coast of Svalbard. In addition to the temperature aspect of seasonality, the maximum stretching of the tongue of cold waters in the winter season is facilitated by the highest speed of ice drift through the Fram Strait in this season (Lipatov, 2021).

The long-term medium sea surface temperature in the Faroe Shetland Strait ranges from 8°C to 12°C. The tongue of warm waters extends to the north, with a gradual decrease in SST to 3°C near the southern borders of the Svalbard archipelago. A branch of this current branches to the west and then brings warm waters to the Barents Sea with the North Cape Current.

The highest SST is typical for the south of the Norwegian Sea (Norwegian and Lofoten basins) in the area of the passage of the North Atlantic Current and its continuation in the form of the Norwegian Current. The water temperature ranges from 8°C to 12°C depending on the season. The system of oceanic ridges (Mona and Knipovich) limits the flow of warm Atlantic waters into the Greenland Basin. And the modernized chilled Atlantic waters will rush into the Fram Strait off the western coast of Svalbard. The absence of ridges in the west of the Barents Sea, in turn, contributes to the flow of warm Atlantic waters in an easterly direction, which makes it possible to use seaports on the shores of Scandinavia all year round due to the absence of ice. From latitude 75°N and to the north in the northeast of the Barents Sea, cold Arctic waters are advected, which manifests itself in the greatest variability in the position of the zero

isotherm in this area depending on the season. The distribution of SST over the surface of the North European Basin in the spring and autumn seasons is almost identical.

## 2.2 Spatio-temporal variability of long-period fluctuations in the sea surface temperature of the seas North European Basin

### 2.2.1 Zoning the sea surface temperature of the seas North European Basin

When studying long-term fluctuations in the thermal state of the sea surface, the SST fields were expanded in terms of natural orthogonal functions (Vainovsky and Malinin, 1992; Belov et al., 2008) and three modes $EOF_1$, $EOF_2$, and $EOF_3$ were obtained. The characteristics of the linear trend are calculated. The linear trend and its characteristics will be discussed in more detail below. The spatial distribution of the principal components is shown in Figure 2.3.

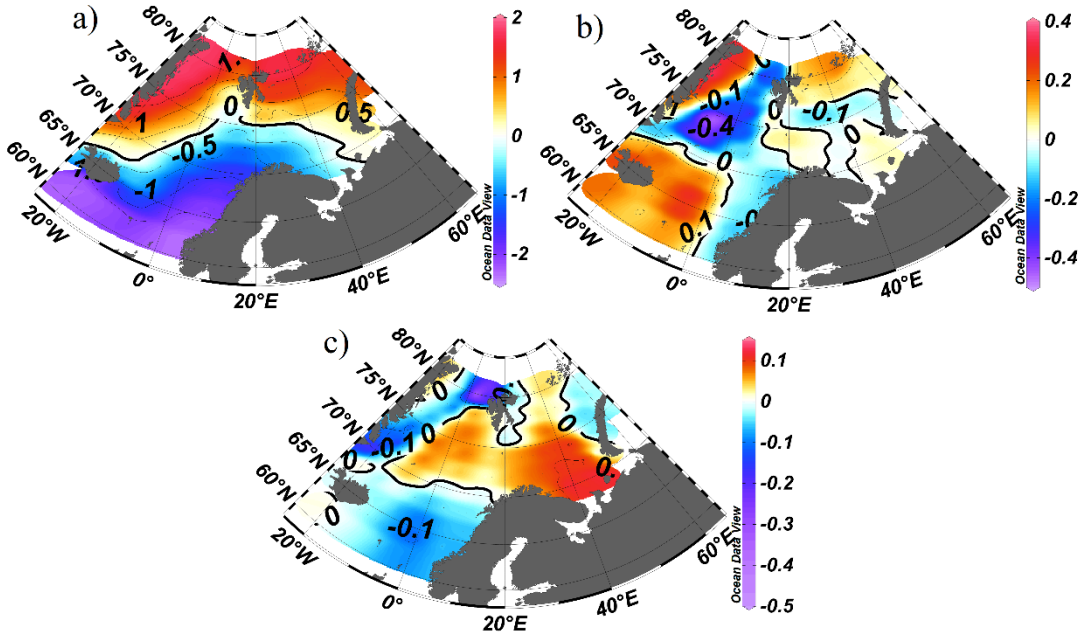


Figure 2.3. Spatial distribution of the main components $EOF_1$, $EOF_2$, $EOF_3$ of the sea surface temperature of the seas of the North European basin for the period 1949-2019.

The distribution of the first mode is characterized by large-scale processes of thermal interaction between the ocean and the atmosphere. Indeed, the correlation between the first mode and the average long-term sea surface temperature (see Figure 2.2.) is almost linear. The lowest correlation coefficient observed in the Barents Sea is – 0.96. The maximum correlation coefficient is noted in the area of the Norwegian Sea - 0.99. Negative mode values are located within the boundary of the Norwegian Sea and cover the southwestern part of the Barents Sea up to the shelf boundaries. The second and third modes are characterized by smaller scale processes and require a separate study.

The next step was the zoning of the basin. For this, a data array was compiled: the main components of $EOF_1$, $EOF_2$, $EOF_3$, the coefficient of determination of the trend and the magnitude of the trend (a1). Using this array with the help of cluster analysis (Ward-Method, Eucidian distance), zoning was performed (Vainovsky and Malinin, 1992; Belov et al., 2008). The first step was to build a dendrogram (Figure 2.4.). According to the dendrogram, it was decided to identify 8 clusters.

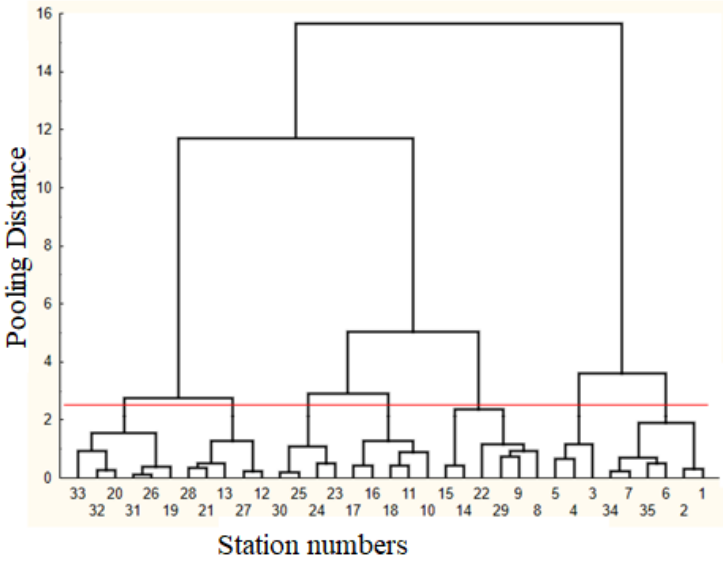


Figure 2.4. Dendrogram for the sea surface temperature of the seas of the North European basin.

*Note:* The red line marks the distance of cluster selection.

Further, using the K-means method (Belov et al., 2008), the grid nodes were combined into regions (Fig. 2.5a).

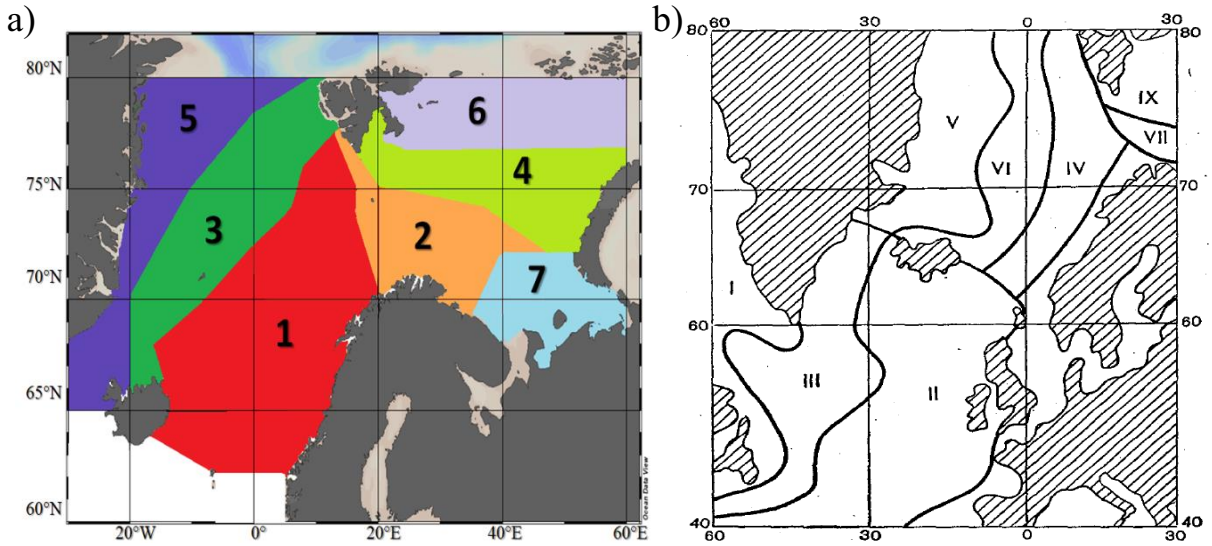


Figure 2.5. Homogeneous areas a) according to the thermal state of the North European Basin, obtained using cluster analysis b) depending on the vertical structure of water masses (Nikiforov and Speicher, 1980).

The third and fourth regions are frontal zones between the warm waters of the Norwegian, Barents and Atlantic waters mixed with them and cold Arctic waters. Also, these areas are the location of the ice edge in different years. The fifth and sixth clusters are located in the northernmost and coldest parts of the Greenland and Barents Seas, respectively. These are areas that are covered with ice in different years in winter (and not only). The first region (corresponding to the Norwegian Sea) is most affected by the Atlantic waters and is also the region with the maximum temperature values and at the same time has the minimum standard deviation. The second area is also strongly influenced by Atlantic waters, but at the same time it is the area with the maximum values of the linear trend, this is the area of the largest increase in SST over the period under consideration. The seventh region is the area of the Pechora Sea, which is subject to the maximum influence of river runoff. It is also worth noting that, in general, the resulting division into regions corresponds to the zoning of the seas of the North

European basin by E.G. Nikiforov and A.O. Speicher 1980 (Nikiforov and Speicher, 1980) depending on the vertical structure of water masses (Figure 2.5.b).

Let's look at each region in more detail. The main characteristics of the districts are presented in Table 2.1.

Table 2.1. Statistical characteristics of the sea surface temperature in the regions of the North European Basin.

| Region | $SST_{Av,}$ °C | SD, °C | $SST_{MAX,}$ °C | $SST_{MIN,}$ °C | $SST_{MAX} - SST_{MIN,}$ °C | SST (winter), °C | SST (summer), °C | Value Trend a1, °C/72 years | $R^2$ |
|---|---|---|---|---|---|---|---|---|---|
| 1 | 6,36 | 1,77 | 10,30 | 4,00 | 6,30 | 4,71 | 8,94 | 0,65 | 0,48 |
| 2 | 4,63 | 1,80 | 8,62 | 2,08 | 6,54 | 2,98 | 7,31 | 0,50 | 0,38 |
| 3 | 2,14 | 1,51 | 5,49 | –0,93 | 6,43 | 0,76 | 4,21 | 0,81 | 0,37 |
| 4 | 1,77 | 1,97 | 5,64 | –1,88 | 7,52 | 0,06 | 4,62 | 0,82 | 0,53 |
| 5 | –0,89 | 0,75 | 1,18 | –1,88 | 3,06 | –1,43 | 0,21 | 0,73 | 0,65 |
| 6 | –0,57 | 1,55 | 2,79 | –1,88 | 4,67 | –1,73 | 1,75 | 0,72 | 0,59 |
| 7 | 4,46 | 2,18 | 9,25 | –1,88 | 11,13 | 2,48 | 7,64 | 0,51 | 0,33 |

Note. $R^2$ – is the coefficient of determination, the trend is significant for all districts (significance level 0,05). –1,88 is a shorthand for the freezing point at which sea ice forms.

*Region 1*

It is located throughout the Norwegian Sea, east of about. Iceland, occupying the Norwegian and Lofoten basins, bounded from the west by the Mona and Knipovich ridges. It is formed mainly under the influence of warm currents: the North Atlantic, Norwegian and North Icelandic Irminger currents; and cold East Icelandic. It is filled with

the warm waters of the Norwegian current, spreading along the coast of Scandinavia. The southern part of the region is adjacent to the Faroe-Iceland Strait, is located mainly outside

the sea in the Atlantic Ocean and is directly under the influence of the North Atlantic Current. The region is characterized by the highest SST (from +4,00 to +10,30°C), with average values of +6,36°C. This is the area with the highest surface water temperatures in the North European Basin. The standard deviation is 1,77°C and is comparable with the standard deviation of the second and fourth districts. This distribution is associated with the distribution of Atlantic waters in the waters of the Norwegian and Barents Seas (see Figure 2.1).

*Region 2*

It is located in the Barents Sea, in the area of passage of the warm Norkap current, the Northern and Central branches. Filled with waters of Atlantic origin. At the same time, the RMS is average relative to other regions RMS = 0,90°C, and the SST is quite high: from +2.08 to +8.62°C. Just like the first region, it is a never-freezing part of the North European basin.

*Region 3*

It is located in the region of the Borey basin and the Greenland basin. The Mona Rapid and the Icelandic-Jan Mayen Ridge serve as the eastern border with the third region. This area is crossed by the Jan Mayen current, which carries cold waters and old ice from the Arctic basin into the Greenland Sea. Here, the bottom waters are overlapped by the central water mass, which is formed during the mixing of the Atlantic and surface Arctic waters. The average values of TPO are positive +2,6° C, varying from negative minimum –0,93°C to +5,49°C. The RMS value is 1,51°C. Which is comparable to the sixth district. The presence of negative temperatures and the average standard deviation for the North European Basin is associated with the proximity to the area where the boundary of multi-year ice is located, which in turn is associated with the

system of surface currents and the speed of ice drift through the Fram Strait. This area is a kind of frontal zone, between the Greenland and Norwegian Seas, separating the area with year-round presence of ice cover (fifth) and the area, year-round ice-free (first).

*Region 4*

It is located along 75°N in the Barents Sea. Cold Arctic waters with the current of the same name flow into this area from the northeast along the Perseus Rise, from the south - warm waters from the Northern branch of the Norkap current and the West Prinovozemelskoye current from the southeast off the coast of Novaya Zemlya. From the south, the area is limited by the Spitsbergen Bank and the central upland. The standard deviation is 1,97°C, practically the highest value in the entire North European basin, slightly higher only in the seventh region. Water temperatures range from the minimum -1,88°C (these temperatures and below are typical for areas with ice cover) to +5,64°C. This area is a kind of frontal zone in the Barents Sea, separating the area with year-round presence of ice cover (sixth) and the area, year-round ice-free (second).

Also, in the area north of Cape Zhelaniya, the inflow of the waters of the Kara Sea is determined. Depending on the intensity of the North Atlantic Current, the state of the atmospheric circulation and other factors in different years, they are the area where the ice edge passes. RMS is 0,84°C, which, as for the fifth region, is the average value within the North European Basin.

*Region 5*

It occupies the western and northern parts of the Greenland Sea, also includes the Fram Strait. If you look at the bottom topography, you can see that the border of the first region with the second one runs along the Greenland Plateau and belongs to the continental shelf of about. Greenland. The area covers a part of the East Greenland (according to the Nikiforov-Speicher nomenclature) and is filled with deep and bottom waters that form in the basin. But on the surface they are blocked by Arctic water,

which is partly carried out by the East Greenland Current, and partly formed in the Greenland Sea.

SST ranges from the minimum freezing temperatures of sea ice, conventionally designated as SST -1,88°C (these temperatures and below are typical for areas with ice cover) to the maximum +1,18°C, typical for the southernmost part of this area. The average TPO is -0,89°C. In general, the area is characterized by the lowest water temperatures in the North European basin. This is due to the fact that in this area there is a year-round drift of ice and cold waters from the Central Arctic Basin, which contributes to additional cooling of the waters formed on the spot. In addition, the formation of the coldest bottom waters in the World Ocean occurs here with temperatures down to -1°C (Nikiforov and Speicher, 1980). The standard deviation of the entire region is +0,75°C, which is the lowest value of variability of all regions. Which is primarily due to the fact that this is an area, most of which is covered with ice all year round. And the presence of ice prevents high variability. In addition, due to the presence of ice, it is not possible to obtain year-round SST data. In this connection, the study of this area will be carried out in the future by analyzing the long-term variability of ice coverage.

*Region 6*

The northernmost and coldest part of the Barents Sea, occupied partially or completely by ice during the cold season in different years. Similarly to the fifth region, located in the Greenland Sea, there is no possibility of obtaining data in the cold season of the year, therefore, the analysis of this area will be presented in the future as a study of the interannual variability of the ice cover in the Barents Sea. RMS is 1,55°C. Which is twice the standard deviation in the fifth region, but less than in the warmer regions (first, second, fourth and seventh). This distribution of RSD is related to the presence of ice in this area, but at the same time, the edge of ice distribution has greater variability

than in the fifth region. The North Atlantic waters, which largely form the hydrological regime of the Barents Sea, are located in lower layers and, although they have a significant influence, are more measured (Alekseev, 2017). Not so long ago, the phenomenon of “atlantification” appeared, in which the intensity of the influence of Atlantic waters in the westernmost part of this region and north of the coast of Svalbard began to increase significantly (Ivanov and Repina, 2018; Ivanov, 2021). Water temperatures range from –1,88°C (these temperatures and below are typical for areas with ice cover) to +2,79°C. Negative average water surface temperatures (–0,57°C) are associated with the year–round presence of ice, as in the sixth region.

*Region 7*

It is located in the region of the Pechersk Sea, where coastal currents dominate: the coastal Murmansk in the southwest, the White Sea in the south, and the Kanin and Pechersk currents in the southeast. This is the only region of the North European Basin affected by river runoff. The largest river flowing into this region of the Barents Sea is the Pechora: the total inflow into the sea from this river for the year is 70% (Lebedev, 2021). Corresponds to the Pechersk region in terms of nomenclature (Nikiforov and Speicher, 1980). The water area is filled mainly with the waters of the coastal water mass, which is underlain by its own Barents Sea waters. Water exchange with the White and Kara seas is characteristic. Due to the complex hydrological structure, it has the highest standard deviation of 2,18°C. The maximum water temperature in this area is up to 9,25°C. The minimum water temperatures are determined by the freezing point of sea water and are conditional –1,88 ° C.

The maximum difference between the minimum and maximum temperatures of 11,13°C is typical for the seventh region. The minimum for the fifth is 3,06°C. For other regions, the difference between the maximum and minimum temperatures ranges from 4,67°C to 7,52°C. This distribution is associated with the year-round presence of ice cover over a large area in the fifth region. Whereas in the seventh region, in the summer season, complete ice clearance occurs, and in the winter season, the water area is almost completely covered with ice: the ice cover reaches a maximum of 99%, and on average in winter it is 65% (Lis and Egorova, 2022).

The magnitude of the trend for the period under review for all regions is close in magnitude. The minimum value of the trend corresponds to the areas of the Barents Sea, which are most affected by the Atlantic waters and coastal currents (second and seventh) 0,5°C/72 years. A slightly larger trend value (by 0,2°C/72 years) in the first, fifth and sixth regions is 0,7°C/72 years. These are areas where there is either year-round absence of ice (the first area) or year-round presence (fifth and sixth). The maximum value of the trend is typical for the border regions (third and fourth) 0,8° C/72 years. The coefficient of determination ranges from 0,37 to 0,65. Whence it follows that the linear trend is statistically significant for all districts at a significance level of 0,05.

Thus, the cluster analysis made it possible to identify two main factors that maximally form the large-scale variability of interannual SST fluctuations – the presence/absence of ice and the system of surface currents.

### 2.2.2 Long-term and cyclic vibrations in the variability of the sea surface temperature

For each of the seas of the North European basin, seasonal averages (winter and summer) were used to calculate linear trends (Figure 2.6.a, b). The trends in SST variability for all seas are the same: there is an increase in temperature over the period

from 1950 to 2019. At the same time, the linear trend is not significant in the Greenland Sea. Those. The SST of the Greenland Sea, when considered for the period 1950–2019, does not have significant fluctuations, the period of which exceeds the length of the series (Table 2.2.).

Table 2.2. Characteristics of linear trends for SST in the Greenland, Barents, and Norwegian Seas for the winter and summer seasons.

| Period 1949–2019 | Summer | | | Winter | | |
|---|---|---|---|---|---|---|
| | NS | BS | GS | NS | BS | GS |
| Difference of SST for the entire period, °C | 0,46 | 0,57 | 0,38 | 0,51 | 0,71 | –0,11 |
| Trend value, °C/year | 0,01 | 0,01 | 0,01 | 0,01 | 0,01 | 0,00 |
| $R^2$, unit | **0,48** | **0,60** | **0,52** | **0,53** | **0,50** | 0,15 |
| Characteristics of trends for selected periods | | | | | | |
| Difference of SST for periods (1950–1985 and 1986–2019), °C | 0,40 | 0,35 | 0,39 | 0,35 | 0,29 | 0,15 |
| Trend value (1950–1985), °C/year | –0,01 | 0,00 | 0,00 | –0,01 | 0,00 | –0,01 |
| Trend value (1986–2019), °C/year | 0,03 | 0,02 | 0,02 | 0,02 | 0,02 | 0,02 |
| $R^2$ (1950-1985), unit | 0,21 | 0,00 | 0,01 | 0,20 | 0,10 | **0,25** |
| $R^2$ (1986-2019), unit | **0,74** | **0,85** | **0,62** | **0,81** | **0,25** | **0,38** |
| Trend index (1950–1985), unit | –3,13 | 0,75 | –2,10 | –3,73 | –16,79 | –92,01 |
| Trend index (1986–2019), unit | 10,52 | 16,37 | 22,46 | 15,39 | 68,72 | 141,30 |

*Note.* SST of the Greenland (GS), Barents (BS) and Norwegian (NS) seas; $R^2$ – trend determination coefficient, significant trends are in bold, at the significance level 0,05; SST – sea surface temperature.

The trend value for all seas is 0,01°C/year and tends to zero in the winter season in the Greenland Sea. The obtained results confirm previous studies on the increase in SST in the seas of the North European Basin (Malinin and Gordeeva, 2003; Fedorova et al., 2015), and an increase in heat inflow from the North Atlantic (Skagseth et al., 2008; Yashayaev and Seidov, 2015; Bashmachnikov et al., 2018). If we analyze the temperature difference between 1950 and 2019, it can be noted that SST increased

maximum in the Barents Sea (by 0,71°C) and slightly decreased in the Greenland Sea (by 0,11°C).

When analyzing the ice coverage of the Russian Arctic seas, it is customary to single out periods called “relatively cold” years 1959–1989 and “relatively warm” years 1990–2021 (Yulin et al. 2019; Egorov, 2020). At the same time, in a number of works (Morison et al., 2000; Polyakov et al., 2010; Chernyavskaya, 2020), slightly different periods are distinguished in the variability of various characteristics of the thermohaline structure. Thus, the work (Chernyavskaya, 2020) considers the years 1970–1989, designated as the second stage, during which a decrease in temperature in the North Atlantic region and the formation of positive salinity anomalies in the surface layer of the Amerasian sub-basin are noted. The authors (Morison et al., 2000) single out the years 1978–1996, when the NAO index was in a deep negative phase for a long time. It is also assumed that changes in salinity and temperature in the surface layer of the Arctic Ocean began in the late 1980s. The cold period of 1960–1970 and the decrease in the frequency of the Väisälä Brand in the Atlantic water layer in the Arctic Ocean by 12% over 1980–1990 are distinguished by the water surface temperature (Polyakov I. V. et al. 2010).

In the studied initial series for the SST of the seas of the North European Basin, using sliding periods for identifying trends, two periods were distinguished: 1950–1985 and 1986–2019 (Figure 2.6c, d).

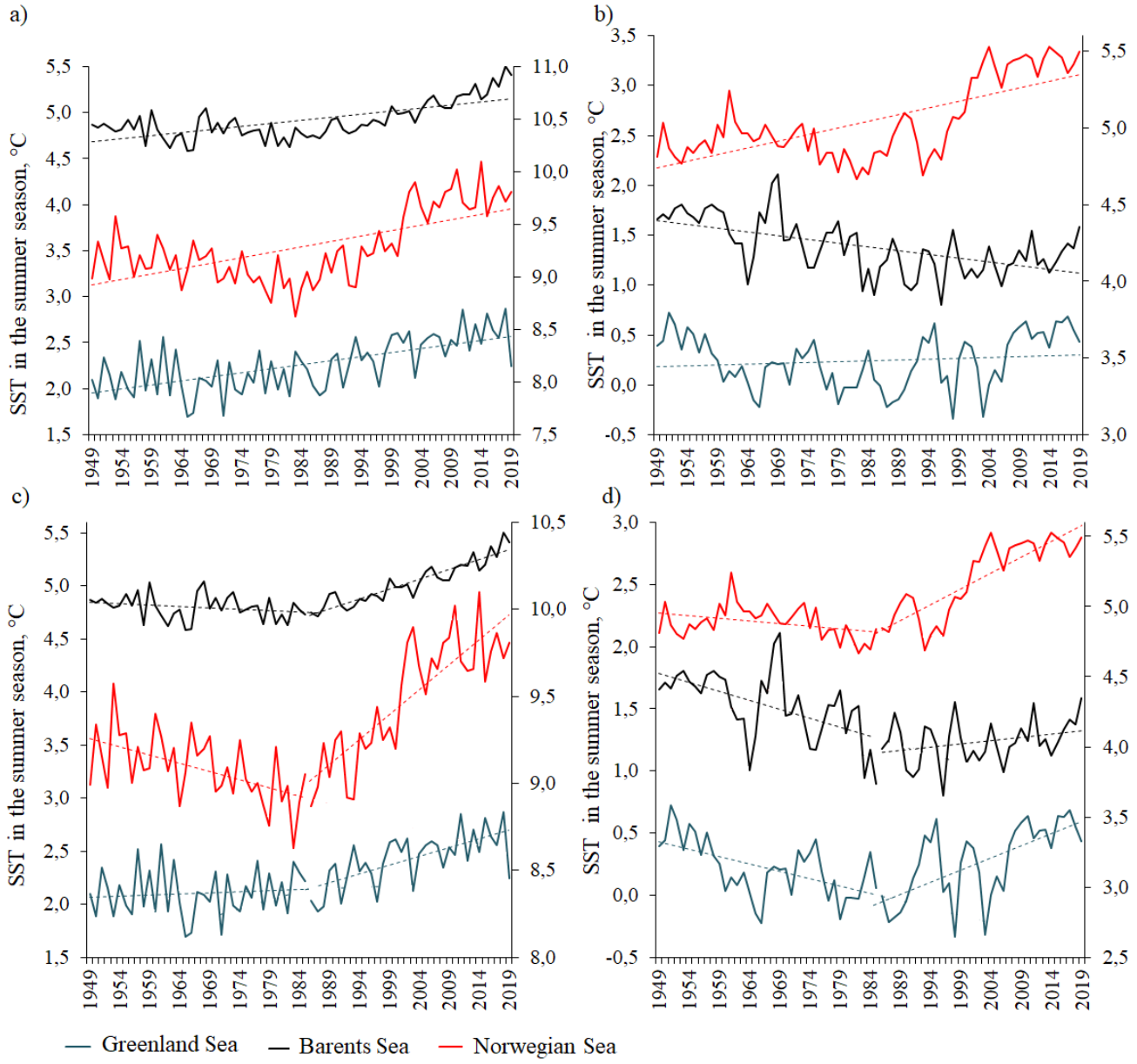


Figure 2.6. Interannual variability of SST in the Greenland (blue, Barents (black) and Norwegian (red, ordinate on the right) seas in summer (a, c) and winter (b, d) seasons with a plotted trend line (dotted lines of corresponding colors) in the periods 1950–2019 years (a, b) 1950–1985 and 1986–2019 (c, d).

Similar periods are distinguished by the ice cover of the Barents Sea (Lis and Egorova, 2022). The period for 1950–1985 is characterized by the absence of statistically significant trends in temperature variability for all seas, except for the Greenland Sea (see Table 2.2.).

It should be noted that the magnitude of the trend of the SST of the Greenland Sea is negative and amounts to 0,01°C/year. That is, over the indicated period, the SST in the Greenland Sea decreased. The temperature difference for the periods (1950-1985 and 1986-2021) varies from 0,15 °C (during the winter season in the Greenland Sea) to 0,40 °C (during the summer season of the Norwegian Sea). The maximum value of the trend falls on the period for 1986–2021 in the Norwegian Sea in the summer season and is 0,03 °C/year.

Since the trend determination coefficient is not a qualitative characteristic for comparing long-term fluctuations, the trend index $I_{tr}$ was used (Malinin and Vainovsky, 2019). Calculated using the following formula:

$$I_{tr} = \frac{100 \cdot a_1 \cdot n}{X_m}, \quad (4)$$

$a_1$ – is the coefficient of the linear trend equation, n – row length, $X_m$ – the average value of the time series. It is a more convenient characteristic for comparison, because it is a dimensionless quantity.

When comparing trend indices, the difference between the periods is obvious. Thus, the maximum difference is noted for the Barents Sea in the summer season, when the trend index for 1950–1985 is 0,75, and for 1986–2019 it is 16,37. The minimum difference stands out for the Greenland Sea in the winter season, when the trend index for 1950–1985 is –92, and for 1986–2019 is 140. In general, it can be concluded that the SST of all seas for the period for 1950–2021. increases, and especially intensively especially in the second period for 1986-2019.

Consider the spatial distribution of trends. At each point, the characteristics of the linear trend were calculated, such as the magnitude of the trend and the coefficient of determination. As can be seen, the largest significant positive linear trend is observed in the area north of Scandinavia in the second part of the period under review for 1986-2019 (Figure 2.7.).

Consider the period 1950-1985 (Figure 2.7.a). In most of the entire North European Basin, the magnitude of the trend has negative values: the entire Norwegian

Sea basin, the western and southwestern parts of the Barents Sea, and the southeastern part of the Greenland Sea. With the highest positive values in the Faroe-Shetland Strait (-0,01°C/37 years) and in the south of the Barents Sea (-0,01°C/37 years).

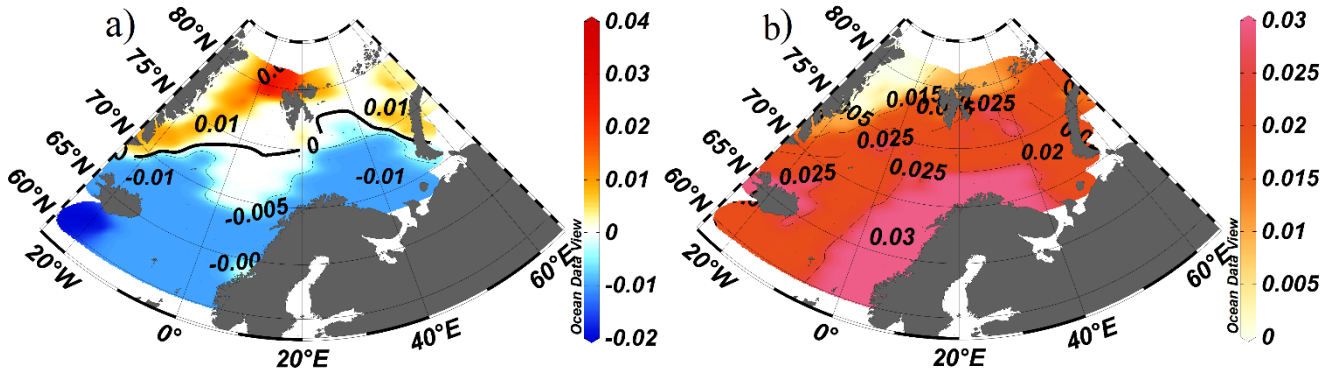


Figure 2.7. The magnitude of the linear trend of SST in the seas of the North European Basin for a) 1949–1985, °C/37 years b) 1986–2019, °C/34 years.

The zone of negative trend values corresponds to the first, second and seventh regions (see Figure 2.5.) with the highest temperatures and the greatest influence of the inflow of warm Atlantic waters. In these areas, the SST decreased over the period 1949–1985 by an average of -0,005°C. The situation in the Fram Strait looks different – the trend value is positive and amounts to +0,04°C/37 years, where SST increased over the period under review. Practically in the entire water area of the Greenland Sea (except for the strip along the western side of the Icelandic-Janmayen Range) and in the north of the Barents, the trend value is positive (+0,01°C/37 years on average).

More interesting is the period for 1986–2019 (Figure 2.7. b), when the trend value $a_1$ exceeds +0,03°C/34 years almost over the entire area of the North European Basin. The maximum values of the trend value $a_1$ are in the coastal zone along Scandinavia and are more than +0,03°C/34 years. On average, the trend value for the entire water area is +0,02°C/34 years, while for the period up to 1985 it was -0,003°C/37 years.

The area of the Fram Strait is singled out, where there is an area of zero values of the trend value $a_1$.

Linear trends were tested for significance. Figure 2.8. the distribution of the value $t_{cr}$ (empirical value of Student's criterion) for a linear trend is presented.

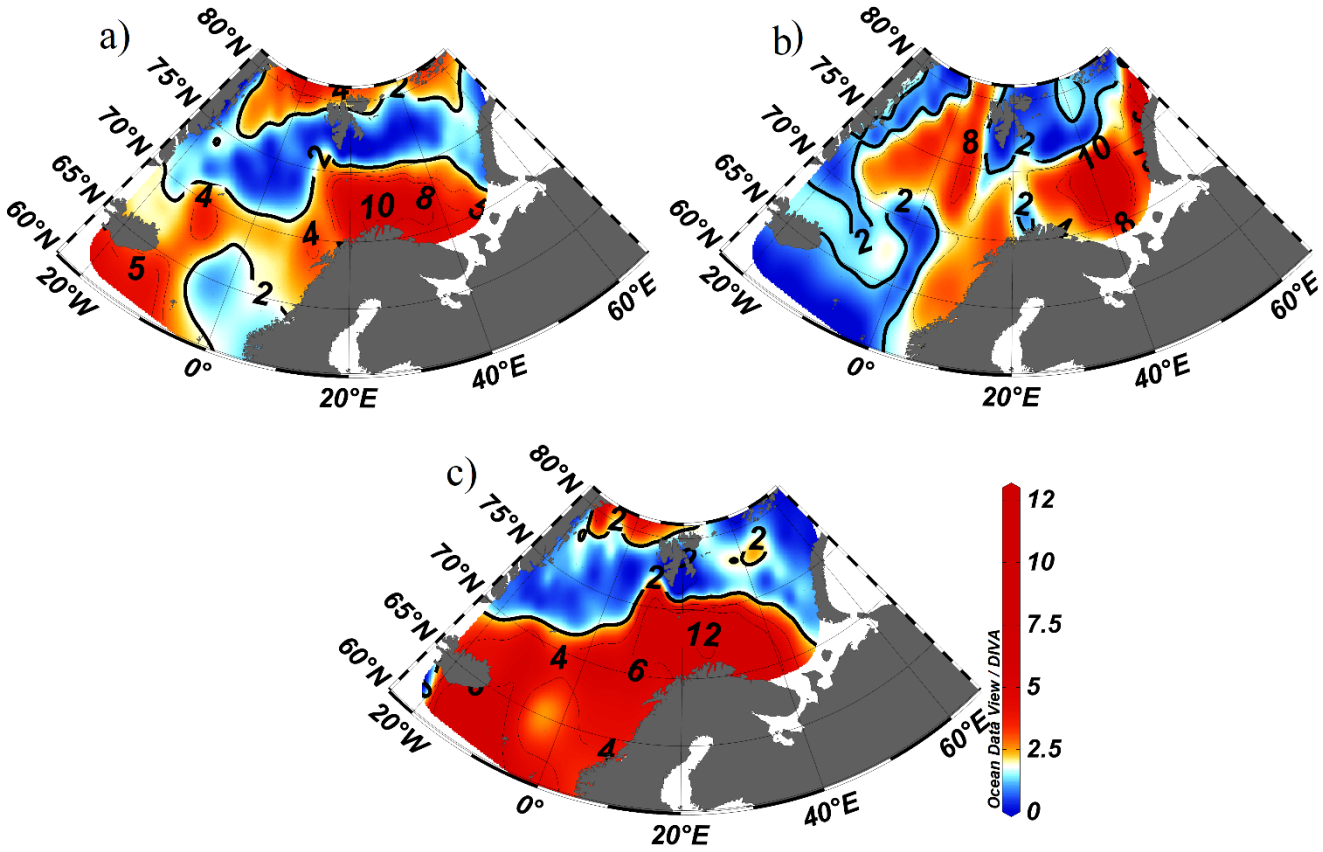


Figure 2.8. Distribution of the sample value of the Student's coefficient $t_{cr}$ for the linear trend of SST in the seas of the North European Basin for the periods: a) 1949-1985; b) 1986-2019; c) 1949-2019.

*Note:* Statistically significant trend are marked in red, the value of Student's $t_{cr}$ is highlighted in thick lines.

This value is significant when it exceeds the critical value of the Student's coefficient (1,99) at a given level of significance (in this case 0,05). On the map, significant coefficients (respectively, a significant linear trend) are indicated by colors from orange to red. A non-significant linear trend is indicated by white and blue colors.

The largest significant positive linear trend is observed in the area north of Scandinavia, both in the first (Figure 2.8. a) and in the second (Figure 2.8. b) part of the period under consideration for 1949-2019. Which does not contradict the hypothesis about the strengthening of the "atlantification" of the western Arctic (Ivanov, 2021).

The SST for each area was averaged and presented as temporal variability in Figure 2.9.

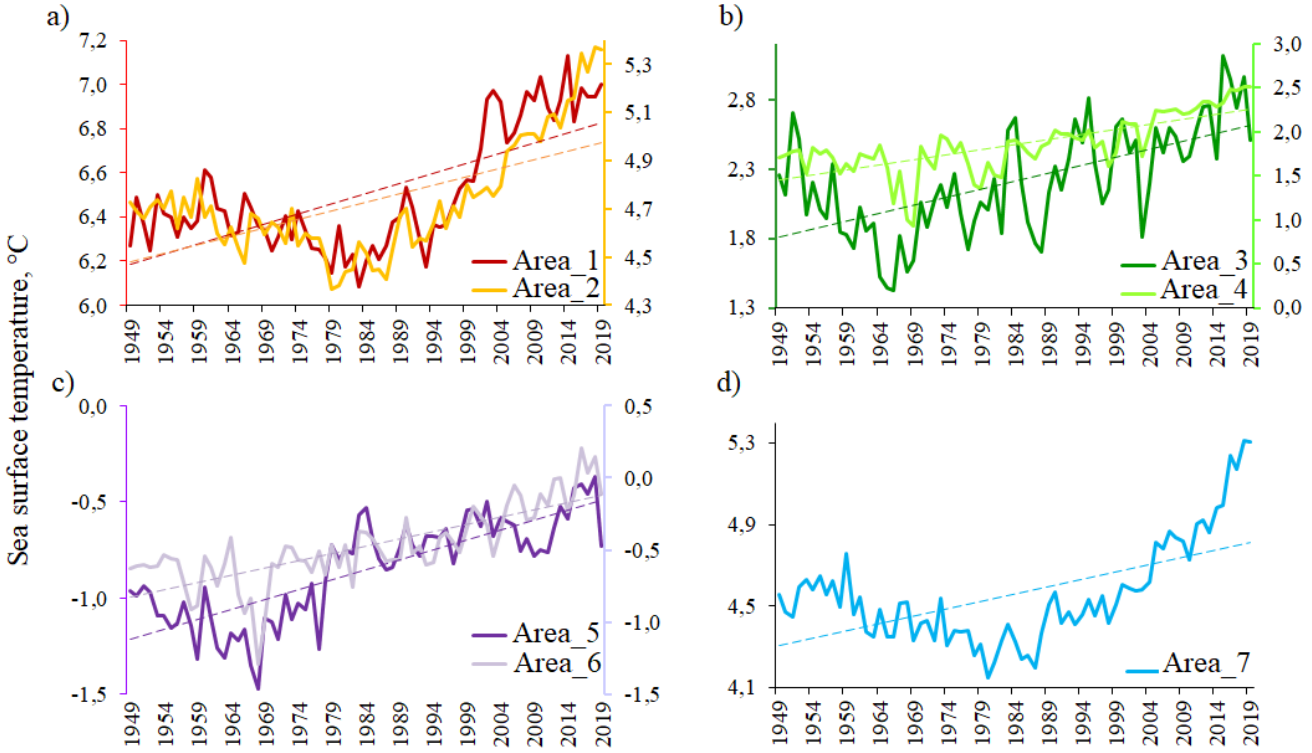


Figure 2.9. Interannual variability of SST in areas of the North European Basin with plotted linear trend lines (dashed lines), for the period 1949–2019.

For all areas, two conditional periods are visually distinguished: a colder one, which tends to decrease in temperature, and a warmer one, which tends to increase in temperature. In districts three through five, the decrease in water temperature occurs until the early 1970s, while in districts one, two, and seven, it occurs in the period 1980–1989. The first, second and seventh regions are the warmest water areas and are subject to the greatest influence of warm Atlantic waters.

It should be noted that for the third, fourth and fifth regions the linear trend until 1985 was significant, negative ($R^2$ was 0,22, 0,39 and 0,60; and the trend value was 0,007°C/year, 0,006°C/year 0,008°C/year, respectively). This indicates a slight, but nonetheless, decrease in TPO. After that, a period of intensive increase in SST begins in 1986-2019. All these three areas are primarily the most sensitive to the intensity of the inflow of warm waters from the North Atlantic (Nikiforov and Shpaikher, 1980; Yashayaev and Seidov, 2015).

*Cyclical fluctuations in ocean surface temperature.*

After removing linear trends from the time series, spectral analysis was performed to highlight the cyclical components (Figure 2.10.). Using the program of the analysis package "Statistica", the Fourier decomposition was performed by the FFT method (Fast Fourier Transform). The following cycles were identified based on the peaks of spectral densities. A 10-year fluctuation is observed in all seas during the summer season and can be associated with an 11-year fluctuation in solar activity (“Schwabe cycle” or “Schwabe-Wolf cycle”). Its length varies from 7 to 17 years. During the winter season, SST cycles range from 8,8 to 14 years. This may also be related to solar activity. There are also periods from 5 to 7 years and a group of lower frequency cycles from 2 to 4 years. Such fluctuations are presumably caused by the influence of atmospheric circulation variability and the interaction of the ocean and the atmosphere (Chen et al., 2013).

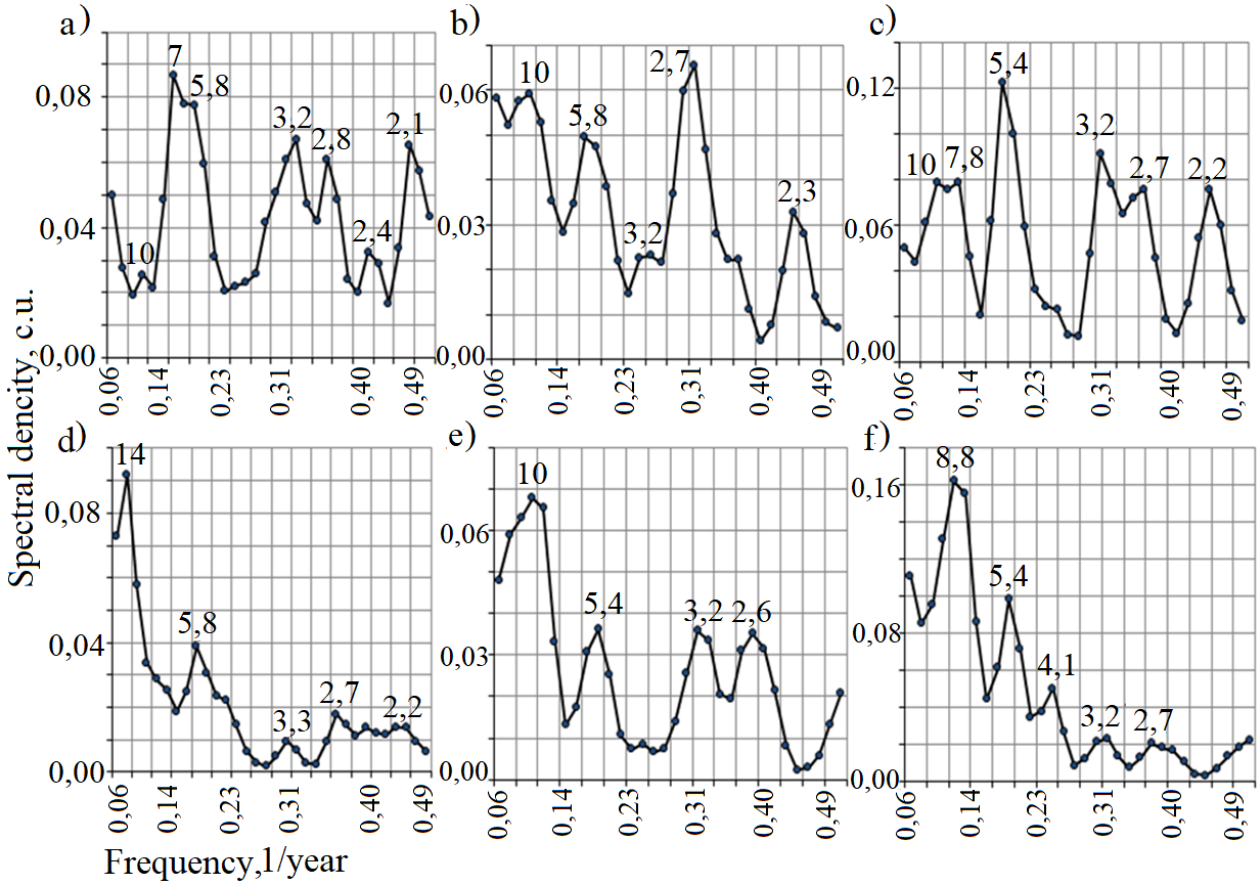


Figure 2.10. Spectral densities of SST fluctuations in the Norwegian (a – summer, d – winter), Barents (b – summer, e – winter) and Greenland (c – summer, f – winter) seas for the period 1949-2019 in the summer and winter seasons. The numbers on the graphs in points indicate the periods of cyclical fluctuations in years.

Variations in these low frequency fluctuations can also be caused by the seasonal variability of SST. Similar cycles of years are distinguished by a number of authors for the surface temperature of the atmosphere. (Minobe, 1997; Alekseev, 2003; Frolov, 2007; Gudkovich et al., 2009; Fyfe et al., 2013)

### 2.2.3 Homogeneous periods of climatic changes in the sea surface temperature

To determine the homogeneous periods, a cluster analysis was performed by constructing tree-like dendrograms using the Ward-Method method for the SST

variability of the seas of the North European basin in the program of the STATISTICA analysis package for the period 1950-2019. The squared Euclidean distances were used as the distance over which the data were combined into clusters. According to the obtained tree-like dendrogram for the SST of each of the seas of the North European basin (Figure 2.11, a, c, f) at a distance level of 5 unit three clusters can be distinguished.

To improve the quality of the results, in addition to constructing dendrograms, to compare the selected groups, clustering was also performed using the K-means method (see Figure 2.11. b, d, g). Euclidean distance was also used as a metric. Due to the fact that three clusters were identified by the dendrogram, three groups were also used in the K-means method when combining. As a result of comparison and refinement of the obtained results, the following periods of years were obtained: the first cluster ($K_1$) - elevated temperatures, the second cluster ($K_2$) - average, the third cluster ($K_3$) - low temperatures. The distribution of average values for each cluster of Greenland Sea SST is shown in Figure 2.11. (b) for the period 1950-2018. Similar studies were carried out for the Barents and Norwegian Seas (see Figure 2.11. d, g).

The first group of years (cluster one) for the Norwegian Sea included the following years: 1952, 1956, 1958, 1962, 1964–1965, 1967–1971, 1973, 1975–1979, 1981–1988, 1993 part of the years is included in the third cluster, see Figure 2.11 c). The second group included: 1950–1951, 1953–1955, 1957, 1959–1961, 1963, 1966, 1972–1974, 1980, 1989–1992, 1994–2000 (corresponding to the second cluster of the dendrogram). The third cluster has no "outliers" and is a continuous group of years 2001-2019 when SST has the highest values (corresponds to the first cluster of the dendrogram).

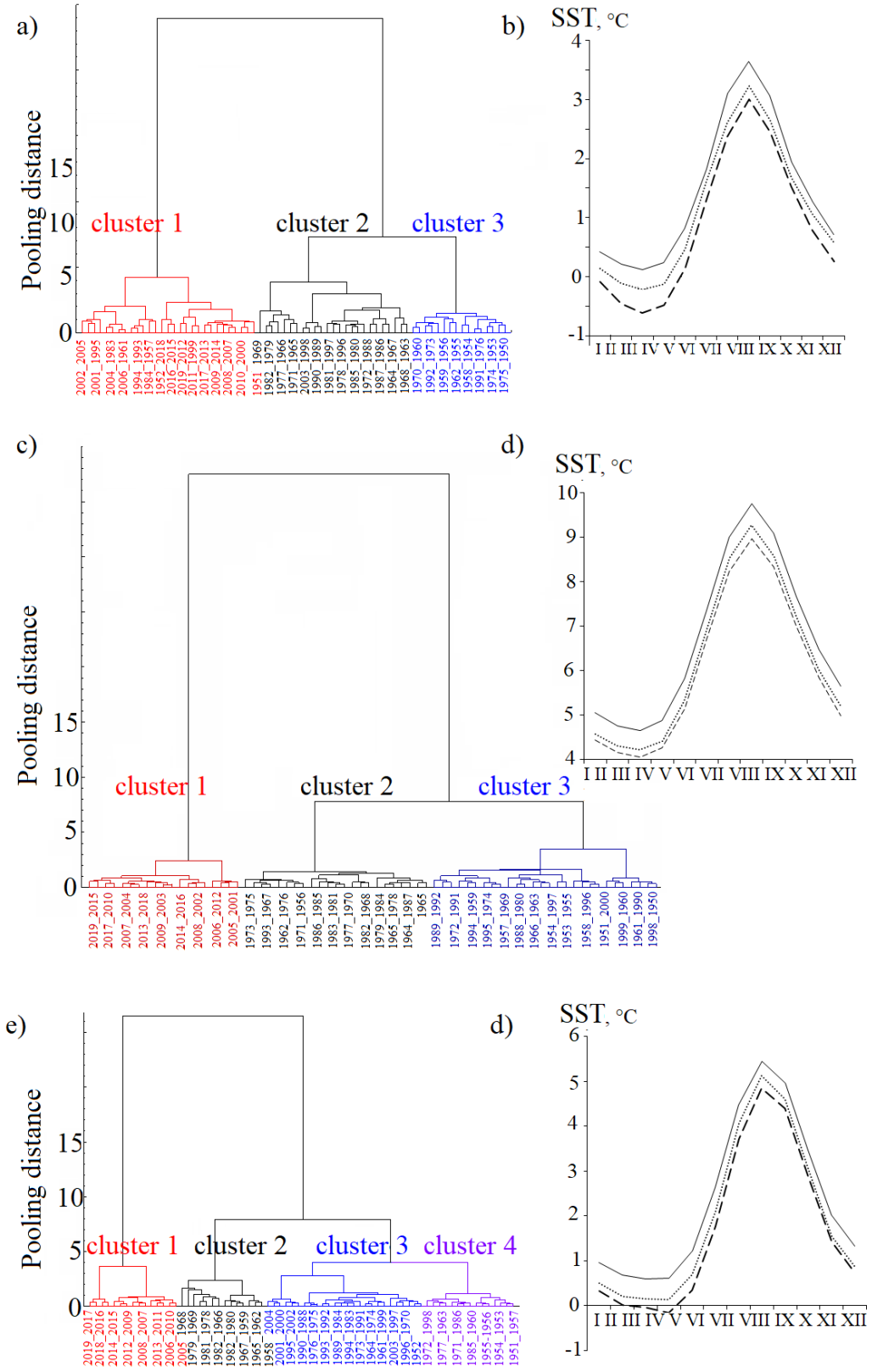


Figure 2.11. Dendrograms and mean values of clusters (cluster 1 – dotted line, cluster 2 – dotted line, cluster 3 – solid line) for SST variability in the Greenland (a, b), Norwegian (c, d) and Barents (f, g) seas for the period 1950– 2019 years.

According to the average values of the clusters (Figure 2.11. d), it can be seen that the third group differs most from the first and second. Even in the autumn-spring seasons, when the difference between the first and second clusters is minimal. The smallest difference between the average values of the first and second clusters falls from January to April and ranges from 0,13°C to 0,16°C (Table 2.3), while the difference between the third cluster and the first and second during this period ranges from 0,44°C to 0,62°C. This suggests that the selected period has very significant differences and correlates with the current period of global climate change. The largest distance between clusters falls on the summer and winter seasons and ranges from 0,30°C (between $K_1$ and $K_2$) to 0,77°C (between $K_3$ and $K_2$).

Table 2.3. Groups of years of similar seasonal SST cycles of three clusters for the Barents, Greenland and Norwegian seas.

| Cluster | Barents Sea | Greenland Sea | Norwegian Sea |
|---|---|---|---|
| Cluster 1 | 1953, 1958-1959, 1962, 1965-1969, 1978-1982,1987. | 1963-1969, 1971, 1977-1982, 1987-1988, 1997. | 1952, 1956, 1958, 1962, 1964-1965, 1967-1971, 1973, 1975-1979, 1981-1988, 1993. |
| Cluster 2 | 1950-1952, 1954-1957, 1960-1961, 1963-1964, 1970-1977, 1983-1986, 1988-2004. | 1950, 1952-1956, 1958-1962, 1970, 1972-1976, 1983-1985, 1989-1993, 1996, 1998, 2003-2004. | 1950-1951, 1953-1955, 1957, 1959-1961, 1963, 1966, 1972-1974, 1980, 1989-1992, 1994-2000. |
| Cluster 3 | 2005-2019. | 1951, 1957, 1994-1995, 1999-2002, 2005-2019. | 2001-2019. |

Let us now consider the selected groups of years for the Greenland Sea (see Table 2.3). The first cluster included: 1963–1969, 1971, 1977–1982, 1987–1988, 1997 (corresponding to cluster 3 of the dendrogram); second cluster: 1950, 1952–1956, 1958–1962, 1970, 1972–1976, 1983–1985, 1989–1993, 1996, 1998, 2003–2004; third cluster: 1951, 1957, 1994–1995, 1999–2002, 2005–2019. Interestingly, in the Greenland Sea, the period of the highest sea surface temperatures (the maximum average value of the third cluster was 3,63°C) included years not only of the last two decades, but also a couple of years in the 1950s. These two years characterize the increased values of SST for the winter season. At the same time, the difference between the average values of the clusters is distributed evenly from 0,16°C to 0,49°C during all months of the year.

In the Barents Sea, the distribution of years according to the dendrogram looks somewhat different than when using the K-means method. If we divide into groups of years according to the union distance of 5, then three clusters will be identified, and if we shift slightly lower to a distance of 4, then four clusters will be identified (see Figure 2.11, e).

To clarify the allocation of the number of clusters, the average values were analyzed when divided into four groups of years. According to the result, it was found that there are no significant differences as such between the third and fourth clusters, the differences in SST are small (less than 0,1°C) and exist only in the winter and summer seasons. In this regard, it was decided to use a combination of three groups of years. The difference between the third cluster and the second is the largest in comparison with other seas. The maximum differences in the average values fall on May-June and amount to 0,54°C, the minimum in August (0,31°C). Which is most likely due to seasonality and different times of the beginning of ice-freeing in the Barets and Greenland Seas.

## Conclusions for Chapter 2

Studies of surface water temperature in the North European Basin made it possible to establish the following: the performed zoning of the North European Basin according to the sea surface temperature as a whole corresponds to the zoning of the seas of the North European Basin by E.G. Nikiforova and A.O. Speicher 1980 (Nikiforov and Speicher, 1980) depending on the vertical structure of water masses and can be used in the analysis of long–term variability of SST; the sea surface temperature has a pronounced latitudinal distribution, which is disturbed only in the form of a tongue of cold waters in the Greenland Sea, due to the removal of ice and water from the Central Arctic Basin; in all selected areas, in general, there is an increase of the sea surface temperature; features of the hydrological structure of the regions are primarily due to the system of surface currents and the presence / absence of ice (which in turn is also associated with the advection of warm and cold waters); based on the results of spectral and cluster analyzes, it can be assumed that in connection with the identified homogeneous periods, when analyzing contingency, it is worth paying special attention to various hydrometeorological and astrogeophysical factors with cyclic fluctuations of 9-14, 10 and 5-7 years, as well as when developing equations using multiple linear regression to include among the predictors factors that have similar significant periods of fluctuations.

# CHAPTER 3 THE STRUCTURE OF THE VARIABILITY ICE COVERAGE OF THE SEAS NORTH EUROPEAN BASIN

## 3.1 Ice coverage of the North European Basin's seas

The term “ice coverage” refers to the proportion of the area occupied by ice of any concentration in relation to the total area of the sea (World Meteorological Organization, 2017). In addition, to characterize the ice cover, the size of the sea area occupied by ice is also used.

The location of the seas of the North European Basin at high latitudes, in the polar region, largely forms a significant distribution of ice coverage on the territory of these seas. The Norwegian Sea (which is also part of the North European Basin), due to the inflow of large volumes of warm water from the North Atlantic, never freezes. Whereas the ice coverage of the Greenland and Barents Seas as a percentage of the North European Basin is comparable - about 30% for the sea (see Table 1.1.). A distinctive feature is that in winter the Greenland and Barents Seas are not completely covered with ice under the influence of the influx of warm Atlantic waters. But in the summer period in recent years, the Barents Sea is completely cleared of ice, while the Greenland Sea is still not completely freed (Dobrovolsky and Zalogin, 1992; Britannica et al., 2013; Brockhaus, 2013; Vize, 1948).

The largest seasonal and long-term changes in sea ice extent are observed in the North European Basin (Fig. 3.1), and in this area sea ice is especially sensitive to climatic changes (Zakharov, 1981, Zubakin, 1987).

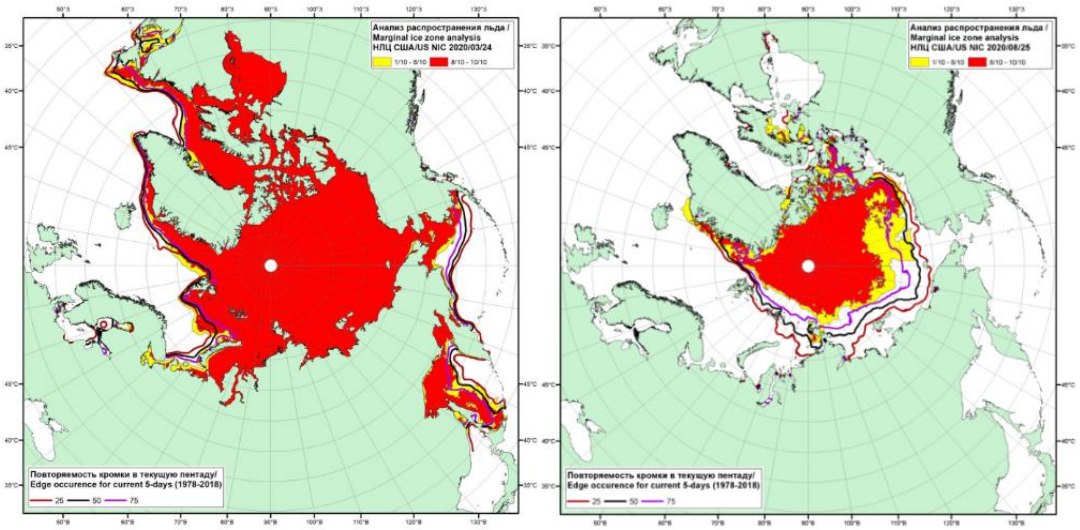


Figure 3.1. The position of the ice edge and zones of rarefied (<8/10) and compacted (≥8/10) ice of the Arctic Ocean (in color) for March 24, 2020 (a) and August 25, 2020 (b) based on the ice analysis of the US National Ice Center and edge (line) frequency for March 21–25 (a) and August 21–25 (b) for the period 1979–2018 according to SSMR-SSM/I-SSMIS observations (algorithm NASATEAM).

The Barents and Greenland Seas play an important role in the processes of interaction between the North European Basin and the Arctic Basin, being an important part of the Arctic climate system. Through their area, the warm and saline waters of the North Atlantic Current enter the Arctic seas and the Arctic Basin, and in the opposite direction, the East Greenland Current transports sea ice and cold and relatively desalinated waters to the North Atlantic (Nikiforov and Speicher 1980; Mironov, 2004).

This feature is one of the most important climatic factors that form the thermal and, accordingly, the ice regimes of the region (Furevik, 2001; Kayet al., 2011; Safonova, 2017; Glock et al., 2019). Through the Faroe-Shetland Strait there is a constant inflow of warm waters of the North Atlantic, forming the Norwegian Current in the Norwegian Sea. The main branch of which is heading northwest, with many branches heading north. At the same time, the main sweat of the Atlantic water mass comes with the Svalbard current through the Fram Strait into the Arctic basin.

Such an inflow of large layers of warm water masses radically changes not only the entire thermal regime of the basin, but also contributes to the displacement of the ice cover edge to the north and east.

Along with such unique features for the polar region of the thermal regime, in the Greenland Sea throughout the year there are cold surface waters in the form of the East Greenland Current. Cold and desalinated water masses enter through the Fram Strait and carry with them the perennial ice of the Central Arctic Basin. Also, the region is under the strong influence of advection of warm Atlantic air masses (Nikiforov and Speicher 1980; Mironov, 2004).

Thus, the North European Basin is a region of contrasts both in the context of the ice and thermal regimes, and in relation to atmospheric circulation.

### 3.2 Internal structure and inertiality ice coverage

To study the effect of winter and summer ice cover conditions on the ice extent in subsequent months, a cross-correlation analysis was performed between the average area of a couple of months, starting with the highest winter ice cover for each sea. The values of the correlation coefficients are given in Table 3.1. The correlation analysis made it possible to establish the influence of the winter and summer conditions of the ice cover on the ice area in subsequent months. The calculation results (Table 3.1) show that the state of ice coverage in winter couples of months (February-March for the Greenland Sea and April-May for the Barents Sea) has a significant relationship (at a significance level of 0,05) with all months until the end of the current calendar year and the next. In the Greenland Sea, the relationship between winter ice coverage and subsequent seasons decreases until August, after which it increases, reaching a maximum of R = 0,66 for ice coverage in December-January (Table 3.1.). In the Barents Sea, the correlation is somewhat different: the relationship of ice coverage in

April-May first decreases to R = 0,25 for October-November, and then increases to R = 0,58 for ice coverage in February-March of the following year (Table 3.1).

Table 3.1. Correlation coefficients R between changes in ice coverage in winter* and summer** and changes in ice coverage in subsequent pairs of months of the current year, the next year*** and the following year****

| Couples of months | Correlation coefficients | | | |
|---|---|---|---|---|
| | Greenland Sea | | Barents Sea | |
| | February-March | August-September | April-May | August-September |
| February-March | 1 | – | – | – |
| April-May | 0,83±0,12 | – | 1 | – |
| June-July | 0,7±0,12 | – | 0,86 | – |
| August-September | 0,52±0,12 | 1 | 0,58 | 1 |
| October-November | 0,54 | 0,73 | 0,25 | 0,55 |
| December-January | 0,66 | 0,67 | 0,52 | 0,52 |
| February-March (+1 year) | 0,59 | 0,57 | 0,58 | 0,46 |
| April-May (+1 year) | 0,55 | 0,57 | 0,52 | 0,38 |
| June-July (+1 year) | 0,37 | 0,53 | 0,52 | 0,46 |
| August-September (+1 year) | 0,42 | 0,54 | 0,50 | 0,63 |
| October-November (+1 year) | 0,54 | 0,51 | 0,37 | 0,45 |
| December-January (+1 year) | 0,61 | 0,58 | 0,39 | 0,29 |
| February-March (+2 years) | 0,45 | 0,55 | 0,29 | 0,28 |
| April-May (+2 years) | 0,49 | 0,56 | 0,33 | 0,29 |
| June-July (+2 years) | 0,36 | 0,39 | 0,37 | 0,31 |
| August-September (+2 years) | – | – | 0,28 | 0,28 |

*Note.* For all correlation coefficients Student's t-test is ±0.21 at the significance level 0,05; * – February–March (Greenland Sea) and April–May (Barents Sea); ** – August–September (Greenland and Barents Seas); *** – +1 year; **** – +2 years.

The statistical relationship between the state of the ice coverage summer and the ice coverage of subsequent seasons is somewhat different in the Greenland and Barents Seas. The value of the correlation coefficient of the summer ice coverage (August–September) of the Greenland Sea with the ice coverage of subsequent months decreases until June–July of the next year, then slightly increases to R = 0,54 in the period August–September of the next year, and after a decrease reaches a maximum of R = 0,58 in December-January of the following year (see Table 3.1). In the Barents Sea, the value of the correlation coefficient of the summer ice coverage (August-September) with the ice coverage of subsequent months decreases until April-May of the following year, and then reaches a maximum of R = 0,63 in August-September of the following year (see Table 3.1).

Thus, the ice coverage of the seas in the summer season retains its influence on the state of the ice coverage in the summer of the next year, and the influence is somewhat greater than the influence of winter on summer.

The result of the correlation analysis is consistent with the results of the cluster analysis. As noted above, the similarity of intra-annual cycles can persist for an average of 2–3 years. In this case, we can talk about the continuity of the state of the ice coverage within the annual cycle, when the prehistory of the state of the ice coverage, to a certain extent, determines the current phase.

The established empirical regularity is important for understanding the process of formation of the ice regime and can be used in the construction of statistical models for diagnosing and forecasting sea ice coverage.

First of all, the inertia of the variability of the ice coverage area attracts attention. Table 3.2 shows the correlation coefficients of ice coverage for each season in the Barents and Greenland Seas with ice coverage in previous years (with negative time lags of -1, -2 and -3 years). The ice coverage of the winter season of the Greenland Sea is characterized by the maximum values of the coefficients of connection with the state of the ice coverage in previous years and ranges from 0,30 to 0,59, i.e. the inertia of

winter ice processes is quite large and persists for up to three years. The inertia is well manifested both in the winter and spring seasons, while for the autumn season the coefficients with a negative lag of three years turned out to be insignificant.

Table 3.2. Paired Significant Coefficients of the Autocorrelation Function of the Ice Coverage in the Seas of the North European Basin.

*Greenland Sea*

| Season | $W_{-1}$ | $S_{-1}$ | $Sp_{-1}$ | $A_{-1}$ | $W_{-2}$ | $S_{-2}$ | $Sp_{-2}$ | $A_{-2}$ | $W_{-3}$ | $S_{-3}$ | $Sp_{-3}$ | $A_{-3}$ |
|---|---|---|---|---|---|---|---|---|---|---|---|---|
| Winter | 0,59 | 0,57 | 0,63 | 0,58 | 0,44 | 0,55 | 0,49 | 0,37 | 0,30 | 0,29 | 0,35 | – |
| Summer | 0,41 | 0,54 | 0,34 | 0,39 | 0,39 | 0,37 | 0,39 | 0,26 | 0,36 | 0,33 | 0,39 | – |
| Spring | 0,36 | 0,53 | 0,49 | 0,49 | 0,35 | 0,38 | 0,35 | 0,27 | 0,24 | – | 0,36 | – |
| Autumn | 0,54 | 0,50 | 0,56 | 0,45 | 0,34 | 0,26 | 0,34 | 0,24 | 0,33 | – | 0,38 | – |

*Barents Seas*

| Season | $W_{-1}$ | $S_{-1}$ | $Sp_{-1}$ | $A_{-1}$ | $W_{-2}$ | $S_{-2}$ | $Sp_{-2}$ | $A_{-2}$ | $W_{-3}$ | $S_{-3}$ | $Sp_{-3}$ | $A_{-3}$ |
|---|---|---|---|---|---|---|---|---|---|---|---|---|
| Winter | 0,73 | 0,70 | 0,59 | 0,73 | 0,57 | 0,46 | 0,28 | 0,53 | -0,55 | 0,96 | 0,33 | 0,48 |
| Summer | 0,70 | 0,70 | 0,39 | 0,56 | 0,59 | 0,56 | 0,22 | 0,38 | 0,38 | 0,39 | 0,22 | 0,33 |
| Spring | 0,59 | 0,41 | 0,41 | 0,43 | 0,34 | 0,31 | 0,28 | 0,33 | 0,34 | – | – | 0,31 |
| Autumn | 0,73 | 0,56 | 0,43 | 0,68 | 0,51 | 0,37 | 0,23 | 0,48 | 0,46 | 0,32 | 0,30 | 0,46 |

*Note.* W - winter ice coverage (December-April); S - summer ice coverage (July-September); A - ice coverage in autumn (October-November); Sp - ice coverage in spring (May-June); -1, -2, -3 - ahead of the parameter by 1, 2 and 3 years, respectively; the sign denotes insignificant correlation coefficients.

The inertial component of the ice coverage of the Barents Sea exceeds that of the Greenland Sea. The maximum correlation coefficient is 0,73 for the winter season with a one-year lag between winter and autumn ice coverage. Except for spring, significant correlation coefficients remain for all seasons for three years (at a significance level of 0,05). At the same time, the lowest values fall on the spring season. And it ranges from insignificant to 0,43 (between spring and last year's autumn) as much as possible. The highest pair correlation is determined for the winter season and varies from 0,28 (with spring with a lag of 2 years) to 0,73 (with last year's winter and autumn).

For summer, the values are somewhat smaller: from 0,22 (with spring with a lag of two and three years) to 0,70 (with last year's summer). The autumn ice coverage has correlation coefficients slightly lower than for the summer season. The values vary from 0,23 (since last year's spring) to 0,68 (with autumn ice coverage with a one-year lag).

The revealed persistence of ice coverage shows that the previous state of the ice coverage and its area is the most important predictor in the development of equations, both for diagnosis and for forecasting, which was previously demonstrated in a number of works (Mironov, 2004; Fedorov, 2016).

## 3.3 The structure of the interannual variability ice coverage

### 3.3.1 Long-term and cyclic fluctuations ice coverage

The time course of the ice coverage of the Greenland and Barents Seas for the period from 1950 to 2021 for the summer and winter seasons is shown in Figure 3.2. The trend of climatic changes in the ice coverage in both seas is the same: in interannual changes, a negative linear trend of ice coverage is distinguished. This pattern of long-term variability of ice coverage has been noted by other authors for several decades (Walsh and Johnson, 1979; Mysak and Manak, 1989; Parkinson et al., 1999). The magnitude of the linear trend for the Barents Sea in the winter season is -0,37%/year (-3,46·$10^3$ $km^2$/year) and –0,20%/year (-2,82·$10^3$ $km^2$/year) in the summer. For the winter season of the Greenland Sea, the trend value is -0,25%/year -4,25·$10^3$ $km^2$/year) and is comparable in the summer season to m0.21%/year (-2,25·$10^3$ km2/year). At the same time, the linear trend for the Greenland Sea is not statistically significant (at a significance level of 0,05), and the coefficient of determination is 0,12. For the Barents Sea, the linear trend is significant (at a significance level of 0,05), and the coefficient of determination is 0,48.

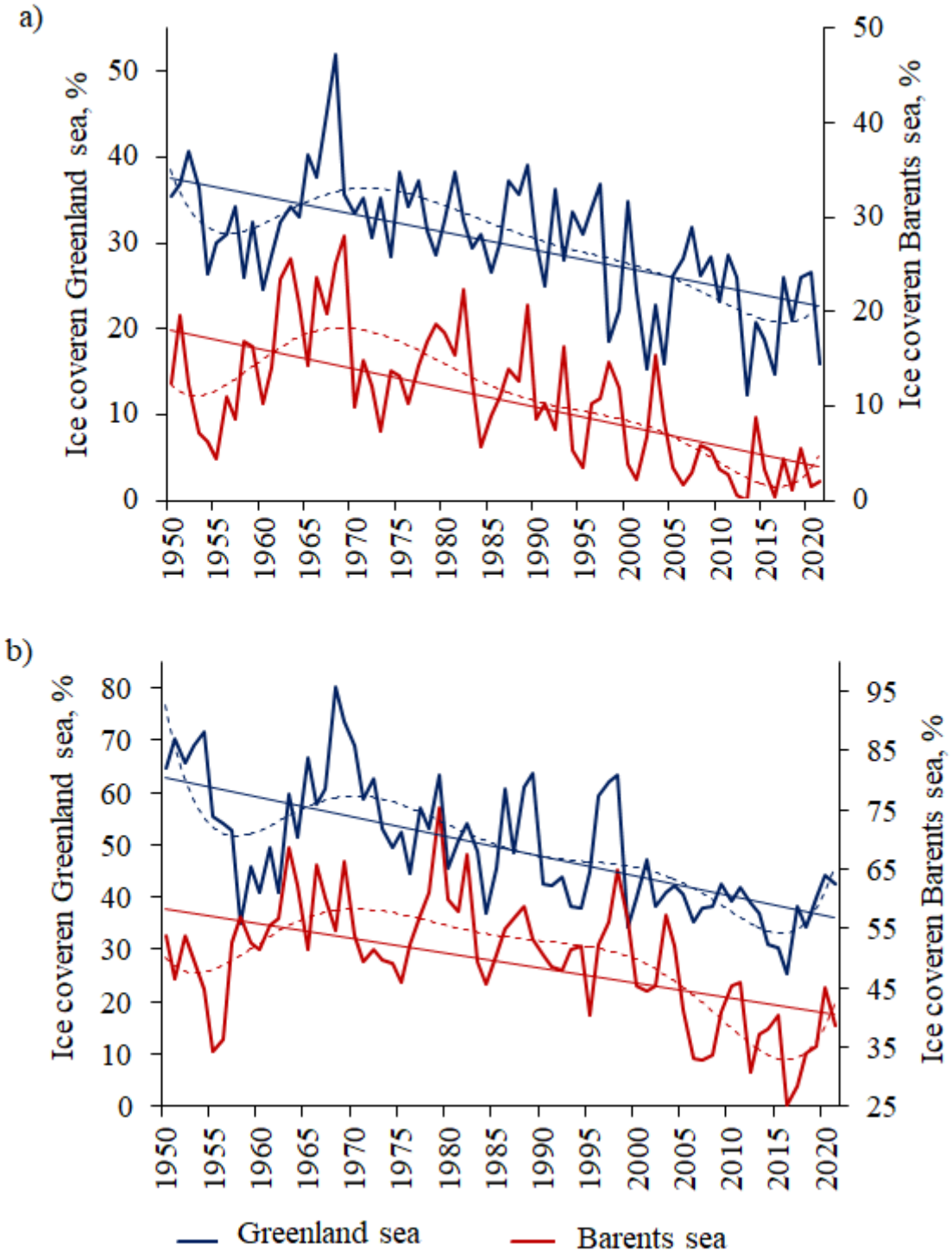


Figure 3.2. Interannual changes in the ice coverage of the Greenland (bold blue line) and the Barents (bold red line) seas in a) summer and b) winter seasons with plotted lines of linear (thin line) and polynomial 6th degree (dashed line) trends for the period 1950–2021 years.

The decrease in the ice coverage of the Greenland Sea in the winter season is somewhat more intense than in the summer. A similar situation is observed in the Barents Sea. The magnitude of the trend in the winter season is somewhat larger than in the summer. This is probably due to the fact that the intensity of the inflow of warm Atlantic waters increases either in the Barents Sea and weakens, respectively, in the Greenland Sea. Or the situation is reversed. At the same time, the flow of warm waters of Atlantic origin enters the Barents Sea more than the Greenland Sea. In recent years, many authors have confirmed the phenomenon of "atlantification" in the Barents Sea (Aksenov and Ivanov, 2018; Barton et al., 2018; Asbjørnsen et al., 2020), in which cold Arctic waters are displaced by Atlantic waters due to their more active inflow.

The polynomial trend of the 6th degree is statistically significant for both seas. Trend determination coefficient: for the Greenland Sea 0,55 and 0,48 in winter and summer seasons; for the Barents Sea 0,54 and 0,55 in winter and summer seasons.

In the study of interannual variability of ice coverage, as well as in the study of SST (Chapter 2), 1985 was chosen as the boundary year. Indeed, the linear trends for the ice coverage of the Greenland and Barents Seas over the period 1950–1985 (Table 3.3.) are not statistically significant (at a significance level of 0,05) for both the summer and winter seasons. The trend value varies from –0,32%/year ($–3.59 \cdot 10^3$ km$^2$/year; winter season, Greenland Sea) to 0,26%/year ($3,29 \cdot 10^3$ km$^2$/year; winter season of the Barents seas). And although the magnitude of the trend in the winter season in the Barents Sea is positive, the trend is not statistically significant (at a significance level of 0,05). This means that the positive trend towards an increase in the ice coverage in 1950–1985 is insignificant.

Table 3.3. Characteristics of linear trends for the ice coverage of the Greenland and Barents Seas for the winter and summer seasons.

| Period 1950–2021 years | Summer season (July-September) | | Winter season (December-April) | |
|---|---|---|---|---|
| | BS | GS | BS | GS |
| Ice coverage difference, $\cdot 10^3$ km$^2$/year | 169 | 124 | 290 | 374 |
| Trend magnitude, $\cdot 10^3$ km$^2$/year | –3,40 | –2,21 | –2,68 | –4,40 |
| $R^2$, unit | **0,24** | **0,31** | **0,30** | **0,41** |
| Characteristics of trends for selected periods | | | | |
| Ice coverage difference for periods | 99,22 | 79,71 | 118,53 | 145,74 |
| Trend value (1950–1985), $\cdot 10^3$ km$^2$/year | 0,72 | –0,40 | 3,29 | –3,59 |
| Trend value (1986–2021), $\cdot 10^3$ km$^2$/year | –5,75 | –4,01 | –10,70 | –6,51 |
| $R^2$ (1950–1985), unit | 0,01 | 0,00 | 0,09 | 0,08 |
| $R^2$ (1986–2021), unit | **0,55** | **0,28** | **0,57** | **0,37** |
| Index trend (1950–1985), unit | 25 | –7 | 31 | –38 |
| Index trend (1986–2021), unit | –193 | –44 | –60 | –45 |

*Note.* GS – Greenland Sea, BS – Barents Sea; $R^2$ trend determination coefficient, significant trends are in bold, at a significance level of 0,05.

For the period 1986–2021, the trend determination coefficient is greater for the Barents Sea for the winter (0,57) summer (0,55) seasons than for the Greenland Sea (in winter $R^2 = 0,37$; summer $R^2 = 0,28$).

For trend analysis, the trend index was calculated (Vainovsky and Malinin, 2019), which is a convenient characteristic for comparison, representing a dimensionless value (see Chapter 2, paragraph 2.2.2). The trend index for the period 1950–1985 for both seas does not exceed 38 unit by absolute value. Whereas for the period for 1986-2020, the lowest values $I_{tr}$ correspond to winter 45 unit and summer 44 unit seasons of the Greenland Sea modulo. In the Barents Sea $I_{tr}$ is 60 c.u. for winter and 193 unit for summer. This indicates a much stronger increase in the intensity of the decrease in the area of ice in the Barents Sea.

At the same time, one should not forget that the variability of the ice coverage in the Greenland Sea is significantly affected by the removal of old ice from the Arctic Basin through the Fram Strait. Therefore, these comparative estimates between the seas can be considered relative.

The polycyclic nature of interannual changes in the ice acoverage in the Arctic seas is indicated in (Frolov et al., 2007). We have performed a spectral analysis of the winter and summer ice coverage of the Greenland and Barents Seas for the period 1950–2021. With a series length of 70 years, the statistically significant values of the periods are in the range of 2–23 years. Figure 3.3 shows plots of spectral density in arbitrary units as a function of oscillation frequency (1/year) for both seas in summer (July-September) and winter (December-April) seasons. For clarity, on the peaks of the spectral density, the periods of cyclicity in years are indicated by numbers.

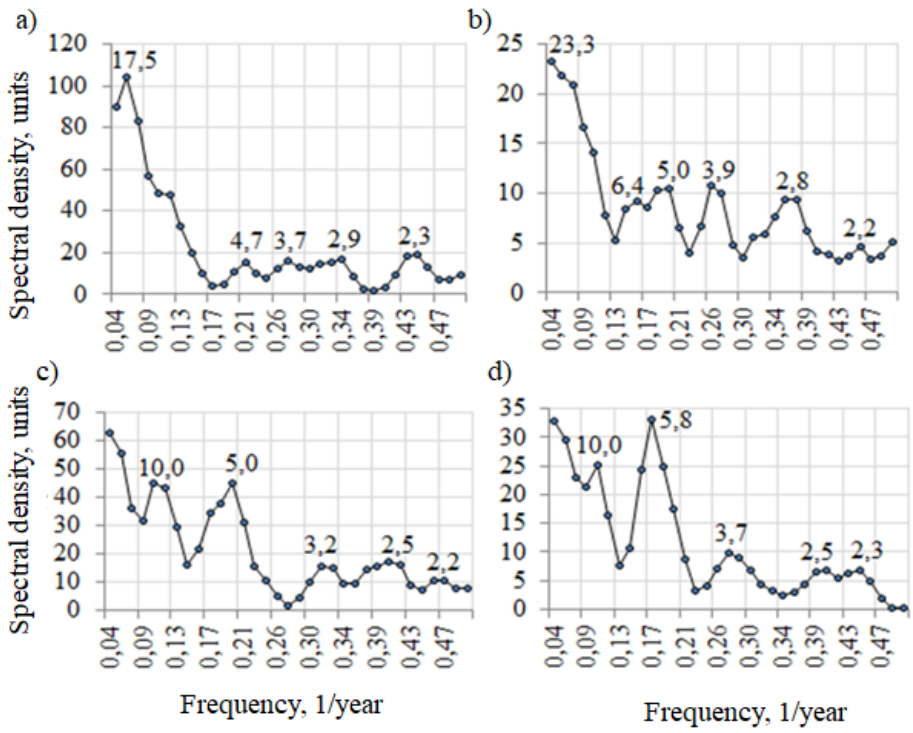


Figure 3.3. Spectral densities of ice coverage fluctuations in the Greenland (a – winter, b – summer seasons) and Barents (c – winter, d – summer seasons) seas for 1950–2021. The numbers on the graphs in points indicate the periods of cyclical fluctuations in years.

Cyclic fluctuations in the high-frequency part of the spectrum with periods less than 3 years are caused, according to the authors of the work (Frolov et al., 2007), by the influence of atmospheric circulation and the interaction of the ocean and atmosphere. This part of the spectrum of the Greenland Sea differs from the similar part of the spectrum of the Barents Sea. The spectra also change from season to season, which can be explained by the seasonal course of meteorological processes and the intra-annual change in the interaction between the atmosphere and the ocean in the presence of ice coverage in this region.

In the low-frequency part of the spectrum of oscillations in both seas, cyclic oscillations of 23 years, 10 years, and 5-6 years are distinguished. Both in the Greenland and the Barents Seas, the spectral density of these oscillations differs from the spectral density of these oscillations from each other. But also the low-frequency spectrum in the Greenland Sea during the summer period is significantly different from the spectrum of the winter season. The spectral density of the noted fluctuations in the Barents Sea in summer is close to that in winter. However, despite these differences, it can be assumed that cyclic fluctuations of 23, 10, and 5-6 years are induced by some global causes common to both seas.

According to many authors (see the review in the monograph (Frolov et al., 2007)), long-term fluctuations in ice coverage depend not only on hydrometeorological processes, but also on astrogeophysical factors. As an argument, the coincidence of cyclic fluctuations in ice coverage and cyclic variations in geophysical and astronomical indices is given. This concept was embodied in the generalizing work of I.V. Maksimov (Maksimov, 1970), who proposed a component-harmonic method for calculating and predicting ice coverage, taking into account the solar-conditioned 11-year cycle, the 6-7-year cycle of the Earth's pole position fluctuation, and the 19-year cycle associated with the action of the long-term lunar declination tide in the ocean. B.A. Sleptsov-Shevlevich and A.M. Bayarinov (Sleptsov-Shevlevich and Bayarinov, 2002) focused on the possibly underestimated role of the Earth's rotation rate in long-term changes in the ocean level and sea ice coverage. I.E. Frolov et al. (Frolov et al., 2007) believe that low-frequency fluctuations in many hydrometeorological characteristics, including sea ice

coverage, are due to a 50–60-year cyclical change in the distance between the Earth and the Sun due to the dissymmetry of the solar system. Since the total solar radiation flux reaching the Earth's surface is inversely proportional to the square of the distance to the Sun, as a result of the dissymmetry effect, a 50–60-year fluctuation in the total solar radiation inflow is formed, which is reflected in changes in the state of the atmosphere and ocean (Medvedev et al., 2018). The relationship with astrogeophysical parameters will be discussed in more detail in the next chapter.

Based on the obtained peaks of the spectral density of the presented Fourier series expansion (the so-called fast transformation), the harmonics with the largest amplitude were selected, and a harmonic analysis was performed. Characteristics were calculated for each harmonic and significance was checked. The table (Table 3.4) presents only significant harmonics (at a significance level of 0,05).

Table 3.4. Characteristics of the periods of cyclical low-frequency fluctuations in the ice coverage of the seas of the North European Basin.

| | Greenland Sea | | | | Barents Sea | | |
|---|---|---|---|---|---|---|---|
| | Winter | Summer | | | Winter | Summer | |
| Period, years | 17,5 | 23,3 | 6,4 | 5,0 | 10,0 | 10,0 | 5,8 |
| Amplitude, $\cdot 10^3 km^2$ | 63,3 | 32,5 | 27,5 | 66,4 | 60,8 | 33,3 | 44,5 |
| Phase, radians | 4,15 | 3,92 | 4,26 | 1,87 | 3,75 | 3,28 | 2,44 |
| Contribution, % | 10,1 | 7,9 | 5,6 | 32,9 | 8,8 | 5,5 | 9,8 |

For the Greenland Sea for the summer season, the largest contribution of 32,9% is made by fluctuations with a period of 5 years. 5-year harmonics correspond to amplitude in $66{,}4 \cdot 10^3 km^2$ and phase 1,87 radians. Also, for the summer season of the Greenland Sea, harmonic oscillations with periods 23,0 years and 6,4 years. For them, the oscillation amplitude was $32{,}5 \cdot 10^3 km^2$ and $27{,}5 \cdot 10^3 km^2$ and the contribution was 7,9% and 5,6% respectively. For the summer season of the Barents Sea, several

significant harmonics are also distinguished. With periods of 10 years and 5,8 years, the contribution of each of which was 5,5% and 9,8%. Which correspond to the following characteristics: amplitude $33{,}3 \cdot 10^3 km^2$ and $44{,}5 \cdot 10^3 km^2$ and phase 3,28 radians and 2,44 radians. It should be noted that for the winter season, a significant harmonic component is allocated with only one period for each series. This is 17,5 years for the Greenland Sea and 10 years for the Barents Sea with contributions of 10,1% and 8,8%. Which correspond to the oscillation amplitudes in $63{,}3 \cdot 10^3 km^2$ and $60{,}8 \cdot 10^3 km^2$.

According to the results of harmonic analysis, it can be assumed that due to the significant contribution of some harmonics to the total dispersion of the series, when analyzing contingency, it is worth paying special attention to various hydrometeorological and astrogeophysical factors with cyclic fluctuations at 23, 17–18.10 and 5–6 years . And also when developing equations using multiple linear regression, include significant harmonics in the number of predictors.

### 3.3.2 Homogeneous periods of seasonal (intra-annual) changes ice coverage

Despite the large intra-annual variability of ice coverage, it is possible to distinguish classes (clusters) of similar seasonal cycles. Two methods were used for their classification: Ward-Method and K-means. The squares of Euclidean distances were chosen as a closeness criterion when using the K-means method (Belov et al., 2008). Data on the variability of ice coverage in the seas of the North European Basin were studied for 1950–2021 (for the Greenland Sea) and for the period 1929–2021 (for the Barents Sea). As a result, using the Statistica program, tree-like dendrograms were constructed for the ice coverage of the Greenland and Barents Seas (Figure 3.4. a, c).

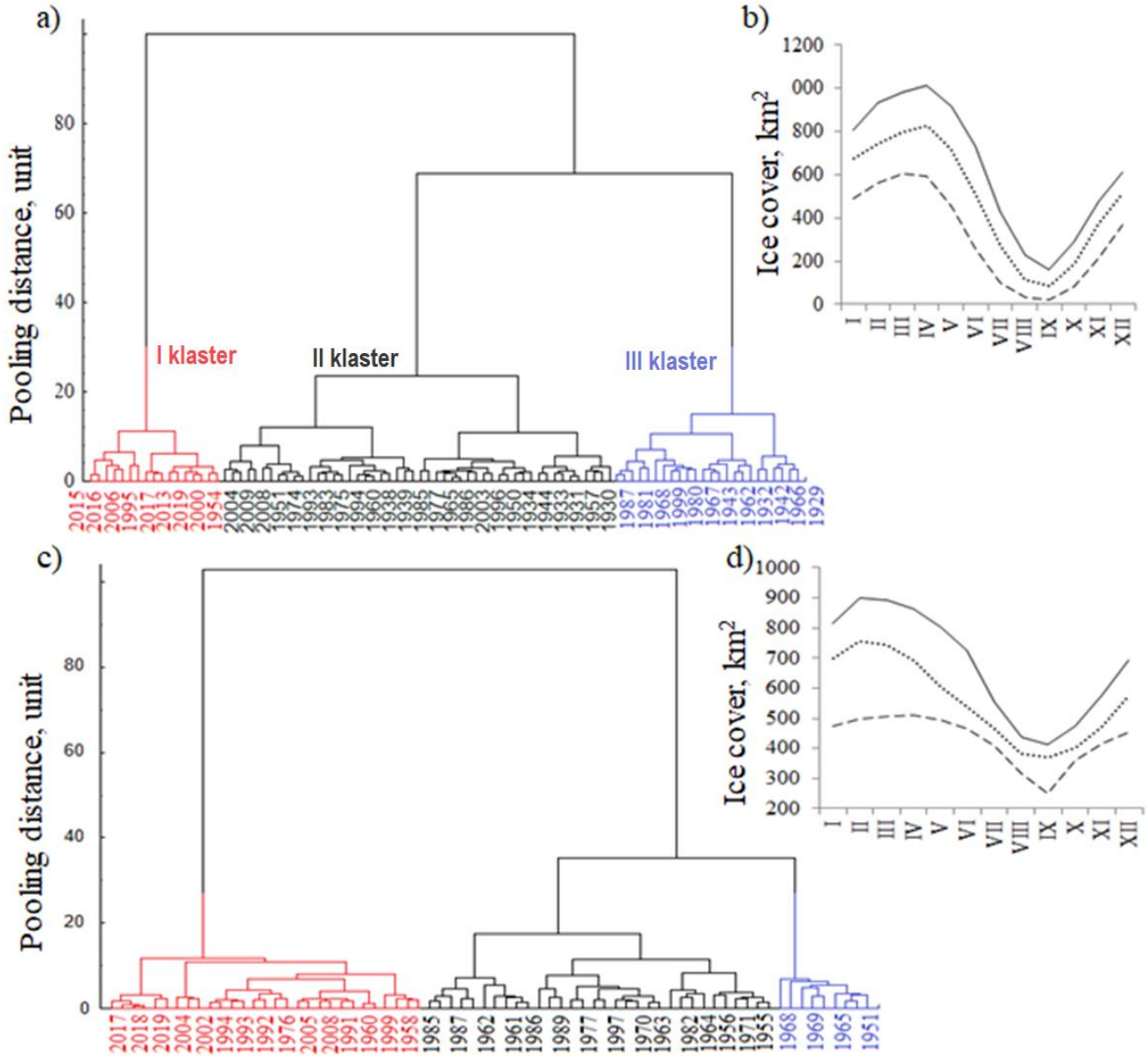


Figure 3.4. Dendrograms and average values of clusters (cluster 1 – dotted line, cluster 2 – dotted line, cluster 3 – solid line) for the variability of the ice cover of the Barents (a, b) and Greenland (c, d) seas for the periods 1929–2020 and 1950–2020, respectively.

To refine the chosen classification, the K-means method was also used. As a result, graphs of average values for selected groups of years were constructed (see Fig. 2.5. b, d). For the Greenland Sea at the level of merging distance 40 units 3 clusters can be distinguished (Figure 3.4. a). Similarly, for the Barents Sea at the level of the pooling distance of 20 units you can also select 3 clusters (Figure 3.4. c). In this case, the second cluster will combine the largest number of years. As a result, 3 clusters were identified

for both the Greenland and the Barents Seas, which included groups of years of similar seasonal cycles, presented in Table 3.4.

Table 3.4. Groups of years of similar seasonal cycles of three clusters for the Barents and Greenland Seas.

| Cluster | Barents Seas | Greenland Seas |
|---|---|---|
| Cluster 1 | 1929–1930; 1932; 1941–1943; 1958; 1962–1964; 1966–1969; 1978–1982; 1987; 1998; | 1950–1954, 1965, 1967–1969; |
| Cluster 2 | 1928; 1931; 1933–1940; 1944–1949; 1950–1953; 1957; 1959–1961; 1965; 1970–1977; 1983; 1985–1986; 1988–1994; 1996–1997; 1999; 2002–2004; | 1955–1957, 1961, 1963–1964, 1966, 1970–1973, 1975, 1977–1982, 1986–1989, 1996–1998; |
| Cluster 3 | 1954–1956; 1984; 1995; 2000–2001; 2005–2021. | 1958–1960, 1962, 1974, 1976, 1983–1985, 1990–1995, 1999–2021. |

The first cluster $K_1$ included years with the largest ice cover in both winter and summer periods. The second cluster $K_2$ united the years of average ice cover, and the third cluster $K_3$ included years with the lowest ice cover of the Greenland and Barents Seas. From the analysis of the years included in the $K_1$–$K_3$ clusters for both water areas, it follows that the similarity of seasonal cycles against the background of low and high ice coverage persists from one season to 6 years. Moreover, for the Greenland Sea, the established regularity is valid for all identified clusters, and for the Barents Sea, the regularity is valid for periods of high ice coverage. This pattern is valid until the period of warming in recent years with low ice coverage: 17 years in the Barents and 23 years in the Greenland Seas. Against the background of average ice coverage in the Barents Sea, the similarity of cycles can last up to 8 years, in the Greenland Sea - up to 6 years.

For the group of years of the first and second clusters, the maximum development of the ice coverage occurred asynchronously: in the Greenland Sea on average in February, and in the Barents Sea in April. The minimum ice coverage on average for both water areas was observed in September. Until 1969 in the Greenland Sea and until 1980 in the Barents Sea, seasonal cycles were formed against the background of high and medium ice coverage. In the period from 1969 to 1998 (Greenland Sea) and from 1981 to 1994 (for the Barents Sea), seasonal cycles developed against the background of average ice coverage in both areas. Since 1999 in the Greenland Sea and since 1995 in the Barents Sea, seasonal cycles have proceeded against the backdrop of a low sea ice coverage. Obviously, there is a general similarity of the selected periods of groups of years with some delay for the Barents Sea relative to the Greenland Sea.

## Conclusions for Chapter 3

Studies on the structure of the long-term variability of ice coverage in the seas of the North European Basin made it possible to establish the following: in all seas, in general, there is a decrease in the ice coverage over the period under consideration, and the decrease in ice coverage in the summer season is more intense both in the Barents and Greenland seas; the system of currents is one of the dominant factors influencing the variability of ice coverage; according to the results of spectral and cluster analyses, it can be assumed that in connection with the identified homogeneous periods, when analyzing contingency, it is worth paying special attention to various hydrometeorological and astrogeophysical factors with cyclic fluctuations of 17, 8–12, 5–7 years, as well as at the development of equations using multiple linear regression to include among the predictors factors that have similar significant periods of fluctuations.

# CHAPTER 4 STATISTICAL MODELS OF LONG-TERM CHANGES OF THE ICE COVERAGE AND SEA SURFACE TEMPERATURE IN THE SEAS OF THE NORTH EUROPEAN BASIN'S

## 4.1 The interaction of long-term fluctuations of the ice coverage and sea surface temperature with hydrometeorological and astrogeophysical parameters

### 4.1.1 The connection of ice coverage and sea surface temperature with hydrometeorological characteristics

*Ice Coverage North European Basin*

In (Gudkovich et al., 2005), a reasonable assumption was made that the high-frequency part in changes in ice coverage is formed mainly as a result of the impact and interaction of the ice coverage with hydrometeorological processes. Other works also emphasize the importance of interaction with the atmospheric circulation of the Atlantic sector (Mikhailova et al. 2021; Sizov et al. 2022).

The character of ten-day changes in the ice coverage of the seas is shown in Figure 4.1, which shows anomalies in the ice coverage of the seas relative to the trend for the period 1950–2019, averaged over decades for the winter and summer seasons.

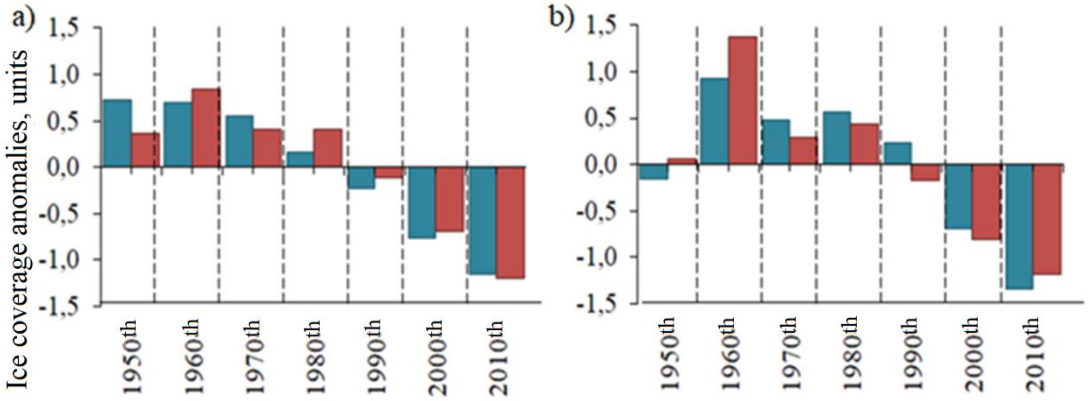


Figure 4.1. Ice coverage anomalies in the Greenland (a) and Barents (b) seas for the winter (blue column) and summer (red column) seasons relative to the average for the period 1950–2019, averaged over 10 years.

The peaks of a significant decrease in ice coverage occur in the 1950s and 2000–2010s, and a period of a significant increase in ice coveragee is noted in the 60s–80s of the last century and a somewhat smaller increase in the 1990s. The sign of ice coverage anomalies in the seas mostly coincided. But in the winter period in the 1950$^{th}$ and 1990$^{th}$, the signs of ice coverage anomalies were opposite. The negative sign of the ice coverage anomaly in the Barents Sea during the winter season in the 1950$^{th}$ can be associated with the influence of the North Atlantic (this period is marked by high sea surface temperature anomalies), as well as increased ice drift from the Central Arctic Basin (Gudkovich, 1997). It follows from the analysis that the predominant conjugat ion of ten-day changes in the ice coverage of the Greenland and Barents Seas is occasionally interrupted by oppositional changes.

To determine the role of hydrometeorological factors in the formation of climatic stages of ice coverage, we constructed histograms of hydrometeorological indices averaged over periods of climatic stages (Figure 4.2).

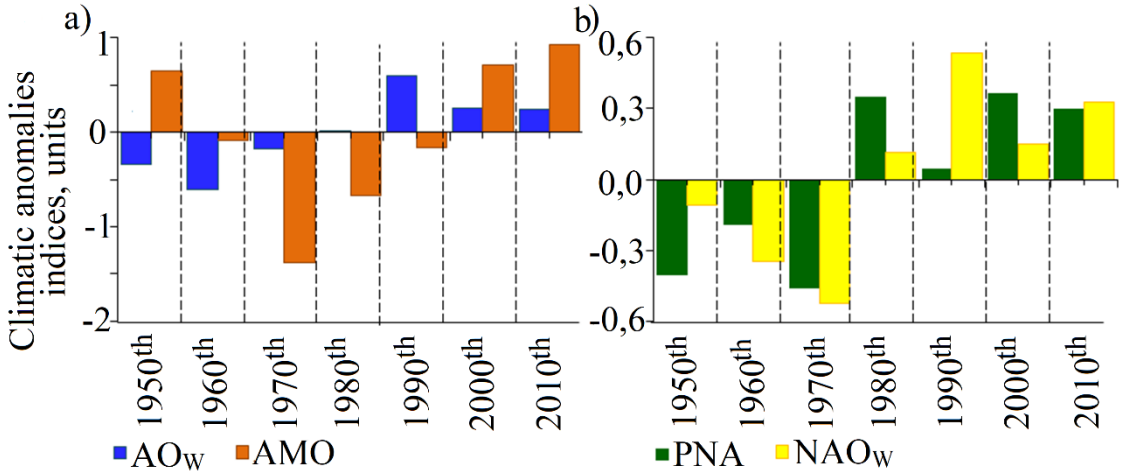


Figure 4.2. Average values of global climate indices for the period 1950–2019, averaged over 10 years.

*Note.* Index designations: Arctic Oscillation $AO_W$ (for winter, blue), Atlantic Multi-Decade Oscillation AMO (for year, orange), Pacific North American Oscillation PNA (for year, green), North Atlantic Oscillation $NAO_W$ (winter, yellow).

As can be seen from Figure 4.2, during the ice coverage period (2003-2019, see Chapter 3, paragraph 3.3.2), climate indices (Arctic Winter AO Oscillation, AMO Atlantic Multi-Decade Oscillation, PNA Pacific North American Oscillation and NAO Winter North Atlantic Oscillation) are on average in a positive phase. The characteristics of the atmospheric circulation indices AO and NAO in the winter season are considered due to the fact that the intensity of atmospheric processes in the near-Atlantic Arctic is maximally manifested in March (Nesterov, 2013), which corresponds to the winter season in the Greenland and Barents Seas. Such baric conditions lead to increased advection of warm Atlantic waters, both into the Barents Sea and into the Greenland Sea. Moreover, there is an increase in the subtropical pressure maximum and a deepening of the Icelandic minimum, there are zones of large gradients between these atmospheric formations and, accordingly, the frequency and strength of winds that carry warm and humid air from the Atlantic to the western Arctic increase. The anticyclonic activity of subtropical origin over Europe is intensifying. With a positive phase of PNA, there is a decrease in pressure over the Kara Sea and the Laptev Sea, and its increase over the Canadian Archipelago, as well as a weakening of the zonal component and an increase in meridional transport, and an increase in anticyclonic activity. An increase in the duration of these processes leads to a significant and long-term decrease in ice coverage.

During periods of increasing ice coverage (1950–1954, 1964–1969, 1976–1981, see Chapter 3, paragraph 3.3.2), either negative or weakly positive values of the AMO index occur. The inflow of warm Atlantic waters during these periods was weakened. The deep negative phase of the AO and NAO indices creates areas of increased pressure in the central Arctic region, which prevents the penetration of warm and humid air from the North Atlantic, carries cold air masses from the northern part of the Pacific sector and causes abnormally cold air temperatures, which leads to a sharp increase in ice. The studies of foreign authors (Sorteber and Kvingedal, 2006; Zhang, 2008; Levitus, 2009b)

also emphasize the importance of air temperature anomalies, large-scale atmospheric circulation, and cyclonic activity. The identified factors are a very important aspect in understanding the formation of the ice regime in the Barents and Greenland Seas and the possibility of forecasting.

*Sea surface temperature of the seas of the North European Basin*

A similar analysis of the anomalies normalized by standard deviation was also carried out for the sea surface temperature (Figure 4.3).

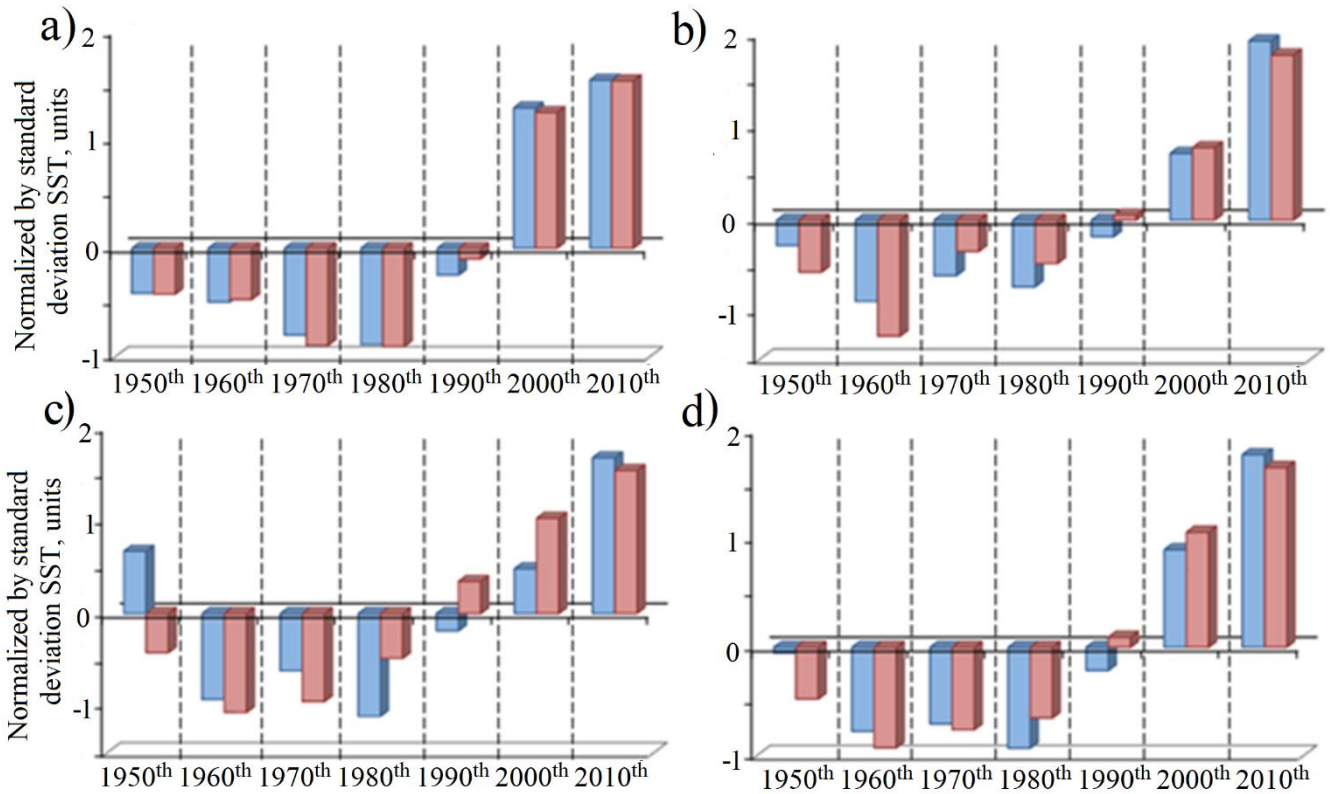


Figure 4.3. Standard deviation normalized SST anomalies for the Norwegian (a) and Barents (b), Greenland (c) seas and the entire water area of the North European Basin (d) for the winter (blue column) and summer (red column) seasons relative to the average for the period 1950–2019 years averaged over 10 years.

If we consider the variability of anomalies in each sea separately, and in the entire North European basin, then we can distinguish a feature that until the 1990$^{th}$, negative anomalies relative to the average were noted. After the 1990$^{th}$, the sign of the anomalies changes to positive. And in the 1990$^{th}$, the anomalies have the minimum values for the entire period. Probably, this may be due to the sharp change of the positive phase to the negative one and the increased deepening of the NAO index in the 2000$^{th}$ (see Fig. 4.2). As well as a decrease in the magnitude of the Atlantic Multi-Decade Oscillation in the 1990$^{th}$ and a transition to a positive phase in the 2000$^{th}$. Changes in the period of the 1990s for the SST of the seas of the North European basin occur more sharply than for the ice coverage of the same water area due to the fact that, as is known, it is the sea temperature that reacts more intensively and primarily to global changes. And as a result of such changes, changes occur in ice coverage.

It is also worth noting that in the Greenland Sea in the 1950$^{th}$ there was a period of positive anomalies, which is not found in any other sea of the North European basin. At the same time, a decrease is noted in the ice coverage anomalies in the indicated period. At the same time, negative anomalies of sea surface temperature are observed in the Greenland Sea during this period, and the removal of ice through the Fram Strait from the Arctic Basin increases (Vyazilova and Smirnov, 2016). In general, the distribution of SST anomalies in the Barents and Norwegian Seas is closest to the variability of anomalies in the entire North European Basin.

### 4.1.2 The connection of ice coverage and sea surface temperature with astrogeophysical parameters

As early as the end of the 18th century, A.I. Voeikov argued that the climate and its variability are mainly affected by the movement of air masses as a result of the influence of the Sun (Voeikov, 1948).

It was the identification of evidence of the direct influence of solar activity on atmospheric circulation that was given special attention in the 1960s by many authors. So I.V. Maksimov, M.S. Eigenson, B.M. Rubashev et al. (Eigenson, 1963; Rubashev, 1964; Maksimov, 1970) showed that long-term ice coverage fluctuations, primarily in the low-frequency part of the fluctuations, can also be influenced by astrogeophysical factors, including: declination and pole tides (Gudkovich et al. ., 1970), the Earth's rotation rate (Gudkovich et al., 2004; Gudkovich et al., 2005), and solar activity (Sleptsov-Shevlevich and Boyarinov, 2002; Abdusamatov, 2009; Fedorov, 2017). MI Pudovkin (Pudovkin, 1996) showed that a change in the incoming solar energy flux causes a change in air temperature and the height of isobaric surfaces in the troposphere, causing noticeable changes in the rate of large-scale atmospheric circulation. An analysis of solar-induced changes in surface and altitude pressure allowed A. G. Egorov (Egorov, 2003, 2005) to establish their connection with the long-term features of ice distribution in the Arctic seas in summer.

According to V. M. Fedorov (Fedorov, 2017), as a result of the low variability of the total solar radiation, the main mechanism for changing the Earth's insolation is associated with celestial-mechanical processes that cause changes in the distance between the Earth and the Sun, changes in the Earth's orbit and the inclination of the Earth's axis of rotation. It was shown in (Fedorov et al., 2016) that the most significant factor determining the variations in the maximum and minimum values of the sea ice coverage in the long-term regime is the variability of the solar radiation arriving at the upper boundary of the atmosphere.

Note that the monitoring of total solar radiation showed that its variations are about 0,1% of the average value (Petrukovich et al., 2008). Such small variations, according to (Pudovkin, 1996), cannot be a direct energy source of atmospheric disturbances, and this is one of the main arguments about the impossibility of solar activity affecting weather phenomena. However, although the energy of the solar wind

is negligible in comparison with the total solar radiation. However, their fluxes increase by tens and hundreds of times during solar disturbances, and they can have an indirect effect on the dynamics and radiation balance of the atmosphere (Pudovkin and Raspopov, 1992). Strengthening (weakening) of the flow of invading particles as a result of physicochemical processes that are not yet fully understood causes a decrease (or increase) in the transparency of the atmosphere and thereby modulates the influx of solar energy into the lower atmosphere. A change in the flow of incoming solar energy causes a change in air temperature and the height of isobaric surfaces in the troposphere, thereby causing noticeable changes in the rate of large-scale atmospheric circulation (Pudovkin, 1996). An analysis of solar-induced changes in surface and altitude pressure allowed Egorov (Rubashev 1964; Gudkovich et al., 1970; Egorov, 2007) to establish their connection with long-term features of ice distribution in the Arctic seas in summer.

According to I. V. Maksimov (Maksimov, 1970), the large-scale structure of the ocean level and the circulation of waters are influenced by the gravitational forces of the Moon and the Sun and fluctuations in the speed of the Earth's rotation. This subgroup of variables acts through a partial change in the gravitational field, which forms a long-term forced tidal wave and the emergence of a partial geostrophic current. J. Darwin (1887) called the “pole tide” wave a forced wave that arises in the World Ocean and is associated with oscillations of the instantaneous axis of rotation of the Earth (Gudkovich et al., 1970). The centrifugal force of the Earth changes as a result of free 14-month oscillations (Chandler oscillation) and 12-month forced oscillations of the Earth's rotation axis or movements of the Earth's instantaneous pole (Medvedev et al., 2018). The superposition of these two oscillations creates a 6–7 cyclic beat.

Figure 4.4 shows the average annual time course of astrogeophysical characteristics and parameters.

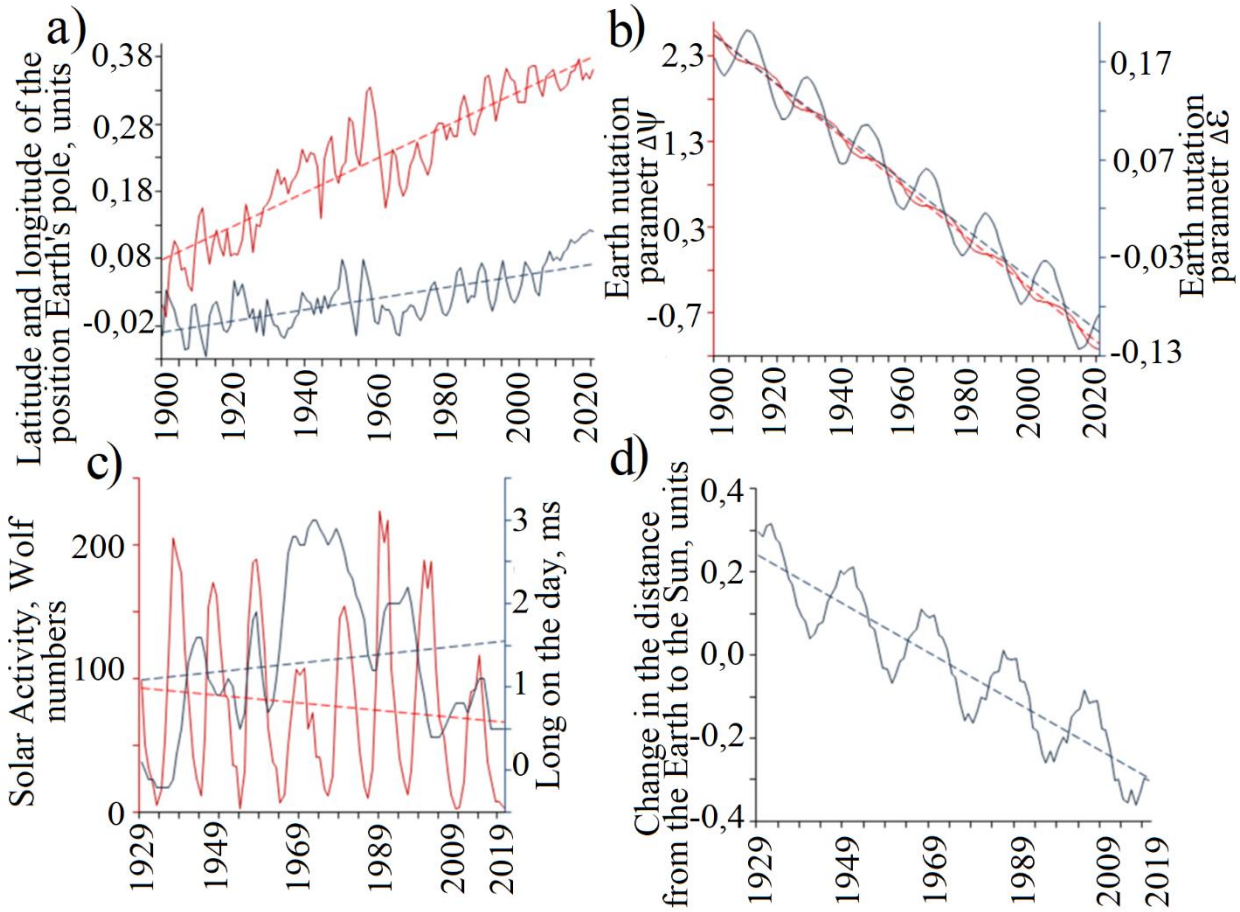


Figure 4.4. Average annual time course of astrogeophysical characteristics and parameters (solid lines) with plotted linear trends (dashed lines): a – latitudinal X (blue) and longitude Y (red) coordinates of the position of the Earth's pole; b – Earth nutation parameters Δψ (red) and Δε (blue) for the period 1900-2020; (c) solar activity (red) and Earth's rotation rate (blue); c - change in the distance from the Earth to the Sun for the period 1929–2020.

Obviously, there are significant negative trends for the long-term variability of the Earth's nutation parameters (Figure 4.4, b) and changes in the distance from the Earth to the Sun (Figure 4.4, d). The contribution of the trend component is 99% (Δψ), 94% (Δε) and 83%, respectively. Also, these parameters have pronounced cyclic fluctuations, which will be discussed in more detail in the next paragraph. In addition to the features of interaction with SST and ice coverage described at the beginning of the paragraph from the point of view of physical interaction, the use of these characteristics

is also due to their good predictability. Which, of course, can be used in the development of ice coverage and SST forecast models.

The latitudinal and longitude coordinates of the change in the Earth's pole have a much less pronounced positive trend in long-term variability (Figure 4.4. a). Whereas in the speed of the Earth's rotation (Figure 4.4 d) and solar activity (Figure 4.4 c), the trend is not significant.

Let us consider in more detail the variability of astrogeophysical characteristics and parameters (Figure 4.5).

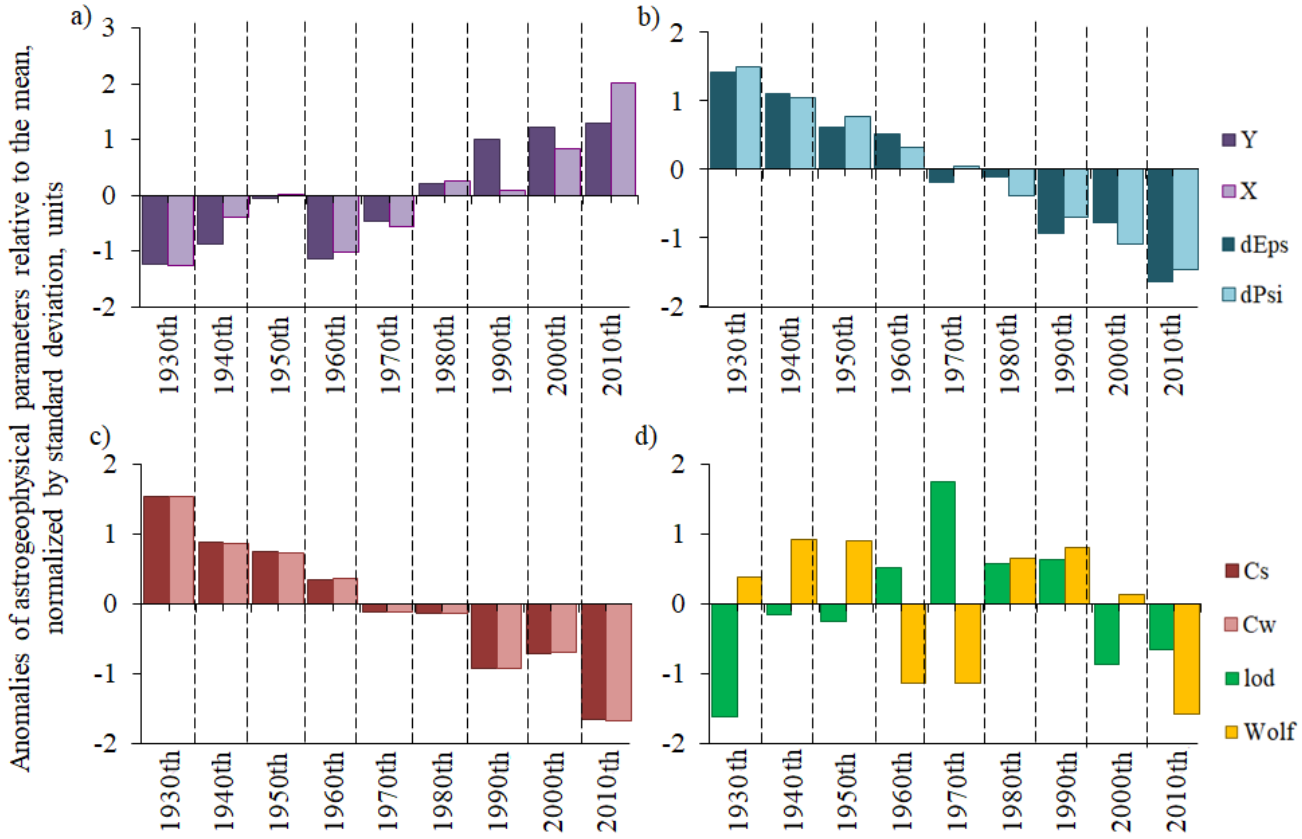


Figure 4.5. Anomalies of astrogeophysical parameters normalized by standard deviation: a – nutation parameters in longitude $\Delta\psi$ and inclination $\Delta\varepsilon$; b – latitudinal X and longitude Y coordinates of the position of the Earth's pole; (c) Wolf solar activity and the Earth's rotation speed lod; d is the change in the distance from the Earth to the Sun in the summer $C_S$ and winter $C_W$ seasons for the period 1930–2019, averaged over decades.

Since the 1980s, the latitude and longitude coordinates of the position of the Earth's pole have changed their sign from negative to positive. Also, during this period, the parameters of the Earth's nutation and the change in the distance from the Earth to the Sun change their sign to the opposite. It is interesting that with a delay of 10 years, the signs and anomalies of both ice coverage and SST change. At the same time, all characteristics and parameters of the cosmic geophysical impact (except for the speed of the Earth's rotation) have the maximum modulus values for the period under study in the last 10 years. Due to the fact that in the 2010s the anomalies in SST variability are positive with maximum values, and in the ice coverage variability the anomalies are negative with maximum values, it should be assumed that astrogeophysical processes are interrelated with such a situation. From which, in turn, follows the need to use astrogeophysical characteristics and parameters in the construction of equations for long-term oscillations of SST and ice coverage.

### 4.1.3 Cyclicity of hydrometeorological and astrogeophysical characteristics and parameters

When establishing relationships, one of the factors in the choice of predictors was the study of the conjugacy of the cyclicity of hydrometeorological and astrogeophysical characteristics and parameters with ice coverage and SST cycles. For each of the proposed predictors, a periodogram was constructed, similar to the plots of the distribution of the spectral density of ice coverage (Figure 3.4) and SST (Figure 2.11). Peaks of spectral densities were identified from the spectrograms. Corresponding to the peaks of the year (periods of fluctuations) are listed in the table (table 4.1).

Table 4.1. Periods of cyclic fluctuations of hydrometeorological indices and astrogeophysical characteristics and parameters, identified by peaks of spectral density.

| Parameter/ index | Periods of cyclic fluctuations in years | | | | |
|---|---|---|---|---|---|
| | over 14 | 8-13 | 6-8 | 3-6 | less than 3 |
| AOw | **17,5** | **8,8** | – | 4,4; 3,7 | **2,8; 2,4** |
| AOs | **17,5** | **10** | **7,0** | 4,4 | **2,8; 2,3** |
| ADw | **17,5** | **14** | **7,0** | 5,0; **3,5** | **2,7; 2,4** |
| ADs | – | 11,7 | **7,0** | 4,1; **3,3** | **2,9; 2,4** |
| PNAw | – | – | **7,8** | 3,7 | **2,5; 2,3** |
| PNAs | – | 11,7 | **7,0** | 4,4; **3,3** | **2,3** |
| AMO | 16,4 | **9,1** | **7,5**; **6,1** | **5,3**; 4,6; **3,6** | **2,5** |
| NAOw | 38,8 | **13,9** | **7,8** | **5,7**; **5,0** | **2,7; 2,4** |
| NAOs | 32,2 | **13,9**; **8,8** | **7,2** | **5,5; 4,0; 3,5** | **2,7; 2,3** |
| lod | **23,0** | 13,1; 8,4 | – | – | – |
| W | – | 11,5; **10,2** | – | **5,4**; 3,8; **3,3** | **2,7; 2,4** |
| Cw | 18,4 | 13,1; 8,4 | **6,1** | 4,0 | **2,7** |
| Cs | 18,4 | **9,2** | **6,1** | 4,0 | **2,7** |
| Δε | 18,4 | **9,2** | – | – | – |
| Δψ | 18,4 | **9,2** | – | – | – |
| X | – | **10,2** | **6,6** | – | – |
| Y | – | **9,2** | **6,1** | – | – |

*Note.* Y, X – longitude and latitude coordinates of the position of the Earth's pole; AD Arctic Dippole index; AO – Arctic Oscillation Index; PNA – Pacific-North American Oscillation Index; W – Wolf numbers; C – change in distance from Earth to Sun; Δε and Δψ – Earth nutation parameters; lod – Earth rotation speed; AMO – Atlantic Multidecade Oscillation; NAO – North Atlantic Oscillation; seasons are denoted in latin letters – S (summer), W (winter); periods in bold type coincide with the cycles of SST and ice coverage.

In the change of the average annual coordinates of the Earth's pole X, Y, a 6-year cycle is distinguished (Table 4.1), which is formed by the superposition of a forced twelve-month oscillation of the Earth's rotation axis and a free fourteen-month Chandler oscillation. The main cyclicity is noted in the components of the Earth's nutation parameter Δε and Δψ, and its period is about 20 (18.4 g) years, which is close to the period of the declination wave. Among the significant periods in the change in the speed of the Earth's rotation, there is a small peak at 13 years. The length of the analyzed series does not allow one to obtain meaningful estimates of cyclicity with periods longer than 30 years. But the polynomial trend of the fifth degree for the series of the average annual speed of the Earth's rotation draws attention to the existence of a long-term cyclicity of 60–70 years (Figure 4.4, c).

Among all periods of cyclic fluctuations of hydrometeorological indices and astrogeophysical characteristics and parameters, there are quite a few such periods that coincide with similar periods for SST and ice coverage. Thus, for the indices of atmospheric circulation AO and AD, fluctuations with periods of 18 are conjugated; 14; 10; 9; 7 and a number of lower frequency cycles from 2 to 4 years. The seven-year cycle also stands out in the Pacific-North American Oscillation. Also, it is worth noting that in all the proposed predictors, an oscillation with a period of 8–14 years is distinguished, which may be associated with the influence of the 11-year cycle of solar activity. Which, as is known, is an average period relative to solar activity minima, and is 8–14 years (Voeikov, 1948).

Among all periods of cyclic fluctuations of hydrometeorological indices and astrogeophysical characteristics and parameters, there are quite a few such periods that coincide with similar periods for SST and ice coverage. Thus, for the indices of atmospheric circulation AO and AD, fluctuations with periods of 18 are conjugated; 14; 10; 9; 7 and a number of lower frequency cycles from 2 to 4 years. The seven-year cycle also stands out in the Pacific-North American Oscillation. Also, it is worth noting that in all the proposed predictors, an oscillation with a period of 8–14 years is distinguished, which may be associated with the influence of the 11-year cycle of solar activity. Which, as is known, is an average period relative to solar activity minima, and is 8–14 years (Voeikov, 1948). Thus, there is every reason to include the components of the nutation of the Earth's axis of rotation, the Earth's poles Δε, Δψ, and the Earth's

rotation rate (anomalies in the length of the day lod) as predictors when finding the statistical equations for the relationship between ice coverage and astrogeophysical factors.

### 4.1.4 The interrelation of ice coverage and sea surface temperature with hydrometeorological astrogeophysical parameters

*Ice coverage of the seas of the North European Basin*

The analysis given in chapters 2 and 3 of the time series confirms the thesis about the polycyclic nature of changes in ice coverage and SST. Trends and fluctuation spectra make up the main part of the variability of both ice coverage and SST in all seas of the North European Basin. Therefore, when establishing the causes of the interannual variability of both the ice coverage and the SST of the seas of the North European Basin, their conjugation with the spectra of external factors can serve as a certain indicator by which the parameter can be used as a predictor for physico-statistical models. However, one more hypothetical reason should also be pointed out when a characteristic cannot be selected based on the spectrum alone: when the factor linearly affects the ice coverage and SST, which, of course, is not reflected in the spectra of the predictor and predictant.

The choice of predictors is helped by a correlation analysis of the relationship between seasonal ice coverage and SST with global indices and astrogeophysical characteristics. In this regard, the next stage of the study was the analysis of the relationship between sea ice coverage and various hydrometeorological characteristics: atmospheric pressure, temperature, as well as various objective hydrometeorological and astrogeophysical indices. To assess the degree of connection between the processes of ice coverage variability and SST of the seas of the North European basin with hydrometeorological and astrogeophysical parameters, cross-correlation coefficients were calculated for the significance level $\alpha$=0,05. The calculation results are presented in Table 4.2 for ice coverage and in Table 4.3 for sea surface temperature.

Table 4.2. Pair significant cross-correlation coefficients of seasonal anomalies in the ice coverage of the Greenland and Barents seas with hydrometeorological factors.

*Hydrometeorological factors*

| GS | $AO_{SP-1}$ | $T_{aW-1}$ | $T_{aS-1}$ | $NAO_{W-1}$ | $NAO_S$ | $T_{a\ Ns-1}$ | $T_{a\ Nw-1}$ |
|---|---|---|---|---|---|---|---|
| Winter | –0,34 | –0,52 | –0,47 | – | 0,30 | –0,49 | –0,72 |
| Summer | –0,43 | –0,41 | –0,54 | –0,29 | 0,26 | –0,68 | –0,54 |
| Autumn | –0,31 | –0,49 | –0,35 | – | – | –0,34 | –0,46 |
| Spring | –0,39 | –0,41 | –0,43 | – | 0,29 | –0,45 | –0,56 |
| BS | $AD_W$ | $AO_W$ | $AO_{S-1}$ | $PNA_W$ | $NAO_W$ | $Ta_{\_Ns-1}$ | $Ta_{\_Nw-1}$ |
| Winter | – | 0,23 | 0,28 | –0,29 | –0,26 | –0,62 | –0,63 |
| Summer | –0,23 | – | 0,28 | –0,39 | –0,25 | –0,51 | –0,54 |
| Autumn | –0,27 | – | – | – | – | –0,53 | –0,46 |
| Spring | – | 0,28 | 0,29 | –0,38 | –0,36 | –0,64 | –0,65 |

*Communication parameters with the Atlantic Ocean*

| GS | $AMO_{-2}$ | $AMO_{-3}$ | $AMO_{-4}$ | $B_{NW-1}$ | $B_{NSP-1}$ | $B_{NS-1}$ | $B_{NAUT-1}$ |
|---|---|---|---|---|---|---|---|
| Winter | –0,35 | –0,43 | –0,50 | – | –0,39 | –0,29 | –0,28 |
| Summer | –0,44 | –0,60 | –0,46 | –0,27 | –0,52 | –0,43 | –0,32 |
| Autumn | – | –0,29 | – | –0,27 | –0,45 | –0,32 | – |
| Spring | – | –0,34 | –0,32 | –0,25 | –0,33 | –0,34 | –0,24 |
| BS | $AMO_{-2}$ | $AMO_{-3}$ | $AMO_{-4}$ | $B_{NW-1}$ | $B_{NSP-1}$ | $B_{NS-1}$ | $B_{NAUT-1}$ |
| Winter | –0,49 | –0,47 | –0,48 | –0,34 | –0,23 | –0,28 | –0,43 |
| Summer | –0,39 | –0,43 | –0,40 | –0,44 | –0,25 | –0,40 | –0,40 |
| Autumn | –0,47 | –0,45 | –0,41 | – | – | –0,33 | –0,22 |
| Spring | –0,50 | –0,46 | –0,45 | –0,37 | –0,29 | –0,39 | –0,47 |

*Note*. -1, -2, -3 - ahead of the parameter by 1, 2 and 3 years, respectively; $T_a$ is the atmospheric temperature in the Greenland Sea; AO, Arctic Oscillation; NAO, North Atlantic Oscillation; $T_{aNW}$ is the atmospheric temperature in the Norwegian Sea; AMO, Atlantic Multi-Decade Oscillation Index; $B_N$ is the heat balance in the Norwegian Sea; seasons are denoted in Latin letters - S (summer), AUT (autumn), W (winter), SPR (spring).

Table 4.3. Pair significant cross-correlation coefficients of seasonal SST anomalies in the Greenland and Barents Seas with hydrometeorological factors over the seasons.

*Hydrometeorological factors*

| GS | $AO_{SP-1}$ | $T_{aW-1}$ | $T_{aS-1}$ | $NAO_{W-1}$ | $NAO_S$ | $T_{a\ Ns-1}$ | $T_{a\ Nw-1}$ |
|---|---|---|---|---|---|---|---|
| Winter | –0,34 | –0,52 | –0,47 | – | 0,30 | –0,49 | –0,72 |
| Summer | –0,43 | –0,41 | –0,54 | –0,29 | 0,26 | –0,68 | –0,54 |
| Autumn | –0,31 | –0,49 | –0,35 | – | – | –0,34 | –0,46 |
| Spring | –0,39 | –0,41 | –0,43 | – | 0,29 | –0,45 | –0,56 |
| BS | $AD_W$ | $AO_W$ | $AO_{S-1}$ | $PNA_W$ | $NAO_W$ | $Ta\_{Ns-1}$ | $Ta\_{Nw-1}$ |
| Winter | – | 0,23 | 0,28 | –0,29 | –0,26 | –0,62 | –0,63 |
| Summer | –0,23 | – | 0,28 | –0,39 | –0,25 | –0,51 | –0,54 |
| Autumn | –0,27 | – | – | – | – | –0,53 | –0,46 |
| Spring | – | 0,28 | 0,29 | –0,38 | –0,36 | –0,64 | –0,65 |

*Communication parameters with the Atlantic Ocean*

| GS | $AMO_{-2}$ | A | $AMO_{-4}$ | $B_{NW-1}$ | $B_{NSP-1}$ | $B_{NS-1}$ | $B_{NAUT-1}$ |
|---|---|---|---|---|---|---|---|
| Winter | –0,35 | – | –0,50 | – | –0,39 | –0,29 | –0,28 |
| Summer | –0,44 | – | –0,46 | –0,27 | –0,52 | –0,43 | –0,32 |
| Autumn | – | – | – | –0,27 | –0,45 | –0,32 | – |
| Spring | – | – | –0,32 | –0,25 | –0,33 | –0,34 | –0,24 |
| BS | $AMO_{-2}$ | A | $AMO_{-4}$ | $B_{NW-1}$ | $B_{NSP-1}$ | $B_{NS-1}$ | $B_{NAUT-1}$ |
| Winter | –0,49 | – | –0,48 | –0,34 | –0,23 | –0,28 | –0,43 |
| Summer | –0,39 | – | –0,40 | –0,44 | –0,25 | –0,40 | –0,40 |
| Autumn | –0,47 | – | –0,41 | – | – | –0,33 | –0,22 |
| Spring | –0,50 | – | –0,45 | –0,37 | –0,29 | –0,39 | –0,47 |

*Note.* -1, -2, -3 - ahead of the parameter by 1, 2 and 3 years, respectively; $T_a$ is the atmospheric temperature in the Greenland Sea; AO, Arctic Oscillation; NAO, North Atlantic Oscillation; $T_{aNW}$ is the atmospheric temperature in the Norwegian Sea; AMO, Atlantic Multi-Decade Oscillation Index; $B_N$ is the heat balance in the Norwegian Sea; seasons are denoted in Latin letters - S (summer), AUT (autumn), W (winter), SPR (spring).

When assessing the relationship between the ice coverage of the Greenland Sea and the Arctic AO oscillation, significant correlation coefficients fall on the spring season of the previous year. Here there is a feedback with a maximum value of 0,43 (modulo) with summer ice coverage (Table 4.2, block "Hydrometeorological factors"). This means that when the anticyclone weakens over the Arctic, the Atlantic air mass

invades Europe and increases the flow of warm and salty waters of the North Atlantic into the North European Basin, which leads to a decrease in ice coverage in the Greenland Sea. Of interest is the fact that the second mode of decomposition of the surface atmospheric pressure $EOF_2$, or the AD index, does not have significant pairwise correlation coefficients (data not shown), but it shows up well in multiple linear regression in combination with other predictors. The feedback of ice coverage with the near-surface temperature of the atmosphere is confirmed by high significant negative correlation coefficients for air temperature, both in the Greenland and Norwegian seas, which persist for more than a year.

In contrast to the situation with the ice coverage in the Greenland Sea, the connection with the second and third modes of expansion of the pressure at sea level in terms of the natural orthogonal functions AD and PNA is rather well manifested. Interestingly, the highest values of the correlation coefficients fall on the winter seasons of these indices and with feedback. During the positive phase of AD (R was 0,23 –0,27 in absolute value), the wind flow intensifies, which strengthens the Transarctic current in the Central Arctic. As a result, the drift of sea ice through the Fram Strait into the Greenland Sea is increasing. In the negative phase of the Arctic dipole AD, the reverse situation is observed. The removal of ice due to anomalous winds from the Central Arctic is decreasing. (Watanabe et al., 2006; Wang et al., 2009) At the same time, the values of correlation coefficients for the ice coverage in the Barents Sea with the Arctic AO oscillation are somewhat lower than for the ice coverage in the Greenland Sea, but are also significant for all seasons except autumn. The highest correlation coefficients between the ice coverage of the Barents Sea and the AO for the winter and previous summer seasons. And they range from 0,23 to 0,29. Which, although small in size, is nonetheless statistically significant. During the positive phase of AO, sea ice outflow into the Greenland Sea increases. At the same time, the AO index characterizes the global features of the atmospheric circulation and determines the sign (Wang and Ikeda, 2000), while the AD index characterizes the location of pressure anomalies at sea level.

Accordingly, the Arctic Oscillation determines whether the influence of the Arctic dipole anomaly, and hence the drift of ice from the Central Arctic Basin, will be stimulated or limited. Thus, a number of authors argue that it was the existence of the Arctic dipole anomaly in 2007 that led to the record low ice coverage (Munshi, 2015). The connection with the North Atlantic Oscillation is also statistically significant. The NAO index characterizes the strength and direction of air flows across the North Atlantic, closely related to the Arctic oscillation, and the influence of their phases is considered together.

The highest correlation coefficients of the ice coverage in the Barents Sea with the temperature of the atmosphere in the Norwegian Sea, ranging from 0,46 to 0,65 modulo with a lead time of 1 year. Such a lag in the interconnection of processes can help in the preparation of prognostic equations.

No less important is the influx of warm and salty waters from the North Atlantic. The connection between the ice coverage of the Greenland Sea and the characteristics of the waters of the North Atlantic, expressed by the multi-decadal Atlantic oscillation index AMO and the surface heat balance in the Norwegian Sea $B_N$, is also quite close (Table 4,2, block "Parameters of connection with the Atlantic Ocean"). This relationship is most significant for the summer and winter seasons of the year with a correlation coefficient of more than 0,60 modulo. An even stronger correlation is determined for the ice coverage of the Barents Sea. The correlation coefficients with the AMO index are significant for all seasons with a lag of up to 4 years inclusive and range from 0,39 to 0,50. Which indicates a greater influence of the North Atlantic on the Arctic regime of the Barents Sea. There are also significant correlations between ice coverage and sea surface temperature in the Norwegian Sea with a delay of 1 year. Which can also be used in the future when developing equations.

Let's consider the relationship between sea surface temperature and various parameters of atmospheric circulation (Table 4.3, block "Hydrometeorological factors"). The dominant role is occupied by the Arctic oscillation. Moreover, it is worth noting that the greatest correlations fall on the spring season of the previous year (0,31–0,43 modulo).

In general, it can be said that the relationship between SST and hydrometeorological factors (see Table 4.3) is similar to that of ice coverage. Which confirms the hypotheses about the influence of meteorological and hydrological processes.

The reality of the influence of permanent currents (direct influence or through the level slope), such as the transarctic drift current from the East Siberian Sea, through the North Pole, the Fram Strait into the Greenland Sea, is beyond doubt. Trajectory maps of drifting buoys over a long period of time convince us of this (Frolov et al., 2007). According to (Maksimov, 1970), the ocean level and water circulation are additionally affected by the gravitational forces of the Moon and the Sun and fluctuations in the Earth's rotation rate. But the question is often asked: can small fluctuations in gravitational forces cause tangible impacts on the ocean?

Let us give estimates of the forces of long-term fluctuations of the gravitational effects of the Moon and the Sun and the speed of the Earth's rotation. Even (Darvin, 1886) the wave of the "pole tide" called the forced wave arising in the World Ocean associated with oscillations of the instantaneous axis of rotation of the Earth - the centrifugal force of the Earth. The centrifugal force of the Earth changes as a result of free fourteen-month oscillations (Chandler oscillation) and twelve-month forced oscillations of the Earth's rotation axis or movements of the Earth's instantaneous pole (Medvedev et al., 2018). Note that earlier only the fourteen-year wave was called the “pole tide”. The superposition of these two oscillations creates a 6–7 cyclic beat.

Maksimov I.V. (Maksimov, 1970) estimated that the long-term part of the tidal and nutational forces in total is only 19 times less than the maximum value of the component of the tide-forming force of the Moon, where semidiurnal and daily tides with an average height of about 70 cm dominate, and in the coastal zone reaching

several meters. But semidiurnal and diurnal tides act half of the period in one direction and the second half (6 and 12 hours) in the opposite direction. And the "pole tide" is valid for 7 months or 5040 hours in one direction and the same in the opposite direction. We have carried out calculations of long-term tidal currents. It is known that, according to the static theory, the variation with latitude of the “pole tide” amplitudes has zero values at the poles and +/– maximum at latitudes 40–600. The authors of the work (Maksimov et al., 1977) empirically established that the level difference h between latitudes 60 and 700 is about 10 mm, therefore, the level gradient is dh/dx= 1/102000=10–6. According to the geostrophic current formula u=–g/f* dh/dx (g is the force of gravity, f is the Coriolis parameter), we obtain, for a latitude of 650 n.l. the maximum geostrophic current velocity equal to 7,8 cm/sec, and the average current velocity for the half-period of the wave is about 4 cm/sec. Then, within 7 months, this flow velocity corresponds to the length of the horizontal displacement orbit of a water particle of 720 km, which is close to the estimate of IV Maksimov (Maksimov, 1970). While the length of the horizontal orbit of displacement of a daily tide particle with an average speed of 40 cm/sec is only 17 km. Thus, the horizontal displacements of water particles due to the action of small forces of the gravitational influence of the Moon and the Sun and the rotation of the Earth, but acting for a long time, turn out to be greater than semidiurnal and diurnal tides. Thus, small forces of long-term fluctuations of the gravitational influence of the Moon and the Sun, including forces of a nutational nature, can be associated with significant horizontal orbits of water particles in the ocean and can cause quite noticeable changes in the location of the core regions and frontal zones of certain sea currents, and as well as ice cover of the seas.

According to the correlation of processes among astrogeophysical factors, the closest relationship for both ice coverage and SST is manifested with the longitude and latitude coordinates of the position of the Earth's pole Y and X, the nutation parameters of the Earth's axis $\Delta\psi$, $\Delta\varepsilon$ with correlation coefficients greater than 0,50 (Table 4.4.).

Table 4.4. Pair significant cross-correlation coefficients of seasonal ice coverage and SST anomalies in the Greenland, Norwegian and Barents seas with astrogeophysical parameters.

*Ice coverage seas of the North European basin*

| Season | X | Y | Δψ | $\Delta\psi_{-3}$ | Δε | lod | $C_S$ | $C_W$ | $Wolf_{-1}$ |
|---|---|---|---|---|---|---|---|---|---|
| | Greenland sea | | | | | | | | |
| Winter | –0,41 | –0,49 | 0,55 | 0,54 | 0,62 | 0,32 | 0,32 | –0,33 | –0,28 |
| Summe | –0,48 | –0,51 | 0,54 | 0,53 | 0,55 | 0,54 | 0,38 | –0,42 | – |
| Autum | –0,29 | –0,56 | 0,49 | 0,46 | 0,57 | 0,25 | 0,33 | –0,46 | – |
| Spring | –0,30 | –0,58 | 0,57 | 0,54 | 0,63 | – | 0,37 | –0,32 | – |
| | Barents sea | | | | | | | | |
| Winter | –0,57 | –0,41 | 0,39 | 0,40 | 0,41 | 0,34 | 0,32 | 0,34 | – |
| Summe | –0,47 | –0,55 | 0,43 | 0,43 | 0,47 | 0,35 | 0,42 | 0,42 | – |
| Autum | –0,34 | –0,23 | – | – | – | 0,37 | – | – | 0,22 |
| Spring | –0,61 | –0,54 | 0,51 | 0,48 | 0,55 | 0,32 | 0,47 | 0,48 | – |

*Sea surface temperature of the seas of the North European Basin*

| | | | | | | | | | |
|---|---|---|---|---|---|---|---|---|---|
| | Greenland sea | | | | | | | | |
| Winter | –0,41 | –0,49 | 0,55 | 0,54 | 0,62 | 0,32 | 0,32 | –0,33 | –0,28 |
| Summe | –0,48 | –0,51 | 0,54 | 0,53 | 0,55 | 0,54 | 0,38 | –0,42 | – |
| Autum | –0,29 | –0,56 | 0,49 | 0,46 | 0,57 | 0,25 | 0,33 | –0,46 | – |
| Spring | –0,30 | –0,58 | 0,57 | 0,54 | 0,63 | – | 0,37 | –0,32 | – |
| | Barents sea | | | | | | | | |
| Winter | –0,57 | –0,41 | 0,39 | 0,40 | 0,41 | 0,34 | 0,32 | 0,34 | – |
| Summe | –0,47 | –0,55 | 0,43 | 0,43 | 0,47 | 0,35 | 0,42 | 0,42 | – |
| Autum | –0,34 | –0,23 | – | – | – | 0,37 | – | – | 0,22 |
| Spring | –0,61 | –0,54 | 0,51 | 0,48 | 0,55 | 0,32 | 0,47 | 0,48 | – |
| | Norwegian sea | | | | | | | | |
| Winter | 0,69 | 0,66 | –0,75 | –0,75 | –0,71 | –0,68 | –0,62 | –0,64 | – |
| Summe | 0,64 | 0,61 | –0,67 | –0,67 | –0,63 | –0,66 | –0,55 | –0,56 | – |
| Autum | 0,62 | 0,56 | –0,61 | –0,60 | –0,60 | –0,71 | –0,59 | –0,58 | – |
| Spring | 0,61 | 0,60 | –0,71 | –0,72 | –0,64 | –0,60 | –0,55 | –0,58 | – |

*Note.* X and Y latitudinal and longitude coordinates of the position of the Earth's pole; Δψ, Δε nutation parameters of the Earth's axis; $C_S$ and $C_W$ distance from the Earth to the Sun in summer and winter, respectively; lod is the speed of the earth's rotation; Wolf it's Wolf numbers; –1, –3 ahead of the parameter by 1 and 3 years, respectively; – the correlation coefficient is not statistically significant.

The statistical relationship of ice coverage with the Earth's rotation speed lod is most pronounced for the summer season with a correlation coefficient of 0,54, and with changes in the distance from the Earth to the Sun CS and CW, the correlation coefficients are determined at the level of 0,32–0,46. The lowest correlation coefficient is observed for the solar activity index (by Wolf numbers) with a time lag of –1 year $Wolf_{-1}$. A similar situation is observed for all seas, both when considering ice coverage and for SST.

Thus, the performed analysis shows that interannual changes in ice coverage and SST in all four seasons of the year in all seas under consideration are statistically related not only to hydrometeorological indices, but also to astrogeophysical parameters.

## 4.2 Statistical models of long-term changes of the ice coverage and sea surface temperature and informativeness of various hydrometeorological and astrogeophysical factors

### 4.2.1 Statistical models of long-term fluctuations of the sea surface temperature

The analysis of the information content of various hydrometeorological and astrogeophysical factors in the problem of describing the variability of SST was carried out by various numerical experiments on physical-statistical equations for winter and summer SST of the seas of the North European basin. Models were built using multi-regression analysis using the Statistics software package (Malinin and Gordeeva, 2003). The prepared series of hydrometeorological characteristics and indices, as well as the series of astrogeophysical parameters (see Chapter 4, paragraph 1) formed the base of test predictors. The procedure for obtaining a statistical equation for the relationship between SST and predictors was carried out by enumerating them and finding an equation with the highest overall correlation coefficient with sufficient statistical significance of the variables included in the statistical model.

*Statistical models of summer and winter seasons*

Static equations of connection of summer SST anomalies in the Greenland, Barents and Norwegian seas with hydrometeorological and astrogeophysical factors are presented in Table 4.5.

Table 4.5. Static equations of connection of summer SST anomalies in the Greenland, Barents and Norwegian seas with hydrometeorological and astrogeophysical factors.

| № | The equation | R | $R^2$ | P,% |
|---|---|---|---|---|
| | | | | 0,67σ |
| **Greenland sea, summer (July–September)** | | | | |
| 4.5.1 | $SST_S = 0{,}32 \cdot AMO_{-2} + 0{,}36 \cdot X - 0{,}44 \cdot C_W + 0{,}18 \cdot PNA_W + 0{,}18 \cdot AO_S$ | 0,85 | 0,72 | 81 |
| 4. 5.2 | $SST_S = 0{,}33 \cdot AMO_{-2} + 0{,}27 \cdot X - 0{,}53 \cdot \Delta\varepsilon + 0{,}17 \cdot PNA_W + 0{,}16 \cdot AO_S$ | 0,87 | 0,76 | 91 |
| 4. 5.3 | $SST_S = 0{,}33 \cdot AMO_{-2} + 0{,}31 \cdot X - 0{,}52 \cdot \Delta\varepsilon$ | 0,84 | 0,71 | 80 |
| **Barents sea, summer (July–September)** | | | | |
| 4. 5.4 | $SST_S = 0{,}32 \cdot AMO_{-2} + 0{,}18 \cdot AD_W + 0{,}14 \cdot AO_S + 2{,}40 \cdot X - 0{,}51 \cdot C_W$ | 0,85 | 0,72 | 80 |
| 4. 5.5 | $SST_S = 0{,}25 \cdot AMO_{-2} + 0{,}16 \cdot AD_W + 0{,}14 \cdot AO_S + 0{,}28 \cdot X - 0{,}53 \cdot \Delta\varepsilon - 0{,}12 \cdot Wolf$ | 0,88 | 0,77 | 92 |
| 4. 5.6 | $SST_S = 0{,}24 \cdot AMO_{-2} + 0{,}31 \cdot X - 0{,}52 \cdot \Delta\varepsilon$ | 0,84 | 0,71 | 80 |
| **Norwegian sea, summer (July–September)** | | | | |
| 4. 5.7 | $SST_S = 0{,}37 \cdot AMO_{-2} + 0{,}29 \cdot X - 0{,}27 \cdot C_S - 0{,}20 \cdot NAO_{W-1} + 0{,}23 \cdot PNA_S$ | 0,83 | 0,69 | 80 |
| 4. 5.8 | $SST_S = 0{,}36 \cdot AMO_{-2} + 0{,}18 \cdot X - 0{,}18 \cdot NAO_{W-1} + 0{,}22 \cdot PNA_S - 0{,}41 \cdot \Delta\psi$ | 0,86 | 0,74 | 85 |
| 4. 5.9 | $SST_S = 0{,}40 \cdot AMO_{-2} + 0{,}21 \cdot PNA_S - 0{,}54 \cdot \Delta\psi$ | 0,83 | 0,69 | 82 |

*Note.* SSTs is the sea surface temperature for the summer season (July–September); AMO, Atlantic Multi-Decade Oscillation Index; X is the latitudinal coordinate of the position of the Earth's pole; NAO, North Atlantic Oscillation; AD is the index of the Arctic Dippole; AO is the Arctic Oscillation Index; PNA is the Pacific-North American Oscillation Index; Δε and Δψ are the nutation parameters of the Earth's axis; seasons are indicated in Latin letters - S (summer), AUT (autumn), W (winter), SPR (spring); -1, -2, -3 - leading the parameter by 1, 2 and 3 years, respectively.

The static equations for the relationship between winter SST anomalies in the Greenland, Barents and Norwegian seas with hydrometeorological and astrogeophysical factors are presented in Table 4.6.

Table 4.6. Static equations of connection of winter anomalies of sea surface temperature in the Greenland, Barents and Norwegian seas with hydrometeorological and astrogeophysical factors.

| № | The equation | R | $R^2$ | P,% |
|---|---|---|---|---|
| | | | | 0,67σ |
| **Greenland sea, winter (December–April)** | | | | |
| 4. 6.1 | $SST_W = 0,46 \cdot AMO_{-2} + 0,46 \cdot X - 0,21 \cdot W - 0,26 \cdot PNA_{W-2} + 0,24 \cdot AD_{W-1}$ | 0,81 | 0,66 | 82 |
| 4. 6.2 | $SST_W = 0,45 \cdot AMO_{-2} + 0,48 \cdot X - 0,24 \cdot Wolf + 0,25 \cdot AD_{W-1} + 0,75 \cdot \Delta\psi_{-3} - 0,65 \cdot \Delta\varepsilon$ | 0,84 | 0,71 | 80 |
| 4. 6.3 | $SST_W = 0,39 \cdot AMO_{-2} + 0,52 \cdot X + 0,70 \cdot \Delta\psi_{-3} - 0,68 \cdot \Delta\varepsilon$ | 0,78 | 0,61 | 78 |
| **Barents sea, winter (December–April)** | | | | |
| 4. 6.4 | $SST_W = 0,36 \cdot AMO_{-2} + 0,15 \cdot AD_W + 0,13 \cdot AO_{AUT-1} + 2,76 \cdot X - 0,29 \cdot C_W$ | 0,85 | 0,73 | 80 |
| 4. 6.5 | $SST_W = 0,36 \cdot AMO_{-2} + 0,14 \cdot AD_{W-1} + 2,31 \cdot X - 0,38 \cdot \Delta\varepsilon - 0,25 \cdot Wolf$ | 0,90 | 0,80 | 93 |
| 4. 6.6 | $SST_W = 0,36 \cdot AMO_{-2} + 2,20 \cdot X - 0,39 \cdot \Delta\varepsilon$ | 0,85 | 0,72 | 90 |
| **Norwegian sea, winter (December–April)** | | | | |
| 4. 6.7 | $SST_{W=} 0,47 \cdot AMO_{-2} + 0,29 \cdot X - 0,36 \cdot C_W - 0,14 \cdot NAO_{W-1} - 0,10 \cdot PNA_{AUT-1}$ | 0,86 | 0,73 | 88 |
| 4. 6.8 | $SST_W = 0,45 \cdot AMO_{-2} + 0,22 \cdot X - 0,45 \cdot \Delta\psi - 0,14 \cdot NAO_{W-1}$ | 0,87 | 0,76 | 90 |
| 4. 6.9 | $SST_W = 0,45 \cdot AMO_{-2} + 0,23 \cdot X - 0,46 \cdot \Delta\psi$ | 0,86 | 0,75 | 89 |

*Note.* $SST_W$ is the sea surface temperature for the winter season (December-April); AMO, Atlantic Multi-Decade Oscillation Index; X is the latitudinal coordinate of the position of the Earth's pole; NAO, North Atlantic Oscillation; AD is the index of the Arctic dipole; AO is the Arctic Oscillation Index; PNA is the Pacific-North American Oscillation Index; Δε and Δψ are the nutation parameters of the Earth's axis; seasons are indicated in Latin letters - S (summer), AUT (autumn), W (winter), SPR (spring); -1, -2, -3 - leading the parameter by 1, 2 and 3 years, respectively.

Both in the summer season (July–September) and in the winter season (December–April), the leading role in the formation of SST is played by the inflow of Atlantic waters (with a lag of 2 years), the latitudinal coordinate of the change in the position of the Earth's pole, and the parameters of the Earth's nutation (Tables 4.5-4.6, equations 4.5.1–4.6.9).

In recent years, the influence of the inflow of Atlantic waters into the Arctic basin has been actively studied (Sizov et al., 2022), as well as the strengthening of the so-called "Atlantification" (Ivanov and Repina, 2018; Ivanov et al., 2014; Polyakov et al., 2017; Ivanov, 2021). Indeed, for all equations, the share of the influence of the inflow of Atlantic waters (expressed using the AMO index) and the latitude coordinate X accounts for at least 30% for each predictor of the total variance.

In table. 4.5-4.6 in the equations with paragraphs 4.5.1, 4.5.4, 4.5.7, 4.6.1, 4.6.4, 4.6.7, equations are presented that use a set of both hydrometeorological (Atlantic water inflow, atmospheric circulation characteristics) and astrogeophysical parameters (change in the distance from the Earth to the Sun and solar activity, expressed by Wolf numbers). When the parameters of the Earth's nutation are included in the equations, the qualitative indicators increase (Tables 4.5-4.6 of Equations 4.5.2, 4.5.5, 4.5.8, 4.6.2, 4.6.5, 4.6.8). Graphically, the results of the equations are presented in Figure 4.6.

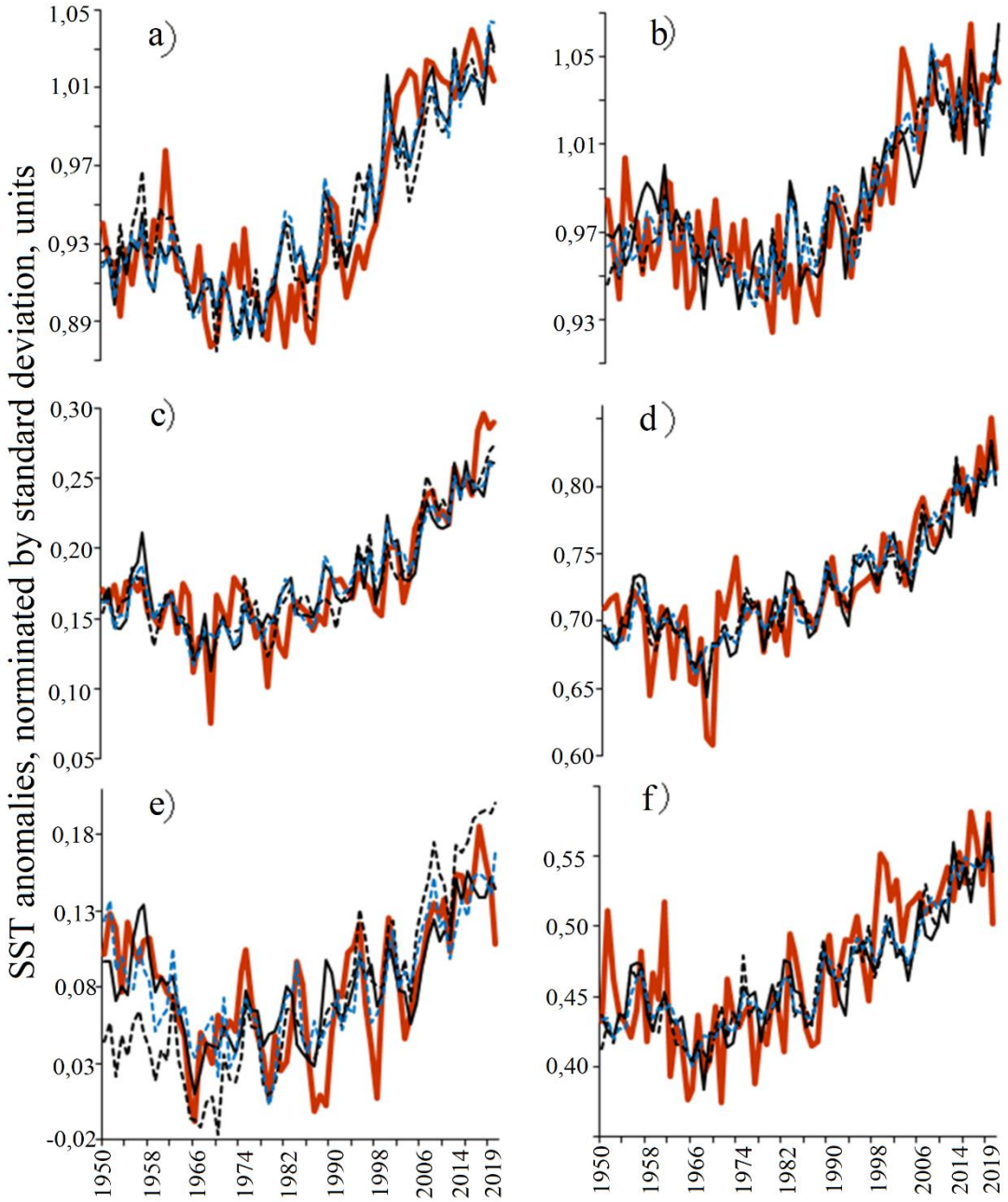


Figure 4.6. Comparison of actual and equationally reconstructed values of SST anomalies in the Norwegian (a – winter, b – summer), Barents (c – winter, d – summer) and Greenland (e – winter, f – summer) seas for the period 1950–2019: red the solid line is the actual SST, the black solid line is equations No._. _.1, _. _.4, _. _.7; dotted black - equations №_. _.2, _. _.5, _. _.8; dotted blue №_. _.3, _._.6, _._.9.

It should be noted that the parameters of the Earth's nutation are of particular importance. An analysis of various combinations of predictors showed that the use of these parameters in the equations helps to increase not only the quality, but also reduce

the number of predictors. What is a very important characteristic in the construction of physical and statistical models (see tables 4.5–4.6).

Interestingly, for the development of SST variability equations for both summer and winter seasons, almost identical predictors and their final combinations are identified, with a difference only in numerical coefficients. In addition, it is worth noting that the SST variability of each of the seas can be described with sufficient accuracy using only three predictors: AMO, $\Delta\varepsilon$ or $\Delta\psi$, and X.

In general, it can be noted that the equations obtained describe to a fairly high degree long-term fluctuations in the surface water temperature of the seas of the North European basin (see Table 4.6 and Figure 4.6) and can be used to describe them.

### 4.2.2 Statistical models of long-term fluctuations of the ice coverage

The study of the information content of various factors in the problem of describing the variability of the ice coverage was carried out similarly to the study of the information content of various factors for SST (see Chapter 4, paragraph 4.2, paragraph 4.2.1).

Note that in previously published works, long-term changes in ice coverage were studied only within the framework of hydrometeorological impact (Mironov, 2004; Frolov et al. 2007) or using only astrogeophysical parameters as predictors (Maksimov 1970; Pudovkin 1996; Sleptsov-Shevlevich and Boyarinov, 2002). In this paper, the study is carried out in a complex manner with the inclusion in the analysis of not only hydrometeorological characteristics, but also astrogeophysical ones. In our opinion, only joint analysis makes it possible to evaluate the contribution of each predictor while simultaneously including other predictors of different nature.

The procedure for obtaining a statistical equation for the relationship between ice coverage and predictors was carried out in a similar way by enumerating them and finding the equation with the highest overall correlation coefficient with sufficient statistical significance of the variables included in the statistical model (see Chapter 4,

paragraph 4.2, subsection 4.2.1). A statistical approach for deriving equations describing changes in

ice coverage in August for the Greenland Sea was previously applied in (Timokhov et al. 2018), while the analysis used a three-year moving ice coverage, and three-year moving hydrometeorological characteristics as predictors. There are no similar studies for the ice coverage of the Barents Sea. In this work, interannual seasonal changes in ice coverage are studied. Based on the initial ice coverage data for the winter and summer seasons and predictors, anomalies were calculated from the averages for the study period, which were normalized by the standard deviation. This made it possible to perform analysis with data of the same dimension, which improves the quality of equations, facilitates work and increases the performance of the Statistics program (statsoft.ru).

The equations for interannual changes in the area of ice in the Greenland and Barents Seas for each season were found by the method of multiregression analysis by enumeration of various predictors: hydrological, meteorological and astrogeophysical parameters and indices. The following parameters were used as an assessment of the quality of the constructed models: correlation coefficient R, determination coefficient $R^2$ and justification of the model P. Verification was calculated with a set standard deviation tolerance $0{,}67\sigma$ (used for short-term, or to assess the accuracy of the diagnosis). According to the guidance (manual on the forecast service, 2011), models for which P is more than 68%. For all correlation coefficients R, Student's test was equal to ±0,21 at significance level $\alpha=0{,}05$. Also, all equations were successfully tested for adequacy by the Fisher criterion. And the standard error $\sigma_\varepsilon$ of the model series did not exceed the standard deviation of the actual ice coverage. For the Greenland Sea, on average $\sigma_{\varepsilon(winter)} = 62{,}41\cdot10^3 km^2$, $\sigma_{\varepsilon(summer)} = 40{,}89\cdot10^3 km^2$, for the Barents Sea $\sigma_{\varepsilon(winter)} = 54{,}72\cdot10^3 km^2$, $\sigma_{\varepsilon(summer)} = 45{,}34\cdot10^3 km^2$, at standard deviation $144{,}19\cdot10^3 km^2$ (winter), $88{,}20\cdot10^3 km^2$ (summer) and $142{,}05\cdot10^3 km^2$ (winter), $96{,}32\cdot10^3 km^2$ (summer).

*Summer Season Statistical Models*

In the summer season (July–September), the leading role in the formation of ice conditions is played by the prehistory of ice coverage (spring period) and surface air temperature (Table 4.7, Equations 4.7.1–4.7.6), which was previously noted in the paper for the ice coverage of the Greenland and Barents Seas ( Mironov, 2004).

In Equations 4.7.1 and 4.7.4, the influence of predictors accounts for 29% and 57% (prehistory of ice coverage), 19% and 40% (air temperature) of the total dispersion of ice coverage in the Greenland and Barents Seas, respectively. The relationship with atmospheric temperature is inverse, but without any time shift, or with a half-year shift (Equation 4.7.6). What is logical is that changes in the near-surface temperature of the atmosphere are a less inertial process than changes in SST.

An equally important factor is the inflow of warm Atlantic waters (Abramov and Zakharov, 1981; Polyakov, 2000), which is modeled in all equations by the AMO index. The relationship between water temperature anomalies in the North Atlantic and ice coverage is inverse, which is manifested in the negative sign (see Table 4.7). Moreover, the time lag for the summer season, both for the Barents and Greenland Seas, is three years $AMO_{-3}$. In the case of developing all equations for the ice coverage in the summer season of the Greenland Sea, the AMO index has a significant contribution from 15% to 19%. Whereas for the Barents Sea, the combination of atmospheric circulation indices and the longitude coordinate of the position of the Earth's pole makes it possible to model the variability of ice coverage without using the AMO index (Equation 4.7.5 of Table 4.7).

Table 4.7. Static equations of connection between summer ice coverage anomalies in the seas of the North European basin and hydrometeorological and astrogeophysical factors.

| № | The equation | R | $R^2$ | P,% |
|---|---|---|---|---|
| | | | | 0,67σ |
| **Greenland Sea, summer (July–September)** | | | | |
| 4.7.1 | $L_S = -0,32 \cdot T_S + 0,23 \cdot L_{SP} - 1,04 \cdot AMO_{-3} - 0,37 \cdot X_{-1} - 0,16 \cdot AD_W - 34,39 \cdot AO_{W-1}$ | 0,87 | 0,75 | 89 |
| 4. 7.2 | $L_S = 0,80 \cdot \Delta\varepsilon - 1,55 \cdot AMO_{-3} - 0,46 \cdot X_{-1} - 0,42 \cdot AD_W - 0,31 \cdot W_{-1} - 0,30 \cdot PNA_{W-1}$ | 0,82 | 0,67 | 79 |
| 4. 7.3 | $L_S = -0,46 \cdot T_S - 0,11 \cdot AMO_{-3} + 0,29 \cdot \Delta\varepsilon$ | 0,81 | 0,65 | 77 |
| **Barents Sea, summer (July–September)** | | | | |
| 4. 7.4 | $L_S = 0,37 \cdot L_{SP} - 0,19 \cdot T_S - 0,29 \cdot PNA_{SPR} - 1,28 \cdot Y - 0,11 \cdot AD_W$ | 0,88 | 0,77 | 92 |
| 4. 7.5 | $L_S = 0,66 \cdot \Delta\varepsilon - 0,12 \cdot AMO_{-3} + 0,12 \cdot AO_W - 0,31 \cdot NAO_W - 0,49 \cdot PNA_{W-1} - 0,60 \cdot X$ | 0,80 | 0,64 | 86 |
| 4. 7.6 | $L_S = -0,19 \cdot T_W - 0,22 \cdot AMO_{-3} - 0,43 \cdot X_{-1}$ | 0,82 | 0,68 | 85 |

*Note.* $L_S$ is the ice coverage for the summer period (July–September); $T_S$ is the surface air temperature for the summer period (July–September); AMO, Atlantic Multi-Decade Oscillation Index; X and Y are the latitude and longitude coordinates of the position of the Earth's pole; NAO, North Atlantic Oscillation; AD is the Arctic dipole index; AO is the Arctic Oscillation Index; PNA is the Pacific-North American Oscillation Index; Δε is the nutation parameter of the Earth's axis; seasons are indicated in Latin letters - S (summer), AUT (autumn), W (winter), SPR (spring); -1, -2, -3 - leading the parameter by 1, 2 and 3 years, respectively.

The influence of atmospheric circulation (indices AO, PNA, NAO and AD) on the ice coverage of the North European Basin is also somewhat different in each sea. The contribution describing the effect of atmospheric circulation on the ice coverage of the Barents Sea (up to 49%) is twice as large as that for the Greenland Sea (up to 22%). This is due to more intense cyclonic activity over the Barents Sea. Thus, it was found

(Smirnova, 2016) that a greater number of polar cyclones (a polar cyclone is a small but rather intense marine cyclone that forms north of the main baroclinic zone (polar front or other main baroclinic zone). The horizontal scale of the PC is approximately between 200 and 1000 km and wind speed in the near-surface layer of about or more than 15 m/s) (Nesterov, 2020) corresponds to a smaller area of ice. This is primarily due to the large area of open water, which contributes to the formation of polar cyclones. The main areas of distribution of polar cyclones in the Barents Sea: the north of the Scandinavian Peninsula, near the North Cape and the western region of the Novaya Zemlya archipelago. In the Greenland Sea, polar cyclones are most active only in the area of the Lofoten Basin (Smirnova, 2016). It should be noted that the highest intensity of polar cyclones is observed in March, which corresponds to the winter season, and manifests itself in the equations in the form of indices characterizing the atmospheric circulation for the period December-April: $AD_W$, $AO_W$, $PNA_W$ and $NAO_W$ (Table 4.7).

Simultaneously with polar cyclones, the baric situation in the Western sector of the Northern Hemisphere also has a significant effect. Let us turn to the physical interpretation of the positive and negative phases of climate indices. As the negative phase of AD and PNA deepens, the pressure over the Kara Sea and the Laptev Sea decreases, and over the Canadian Arctic Archipelago it increases, the zonal component also weakens and the meridional transport increases, which contributes to the strengthening of winds from the Atlantic towards the Fram Strait (Wallace and Gutzler, 1981; Barnston and Livezey, 1987; Watanabe et al., 2006; Wang et al., 2009) and results in reduced sea ice exports from the Arctic Basin through this strait (Table 4.7 Equations 4.7.1 and 4.7.2). At the same time, the action of the warm AO phase in the previous winter (Table 4.7 Equation 4.7.1) contributes to a greater inflow of warm and saline water from the North Atlantic into the North European Basin (Rigor et al., 2002; Wang and Ikeda, 2000). The combination of these phases of atmospheric circulation

leads to a decrease in the ice coverage of the Greenland and Barents seas (table 4.7 of the equation 4.7.1, 4.7.2, 4.7.4 and 4.7.5).

It is worth noting the latitudinal X and longitude Y coordinates of the position of the Earth's pole included in the equations, which are included in almost all equations (Table 4.7). The relationship between the ice coverage of the seas of the North European basin and these parameters is inverse. With a positive X value, the geostrophic flow has a dominant direction towards the Central Arctic Basin from a latitude of 45° due to a change in the level slope (Maksimov, 1970). This leads to an increase in the inflow of warm Atlantic waters from the North Atlantic into the seas of the North European basin and, accordingly, contributes to a decrease in ice coverage. Which is modeled in the presented equations.

For positive values of the nutation parameter $\Delta\varepsilon$, the ocean level, on the contrary, to the latitude 45° from the center of the Arctic Ocean, in which case the dominant flow direction – southwestern, which contributes to increased ice removal from the Arctic basin, leading in turn to an increase in ice coverage in the seas of the North European basin.

Let us return to the assessment of the information content of the predictors of the obtained ice coverage models for the Greenland Sea. Latitudinal coordinate of the position of the Earth's pole X (Equation 4.7.1, Table 4.7). The contribution of this parameter is estimated at 8%. The use of both previous ice and hydrometeorological conditions (described above) and astrogeophysical parameters made it possible to achieve up to 87% reliability of the constructed equations, which is a high indicator of the quality of the model.

In the course of the next experiment, the previous ice coverage was excluded from the predictors (Equation 4.7.2). In this case, the correlation coefficient decreases from 0,87 to 0,82, and the skill from 87% to 79% (Table 4.7, Equation 4.7.2, with a tolerance level of 0,67σ), but the remaining set of predictors also has enough high information content (correctness exceeds the threshold of 68%) (Manual on the service of forecasts, 2011).

Equation 4.7.3 was obtained after excluding the previous ice coverage and atmospheric circulation indices. The qualitative indicators of which decreased, but not significantly (the accuracy dropped to 77%, and the coefficient of determination to 0,65), despite the small number of predictors, equal to three. Similarly, an equation consisting of three characteristics for the variability of the ice coverage in the Barents Sea was obtained (table 4.7, equation 4.7.6). In general, the final three-predictor equations are structurally similar: the surface temperature of the atmosphere, the inflow of Atlantic waters, and the heliophysical parameter. Only in the case of the ice coverage of the Barents Sea, instead of the longitudinal characteristic of the Earth's nutation, the latitudinal coordinate of the position of the Earth's pole is used, and the qualitative characteristics of the model are slightly higher (correction rate 88%, coefficient of determination 0,68).

The experiment shows that with the help of only three predictors in physical-statistical models it is possible to describe quite informatively the long-term variability of the ice coverage in both the Barents and Greenland seas.

*Statistical models of the winter season*

Statistical equations of long-term ice coverage variability in the winter season of the seas of the North European Basin with hydrometeorological and astrogeophysical factors for the period 1951–2021 are presented in Table 4.8.

For the winter period (December–April), equations 4.8.1–4.8.6 in Table 4.8 used as predictors: the inflow of warm Atlantic waters (index *AMO*) with a lead time of 4 years for the Greenland Sea and 2 years for the Barents Sea, surface air temperature (Greenland *T* and Norwegian Seas $T_N$), previous year's solar activity represented by Wolf numbers *W*. These predictors enter the equation with a minus sign, i.e. positive anomalies of these predictors cause a decrease in ice coverage. The equations also include the ice coverage of the autumn period (prehistory $L_{AUT-1}$) (equation 4.8.2) with a plus sign. This means that a large ice coverage in the autumn of the previous year leads to an increased ice coverage in the subsequent winter period, which is confirmed by a rather high inertia (see paragraph 3, table 3.2).

Atmospheric circulation indices such as the Arctic Dipole *AD*, the Arctic Oscillation *AO*, the North Atlantic Oscillation *NAO* and the Pacific-North American Oscillation *PNA* also make important contributions. Together, these global climate indices characterize the baric situation and the movement of air mass flows in the Northern Hemisphere.

The resulting equations were used to evaluate the contribution of each predictor. For equation 4.8.1, which models the ice cover of the Greenland Sea, the main contribution of 87% to the total variance of the series falls on the surface winter air temperature of the Greenland Sea in the winter season $T_W$. This parameter "interrupts" all the others with its influence and is dominant. The influence of atmospheric circulation remains a very small, albeit no less important, percentage of the contribution of 4%.

At the same time, the influence of Atlantic waters (AMO index) manifests itself with a temporary negative lag of 4 years and is estimated at 9%, 13% and 10%, respectively, for equations 4.8.1, 4.8.2 and 4.8.3 (Table 4.8).

Table 4.8. Static Equations for the Relationship of Winter Ice Coverage Anomalies in the Seas of the North European Basin with Hydrometeorological and Astrogeophysical Factors for the Period 1951–2021.

| № | The equation | R | $R^2$ | P,% |
|---|---|---|---|---|
| | | | | 0,67σ |
| **Greenland Sea, winter (December–April)** | | | | |
| 4.8.1 | $L_W = -0{,}31 \cdot T_W - 0{,}17 \cdot AMO_{-4} + 0{,}23 \cdot AD_{W-1} - 0{,}22 \cdot PNA_W$ | 0,85 | 0,72 | 86 |
| 4.8.2 | $L_W = -0{,}19 \cdot T_W + 0{,}56 \cdot L_{AUT-1} - 0{,}16 \cdot AMO_{-4} - 0{,}39 \cdot Wolf_{-1} + 0{,}44 \cdot \Delta\varepsilon$ | 0,90 | 0,81 | 91 |
| 4.8.3 | $L_W = -26{,}43 \cdot T_W - 159{,}17 \cdot AMO_{-4} + 5593{,}48 \cdot \Delta\varepsilon$ | 0,85 | 0,72 | 87 |
| **Barents Sea, winter (December–April)** | | | | |
| 4.8.4 | $L_W = -0{,}33 \cdot T_W + 0{,}36 \cdot L_{W-1} - 0{,}58 \cdot \Delta\psi + 0{,}80 \cdot AO_{S-1} + 0{,}28 \cdot PNA_W$ | 0,93 | 0,86 | 90 |
| 4.8.5 | $L_W = -0{,}10 \cdot T_{AUT\_N-2} - 0{,}96 \cdot NAO_{W-1} - 0{,}42 \cdot Wolf - 0{,}52 \cdot AO_{AUT-1} + 0{,}11 \cdot AO_{W-1} - 0{,}21 \cdot AMO_{-2}$ | 0,81 | 0,66 | 83 |
| 4.8.6 | $L_W = -0{,}35 \cdot T_W + 0{,}32 \cdot L_{W-1} - 0{,}62 \cdot \Delta\psi$ | 0,92 | 0,84 | 91 |

*Note.* $L_w$ – ice coverage for the winter period (December–April); $L_{AUT}$ – ice coverage for the autumn period (October–November); $T_W$ – surface air temperature for the winter period (December–April); $T_{AUT\_N}$ – surface air temperature for the autumn period (October–November) in the Norwegian Sea; Δε – nutation parameter of the Earth's rotation axis; NAO – North Atlantic Oscillation; AMO – Atlantic Multi-Decade Oscillation index; seasons are denoted in latin letters – S (summer), AUT (autumn), W (winter), SPR (spring); Wolf are Wolf numbers; -1, -2, -3 - leading the parameter by 1, 2 and 3 years, respectively.

In the course of further experiments, atmospheric circulation was excluded from a number of predictors, and a predictor was introduced that characterizes the state of ice coverage in the Greenland Sea in the autumn season (24% contribution). This made it

possible to obtain equation 4.8.2 (table 4.8). As can be seen from the above results, the atmospheric circulation indices of the Arctic Dipole AD and the Pacific-North American Oscillation PNA are successfully replaced by solar activity in the form of Wolf numbers with a delay of one year and the longitudinal parameter of the Earth's nutation $\Delta\varepsilon$ (with a contribution of 7% and 8%, respectively). And the dominant contribution is still made by the surface temperature of the atmosphere in the winter season. $T_W$ 48%. At the same time, the justification of the equation slightly increases, from 86% to 91% (Table 4.8).

It should be noted that the total contribution of atmospheric circulation indices is 4%. In general, it can be said that it is possible to successfully model the variability of the ice cover in the Greenland Sea without using atmospheric circulation indices. In the next experiment, after excluding the ice coverage of the previous autumn season, Equation 4.8.3 was obtained.

The largest contribution to the total dispersion of ice coverage is the surface temperature of the atmosphere, 79%. The nutation parameter of the Earth's axis $\Delta\varepsilon$ and the AMO index with a lead time of 4 years account for a significantly smaller contribution of 11% and 10%, respectively. The performance of the equation is comparable to 4.8.1, where only hydrometeorological characteristics were used without using astrogeophysical parameters as predictors. So the coefficient of determination for these equations is the same and is 0,72. But justification for an acceptable error $0{,}67\sigma$ for 4.8.3 is slightly higher than 87% versus 86%. If we take into account the number of predictors (the smaller their number, the lower the error in the quality of the predictors), then the third version of the equation looks more profitable than the first one with almost equal characteristics of the quality of the models. The use of a set of astrogeophysical and hydrometeorological predictors (Equation 4.8.2), as in the case of the summer season (Table 4.7), makes it possible to simulate the result closest to reality with a 91% justification with an acceptable error $0{,}67\sigma$.

It should be noted that the influence of the inflow of Atlantic waters into the seas of the North European basin manifests itself with different time shifts: after 4 years in the Greenland Sea and 2 years in the Barents Sea in the winter season and 3 years in the summer season for both seas (Tables 4.7 and 4.8) . The fact is that in the winter season, the Icelandic depression deepens and the Siberian anticyclone strengthens, and their interaction leads to an aggravation of the Arctic front (Dobrovolsky and Zalogin, 1982; Nesterov, 2013; Bardin et al., 2015). This leads to an increase in westerly and southwestern winds and contributes to a more intense inflow of Atlantic waters into the Barents Sea. Whereas the inflow of these waters into the Greenland Sea is slowing down. The fluctuations of the warm North Atlantic Current and the cold East Greenland Current show conjugation: as the intensity of the warm current increases, the intensity of the system of cold currents weakens somewhat (Seryakov, 1979). What is manifested in the two-year delay of the AMO index in the equations for the ice cover of the Barents Sea and the four-year delay for the Greenland Sea. In summer, the Icelandic low weakens, and the Siberian anticyclone completely breaks up. The influence of atmospheric circulation is weakening and the inflow of Atlantic warm waters is relatively "comparable" in both seas.

We will demonstrate the productivity of the obtained models of interannual variability of ice cover for four seasons by comparing diagnostic calculations using equations 4.7.1–4.8.6 with actual ice cover data. Graphs of actual and calculated ice cover for the period 1951–2021. The Greenland Sea is shown in Figure 4.7 (a, b), the Barents Sea - Figure 4.7 (c, d). The selected predictors and the constructed physical-statistical equations 4.6.1–4.8.6 are quite informative and describe well the variability of ice cover.

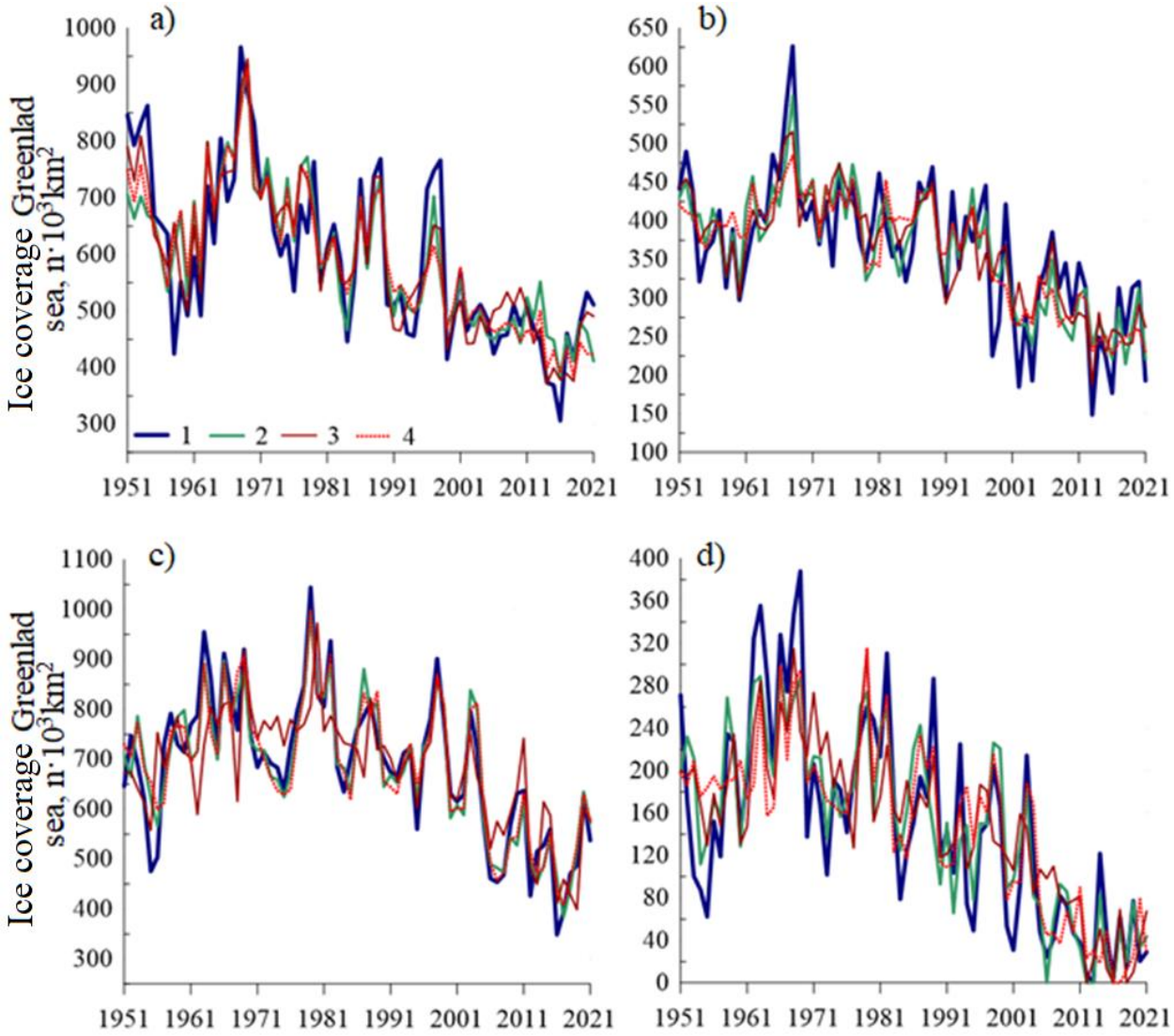


Figure 4.7. Comparison of the actual and equationally reconstructed values of the ice cover of the Greenland (a - winter, b - summer seasons) and the Barents (c - winter, d - summer seasons) seas for the period 1951–2021: 1 - factual data, 2 - equations No. 4._.1, 3 - equations No. 4._.2, 4 - No. 4._.4.

To check the stability of the obtained statistical equations, the following experiment was performed. The time series of predictors was divided into two parts 1951–2000 and 2001–2021. Based on the data for 1951–2000, new numerical coefficients were obtained for the previously obtained statistical equations for the connection between ice coverage and hydrometeorological and astrogeophysical characteristics (Tables 4.6 and 4.8). Next, the ice coverage was calculated for the independent series 2001–2021. The equations for this test were selected with the highest

quality characteristics. As a result, the values of the coefficients of determination have changed somewhat (Table 4.9).

Table 4.9. Criteria for the quality and stability of static equations for the connection of the ice coverage of the seas of the North European basin in winter and summer seasons.

| № equation | R | $R^2$ | P (1951–2000), % | P (2001–2021), % |
|---|---|---|---|---|
| | | | 0,67σ | 0,67σ |
| **Greenland Sea** | | | | |
| 4.7.2 (W) | 0,89 | 0,80 | 89 | 91 |
| 4.5.1 (S) | 0,86 | 0,75 | 84 | 83 |
| **Barents sea** | | | | |
| 4.7.4 (W) | 0,92 | 0,86 | 87 | 93 |
| 4.5.4 (S) | 0,87 | 0,76 | 82 | 80 |

*Note.* W – winter and S – summer seasons; P –justification, R – correlation coefficient; $R^2$ – coefficient of determination.

Some decrease in quality characteristics is associated primarily with a shorter row length (by 20 years). Let's compare the quality characteristics of the models. The coefficient of determination for the equations of ice coverage variability in the Barents and Greenland seas decreased by no more than 0.01. This indicates the high stability of the obtained models.

The justification of the equations obtained from a shorter series was 72–89% (with an allowable error of 0,67σ), which is a high indicator. The indicated values of the parameters are somewhat less than the parameters of the equations obtained on the series for 1951–2021, but also turned out to be satisfactory.

The result obtained testifies to the stability of the obtained statistical equations 4.6.1–4.8.6, at least over the interval of 21 years. A slight decrease in the efficiency of the equations for the 1951–2000 series is most likely due to the fact that this sample does not cover the anomalously warm years of 2007 and 2012.

A graphical representation of the actual and calculated values of the ice coverage variability in the Greenland and Barents Seas is shown in Figure 4.8.

On the whole, the simulated ice coverage repeats the actual variability with a sufficiently high synchronicity. Moreover, this pattern only slightly changes on an independent series, starting from 2001. There are also several years when the model values overestimate the ice area by 0,67σ:

– winter season of the Greenland Sea (Figure 4.8, a) 1958, 1976;

– summer season of the Greenland Sea (Figure 4.8, b) 1954, 1961, 1962, 1974, 1978, 1995, 2002;

– winter season of the Barents Sea (Figure 4.8, c) 1952, 1955, 1987;

– summer season of the Barents Sea (Figure 4.8, d) 1952, 1953, 1986.

The model values *underestimate* the ice coverage by 0,67σ:

– winter season of the Greenland Sea (Figure 4.8, a) 1996;

– summer season of the Greenland Sea (Figure 4.8, b)1998, 2006, 2009, 2019;

– summer season of the Barents Sea (Figure 4.8, d) 1980, 1993, 1994.

It is interesting that the model values of ice coverage up to 2002 never underestimate the size of the ice area. And the 1950s are modeled worst of all, especially the first half, as well as ice coverage in the summer season for both seas.

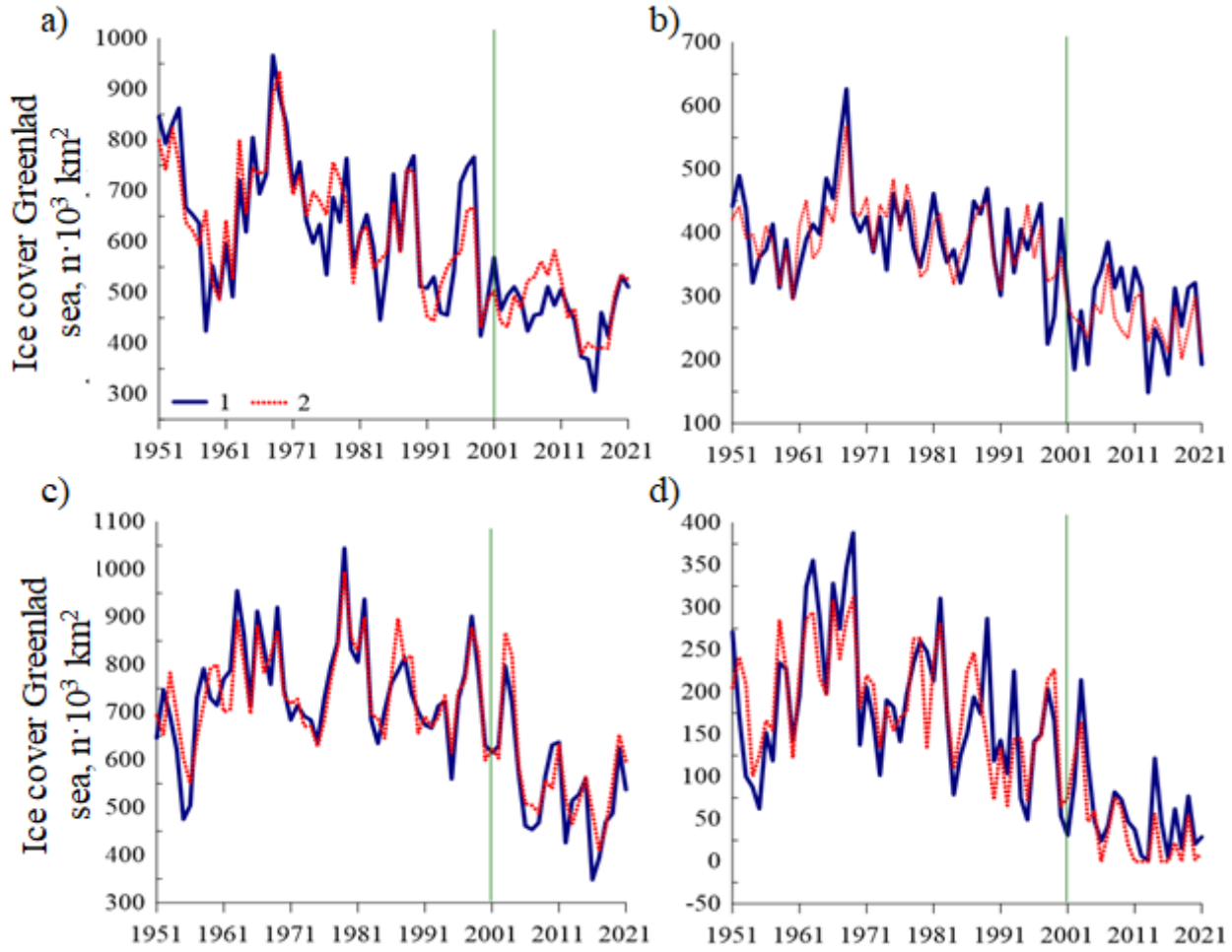


Figure 4.8. Comparison of actual and equationally reconstructed ice cover values of the Greenland (a – winter, b – summer seasons) and Barents (c – winter, d – summer seasons) seas for the period 1951–2021: 1 – factual data, 2 – simulated area by equations.

*Note*. The green vertical line marks the boundary between the dependent (1951–2000) and independent (2001–2021) samples.

Let us compare the obtained results with some models of other authors. (Sandø et al., 2014) suggest that the influence of the ocean on changes in ice coverage in terms of freezing and melting is more dominant than the atmosphere, including in relation to long-term variability. In the models described by us, the ratio of the influence of the ocean and the atmosphere is assumed to be more equivalent and varies depending on the season. The authors of another work (Glock et al., 2019), as in our study, use the

thermal state in more southern latitudes to model ice coverage variability, suggesting using sea surface temperature anomalies in the region of 5–25°N and 20–60° W as the main predictor. The proposed models have fairly high quality indicators, the justification on an independent sample was 64–93%. In the models proposed in our work, the justification on an independent sample exceeds 95%. Presumably, this difference in the results is due to the fact that in the work (Glock et al., 2019) the lead time is up to 32 months, and the models do not include astrogeophysical parameters. Based on the physical-statistical model (Onarheim et al., 2015), a forecast of the ice coverage in the Barents Sea for one year was developed. The main predictors are proposed to use heat transfer in the ocean and meridional air transfer, which has a direct impact on the increase or decrease in heat input. However, sea currents stand out as the dominant factor. The security of the proposed regression models is 88%. Researchers of the Greenland Sea, considering the variability of ice volume and sea temperature (Selyuzhenok et al., 2020), highlight the influence of the North Atlantic Oscillation (NAO index) as a special role. The authors suggest that the simultaneous increase in ice drift from the Arctic Basin through the Fram Strait and an increase in heat fluxes from the North Atlantic are associated with a higher intensity of atmospheric circulation during the positive phase of the North Atlantic Oscillation (NAO index). In (Pope et al., 2020 ) it is also noted that atmospheric circulation is the key driver for increasing the flow of heat from the North Atlantic to the Greenland Sea.

Summing up, we can conclude that the influence of the inflow of Atlantic waters (including heat fluxes) and the variability of atmospheric circulation are used as the main predictors in all works. On the whole, our models take into account the dominant factors that form climatic variability for both ice coverage and SST of the seas of the North European Basin and have similar results with other authors.

# CONCLUSIONS

A working database has been compiled for the period 1951–2021, which includes: the studied characteristics (ice coverage and sea surface temperature of the seas North European basin); hydrometeorological characteristics (atmospheric circulation indices (NAO North Atlantic Oscillation, AO Arctic Oscillation Index, AD Arctic Dipole, PNA Pacific-North American Oscillation); North Atlantic Thermal State Index (AMO Atlantic Multidecadal Oscillation); surface heat balance for the seas of the North European Basin); astrogeophysical characteristics (parameters of the Earth's orientation; Solar activity (Wolf number W); change in the distance from the Earth to the Sun).

For interannual changes in the ice area and surface water temperature of the seas of the North European Basin in the winter and summer seasons, the presence of a linear trend and polycyclic oscillations are confirmed. The identified cycles in the ice coverage and SST of the seas of the North European Basin are associated with fluctuations with periods of atmospheric circulation indices, such as the Arctic Oscillation and the Arctic Dipole: 18, 14, 10, 9 and 7 years. The seven-year cycle also stands out in the Pacific-North American Oscillation. A fluctuation with a period of 8–14 years stands out in all rows of the compiled database.

Statistical relationships were obtained between the interannual variability of both the ice coverage and sea surface temperature, not only with hydrometeorological factors, but also with astrogeophysical parameters. High significant cross-correlation coefficients (up to 0.62) of ice coverage and sea surface temperature with astrogeophysical parameters give reason to believe that there is a relationship between them and the need to include them among the predictors when developing physical and statistical equations to describe long-term changes in seasonal ice coverage and sea surface temperature of the seas North European basin.

Eight regions of the North European Basin have been identified, which have their own characteristics in hydrometeorological and ice regimes. The result will allow further studies to improve the quality of the equations modeling the surface temperature variability, which will help the development of long-term forecasts.

For the first time, physico-statistical equations of the long-term variability of the sea surface temperature and ice coverage of the seas of the North European Basin were obtained not only with hydrometeorological, but also with astrogeophysical factors. The justification of the developed models ranges from 77 to 92% for ice coverage and from 78 to 93% for sea surface temperature. Model data describe a high percentage of the total dispersion of long-term fluctuations in ice coverage (up to 86%) and sea surface temperature (up to 80%) in the seas of the North European Basin.

A sufficiently high information content of the predictors included in the equations for both ice coverage and SST was revealed. The largest contribution (from 23% to 87%) to the total dispersion of ice coverage is made by the ice coverageof the previous season. In models where the predictor “ice coverage of the previous season” was excluded, the contribution to the total dispersion of hydrometeorological factors was up to 94%, and the contribution of astrogeophysical factors was up to 60%. In this case, the contributions of the nutation parameter of the Earth's axis, the longitude and latitude coordinates of the position of the Earth's pole, and the Wolf number can reach 42, 43, and more than 8%, respectively.

The proposed approach to the construction of physical-statistical models for describing long-term fluctuations on the example of ice coverage and sea surface temperature of the seas of the North European basin has shown itself quite well. And the proposed statistical models can be used both for diagnosis and as a basis for developing forecasting methods with a long lead time of two or more years ahead. That requires further research in the proposed direction.

***Acknowledgments*:**

— Ministry of Education and Science of the Russian Federation (Russian-German project CATS (The Changing Arctic Transpolar System) – RFMEFI61617X0076);

— NITR of Roshydromet 5.1 Development of models, methods and technologies for monitoring and forecasting the state of the atmosphere, ocean, sea ice coverage, glaciers and permafrost (cryosphere), processes of ice interaction with natural objects and engineering structures for the Arctic and technologies for hydrometeorological support of consumers;

— Russian Science Foundation within the framework of the scientific project "Investigation of the state of the ice coverage of the Greenland and Barents Seas in the context of modern climate change" № 22–27–00443.

## REFERENCES


1. Abdusamatov Kh. I. The sun dictates the climate of the Earth. SPb.: Publishing house «Logos». – 2009. – 197 p. (in rus).
2. Abramov V.A., Zakharov V.F. On the question of the relationship between changes in water temperature in the North Atlantic and the area of polar ice // Proceedings of the AARI. – 1981. – T. 372. – pp. 5-17 (in rus).
3. Averkiev A. S. et al. Guidelines for the use of the method of ultra-long-term forecasting of hydrometeorological elements and the software package "Prism" //Ed. A.S. Averkiev, V.M. Bulaeva and others - Murmansk: PINRO. – 1997. – 39 p. (in rus).
4. Aksenov P. V., Ivanov V. V. “Atlantification” as a probable reason for the reduction in the area of sea ice in the Nansen basin in the winter season //Problems of the Arctic and Antarctic. – 2018. – T. 64. – №. 1. – pp. 42-54 (in rus).
5. Alekseev G. V. et al. The influence of the Atlantic on warming and the reduction of sea ice cover in the Arctic //Ice and Snow. – 2017. – T. 57. – №. 3. – pp. 381-390 (in rus).
6. Alekseev G. V. et al. Natural and anthropogenic components of changes in surface air temperature in the Arctic in the 20th century according to observations and modeling // Proceedings of the AARI. – 2003. – T. 446. – pp. 22-30 (in rus).
7. Alekseev G.V., Korablev AA Oceanographic conditions for the development of deep convection //Regularities of large-scale processes in the Norwegian energy-active zone and adjacent areas. St. Petersburg: Gidrometeoizdat. – 1994. – 79 p. (in rus).
8. Alekseev G. V. Manifestation and strengthening of global warming in the Arctic //Fundamental and applied climatology. – 2015. – №1. – pp. 11-26 (in rus).
9. Alekseev G.V., Glock N.I., Smirnov A.V., Vyazilova A.E. Influence of the North Atlantic on climate fluctuations in the Barents Sea and their predictability //Meteorology and Hydrology. – 2016 – T. 8. – pp. 38-56 (in rus).

10. Alekseev G.V., Nikolaev Yu.V., Romantsov V.A. Norwegian energy active zone //Results of science and technology. Atmosphere, ocean, space: The "Cuts" program. – M.: Nauka. – 1985. – T. 3. – pp. 45-52 (in rus).
11. Atlas of the oceans. Arctic Ocean. GUNIO MO USSR. – 1980. – 190P. (in rus).
12. Baranov E. N. Structure and dynamics of the waters of the Gulf Stream //M.: Gidrometeoizdat. – 1988. – 252 p. (in rus).
13. Bardin M. Yu., Platova T. V., Samokhina O. F. Peculiarities of the variability of cyclonic activity in the temperate latitudes of the Northern Hemisphere associated with the leading modes of atmospheric circulation in the Atlantic-European sector //Fundamental and applied climatology. – 2015. – T. 2. – pp. 14-40 (in rus).
14. Bashmachnikov I. L. et al. Seasonal and interannual variability of heat fluxes in the Barents Sea area. Izvestiya Rossiiskoi Akademii Nauk. Physics of the atmosphere and ocean. – 2018. – T. 54. – №. 2. – pp. 239-250 (in rus).
15. Belov A. A., Ballod B. A., Elizarova N. N. Probability theory and mathematical statistics: textbook //Modern problems of science and education. – 2009. – №. 1. – 53-54 p. (in rus).
16. Berezkin, V.A., Greenland Sea and the Polar Basin, Tr. The first high-latitude expedition to "Sadko". – L.: – 1939. – №. 1935. – 167 p. (in rus).
17. Boytsov V.D. Variability of water temperature in the Barents Sea and its impact on the biological components of the ecosystem //Abstract of the thesis. diss… doc. geogr. Sciences. St. Petersburg. – 2009. (in rus).
18. Boytsov V.D. Cosmogeophysical factors and interannual fluctuations in water temperature in the Barents Sea //Fishery. – 2007. – № 1. – pp. 57-60 (in rus).
19. Bochkov Yu. A. On long-term oscillations of the thermals of the Barents and Norwegian seas//Tr./PINRO. – 1964a. – Release 16. – pp. 277-288 (in rus).

20. Bochkov Yu. A. Long-term changes in thermals in the southern part of the Barents Sea //Materialy fish farm. research northern basin – Release 4. – Murmansk. – 1964b. – pp. 86-89 (in rus).
21. Bochkov Yu. A. Super-long-term forecasts of water temperature in the Kola meridian section //Methodological recommendations for forecasting water temperature in the Northern fishing basin. – Murmansk. – 1979. – pp. 125-164 (in rus).
22. Bochkov Yu. A. Long-term average water temperature of the section along the Kola meridian for a period of 90 years (1871-1961) for a layer of 0-200 m //Materialy fish farm. research northern basin – Release 2. – Murmansk. – 1964b. – pp. 62-67 (in rus).
23. Bochkov Yu. A. Accounting for 11-year fluctuations in solar activity in the background forecasts of water temperature in the Barents Sea // Proceedings of PINRO. – 1978. – Release40. pp. – 33-43 (in rus).
24. Brockhaus F. A. Encyclopedic Dictionary of Brockhaus and Efron. – Ripol Classic. – 2013. (in rus).
25. Buzin I. V. Assessment of the state of the ice cover and conditions for the formation of heavy ice seasons in the Barents Sea //Dissertation. Cand. Geogr. Nauk, AARI. – 2008. (in rus).
26. Buzin I. V., Gudkovich Z. M. Seasonal features of climatic changes in the Barents Sea //Problems of the Arctic and Antarctic. – 2011. – №. 3. – pp. 20-32 (in rus).
27. Bulaeva V.M. On the possibility of ultra-long-term forecasting of water temperature in the northeast Atlantic //Proceedings of the Leningrad State Medical Institute. – 1987. – Release 99. – pp. 21-99 (in rus).
28. Vainovsky P. A., Malinin V. N. Methods of processing and analysis of oceanological information. Multivariate analysis. – 1992. – 96 p. (in rus).
29. Vize, V. Yu., The Significance of the Spring Ice Regime in the Greenland Sea and the East Icelandic Current for Air Temperature in the Subsequent Winter in Europe //Izv. Russian Hydrological Institute. – 1925. – № 14. (in rus).

30. Vize V. Yu. Climate of the seas of the Soviet Arctic. – Glavsevmorputi. – 1940. – 124 p. (in rus).
31. Vize V. Yu. Ice in the Barents Sea and air temperature in Europe //Izvestia Center, Hydrometeorological Bureau. – 1924. – №. III. – 10 p. (in rus).
32. Vize V. Yu. Seas of the Soviet Arctic //M .: Glavsevmorput. – 1948. – 200 p.
33. Vize V. Yu. On the possibility of predicting the state of ice in the Barents Sea. Izv. Center. hydromet. the Bureau. – 1923. – №. 1. – pp. 1-41 (in rus).
34. Vize V. Yu. Fundamentals of long-term ice forecasts for the Arctic seas // Proceedings of AARI. – 1944. – T. 190. – 273 p. (in rus).
35. Vize V.Yu. On the importance of a systematic study of the Barents Sea for meteorological and hydrological forecasts //Research of the Seas of the USSR. – 1930. – № 11. (in rus).
36. Voeikov A. I. Selected works. Climates of the Globe, in particular Russia //M.-L.: Izd. USSR Academy of Sciences. – 1948. – T.1. – 751 p. (in rus).
37. Vyazigina N. A. et al. Informativity of hydrometeorological and astrogeophysical factors in the problem of describing interannual fluctuations in the ice cover of the Greenland Sea //Ice and Snow. – 2021. – T. 61. – №. 3. – pp. 431-444 (in rus).
38. Vyazilova A. E., Smirnov A. V. Conditions for the formation of anomalous desalination in the NEB // Proceedings of the Hydrometeorological Research Center of the Russian Federation. – 2016. – №. 361. – pp. 192-202 (in rus).
39. Gvozdeva V. G., Kondratovich K. V., Krylova V. V., Seryakov E. I., Bochkov Yu. A. Development of methods for long-term forecasting and making operational forecasts of water temperature in the Barents and Norwegian Seas. Northern Basin research. – 1970. – Release 16. – pp. 26-38 (in rus).
40. Terziev F. S., Girdyuka G. V. Hydrometeorology and hydrochemistry of the seas of the USSR. Barents Sea //L.: Gidrometeoizdat. – 1990. – T.1. – Release 1. – 280 p. (in rus).

41. Glock N. I., Alekseev G. V., Vyazilova A. E. Seasonal forecast of ice coverage in the Barents Sea //Problems of the Arctic and Antarctic. – 2019. – T. 65. – №. 1. – pp. 5-14 (in rus).
42. Golubev V.A., Zhevnovaty V.T. Fuchs Yu.A. Inertial method for forecasting water temperature in the southern part of the Barents Sea // Proceedings of AARI. – 1980. – T. 348. – pp. 70-74 (in rus).
43. Gordeeva S. M. Statistical methods of processing and analysis of hydrometeorological information: textbook [in the discipline Statistical methods of processing and analysis of hydrometeorological information] //St. Petersburg: RSHU. – 2010. – 74 p. (in rus).
44. Gudkovich Z. M. et al. Changes in the sea ice cover and other components of the climate system in the Arctic and Antarctic in connection with the evolution of polar vortices //Problems of the Arctic and Antarctic. – 2008. – №. 1. – 48 p. (in rus).
45. Gudkovich Z. M. et al. On the nature and causes of changes in the Earth's climate //Problems of the Arctic and Antarctic. – 2009. – №. 1. – pp. 15-23 (in rus).
46. Gudkovich Z. M., Karklin V. P., Frolov I. E. Intrasecular climate changes, ice cover areas of the Eurasian Arctic seas and their possible causes //Meteorology and Hydrology. – 2005. – № 6. – pp. 5-14 (in rus).
47. Gudkovich Z. M., Kovalev E. G., and Nikiforov E. G., “On the relationship between the angular velocity of the Earth’s rotation and climate change,” Izv. R.G.S. – 2004. – №. 6. – pp. 1-10 (in rus).
48. Gudkovich Z. M., Nikolaeva A. Ya. Ice drift in the Arctic basin and its relationship with the ice cover of the Soviet Arctic seas //Proceedings AARI. – 1963. – T. 104. – pp. 5-186 (in rus).

49. Gudkovich Z.M., Sarukhanyan E.I., Smirnov N.P. "Polar tide" in the atmosphere of high latitudes and fluctuations in the ice cover of the Arctic seas // Dokl. USSR Academy of Sciences. – 1970. – T. 190. – № 4. – pp. 954-957 (in rus).
50. Dementiev A.A., Zubakin G.K. Assessment of long-term fluctuations of some climate-forming factors of the North European Basin // Proceedings AARI. 1987. – T. 404. – pp. 24-33 (in rus).
51. Dobrovolsky A. D., Zalogin B. S. Seas of the USSR. //M.: MGU Publishing House. – 1982. – 192 p. (in rus).
52. Dobrovolsky A. D., Zalogin B. S. Regional Oceanology //M.: MGU Publishing House. – 1992. – 224 p. (in rus).
53. Egorov A.G. Solar cycle and long-term baric wave in the surface atmosphere of the Arctic // Reports of the Academy of Sciences. Federal State Budgetary Institution"Russian Academy of Sciences". – 2003. – T. 393. – №. 3. – pp. 402-406 (in rus).
54. Egorov A.G. The solar cycle and two regimes of long-term changes in surface pressure in high and temperate latitudes of the northern hemisphere of the Earth in winter //Reports of the Academy of Sciences. – 2007. – T. 414. – № 3. – pp. 402-407 (in rus).
55. Egorov A.G. Spatial position of the ice edge in August - September in the eastern seas of Russia at the beginning of the 21st century. //Problems of the Arctic and Antarctic. – 2020. – T. 66. – Release 1. – pp. 38-55 (in rus).
56. Egorov A.G. Solar-induced changes in surface air pressure in the Arctic and long-term features of the distribution of ice in the Arctic seas of Russia in summer // Meteorology and Hydrology. – 2005. – № 8. – pp. 14-24 (in rus).
57. Zalogin B.S., Kosarev A.N. Morya //M.: Thought. – 1999. – 400 p. (in rus).
58. Zakharov V.F. Ices of the Arctic and modern natural processes //L.: Gidrometeoizdat. – 1981. – 136 p. (in rus).
59. Zolotokrylin A.N., Titkova T.B., Mikhailov A.Yu. Climatic variations of the Arctic front and ice coverage of the Barents Sea in winter // Ice and snow. –2014. – № 1. – pp. 85-90 (in rus).

60. Zubakin G.K. Large-scale variability of the state of the ice cover of the seas of the North European basin //L .: Gidrometeoizdat. – 1987. – 160 p. (in rus).
61. Zubakin G.K., Buzin I.V., Skutina E.A. Seasonal and long-term variability of the state of the ice cover of the Barents Sea // Ice formations of the Western Arctic seas, ed. G.K.Zubakina. - St. Petersburg: AARI. – 2006. – pp. 10-26 (in rus).
62. Zubov N. N. The problem of long-term ice forecasts. //Soviet Arctic. – 1935. – №. 1. (in rus).
63. Zubov N.N. Ices of the Arctic // M.: Izd. Glavsevmorputi. – 1945. – 360P. (in rus).
64. Ivanov V. V. Modern changes in hydrometeorological conditions in the Arctic Ocean associated with the reduction of sea ice cover //Hydrometeorology and Ecology. – 2021. – №. 64. – pp. 407-434 (in rus).
65. Ivanov V. V., Alekseev V. A., Repina I. A. Increasing impact of Atlantic waters on the ice cover of the Arctic Ocean //Turbulence, Atmospheric and Climate Dynamics. – 2014. – pp. 336-344 (in rus).
66. Ivanov V. V., Repina I. A. Strengthening the "atlantification" of the Arctic Ocean // Turbulence, Atmospheric and Climate Dynamics. – 2018. – 187-187 pp. (in rus).
67. Izhevsky G.K. On the early determination of the type of regime of the Barents Sea // Fishery. –1957. – № 12. – pp. 48-55. (in rus).
68. Izhevsky G.K. Oceanological foundations of the formation of commercial productivity of the seas //M .: Pishchepromizdat. – 1961. – 216 p. (in rus).
69. Official website of the representative office of StatSoft Inc. on the territory of Russia and CIS countries [Internet resource] http://statsoft.ru/. Date of the application: 23.04.2020.
70. Solar dynamics, climate and science in real time [Internet resource] https://www.attivitasolare.com/raffreddamento-corso-il-punto-della-situazione/. Date of the application: 14.05.2021.
71. Karakash A.I. The ice coverage of the Greenland Sea and the Possibility of Predicting the State of Ice in the Seas of the Western Sector of the Arctic //Release CIP. – 1950. – Release 17. – pp. 40-55 (in rus).

72. Karakash A.I. Method for predicting water temperature in the Barents Sea //Release CIP. – 1957. – Release 57. – pp. 3-59 (in rus).
73. Karakash A.I. Forecast of water temperature in the Barents Sea //Proceedings of the Hydrometeorological Center of the USSR. – 1976. – Release 182. – pp. 93-96 (in rus).
74. Karsakov A.L., Sentyabov E.V., Bochkov Yu.A. Temperature of the surface of the North Atlantic and long-term forecasting of abiotic and biotic parameters of the ecosystem of the Northern Basin // Proceedings of the reporting session of PINRO based on the results of research work in 1998–1999. - Murmansk: Ed. PINRO. – 2000. – pp. 188-199 (in rus).
75. Kirillov A. A., Khromtsova M. S. On the long-term variability of the ice cover of the Greenland Sea and the method of its forecast //Proceedings AARI. – 1970. – T. 303. – pp. 46-54 (in rus).
76. Kirillov A.A., Khromtsova M.S. Ice cover of the Greenland Sea and methods of its prediction //Research report. - AARI funds. – L. – 1973. – 27 p. (in rus).
77. Lappo S.S., Gulev S.K., Rozhdestvensky A.E. Large-scale thermal interaction in the ocean-atmosphere system and energy-active regions of the World Ocean //L:.Gidrometeoizdat. – 1990. – 335 p. (in rus).
78. Lebedev S. A., Kostyanoy A. G., and Popov S. K., Satellite altimetry of the Barents Sea //in the book The Barents Sea System, edited by Lisitsyn A.P., M., GEOS – 2021. – pp. 194-212 (in rus).
79. Lebedev A. A., Uralov N. S. Forecasting the ice cover of the Greenland Sea in connection with the peculiarities of the thermal state of the Atlantic Ocean and atmospheric circulation // Problems of the Arctic and Antarctic. – 1977. – Release 50. – pp. 36-39 (in rus).
80. Lebedev A.A. Conditions for the formation of large anomalies in the water temperature of the Barents Sea // St. Petersburg. – AARI funds. – 1993. – 35 p. (in rus).
81. Lebedev A.A., Uralov N.S. Results of the assessment of the annual ice exchange cycle of the Arctic Basin with the seas of the North Atlantic //Proceedings AARI. – 1981. – T. 384. – pp. 78-89 (in rus).

82. Lebedev A.A., Mironov E.U. Climatic changes in the area of ice in the Barents Sea. //Abstracts of reports. 3 int. conf. "Development of the shelf of the Arctic seas of Russia". St. Petersburg: Ed. Central Research Institute. ak. A.N. Krylova. – 1997. – pp. 216-217. (in rus).
83. Lebedev A.A., Uralov N.S. On the features of the thermal state of the North Atlantic and atmospheric circulation during the formation of anomalous ice cover in the Greenland Sea //Proceedings AARI. – 1976. – T. 320. – pp. 47-64. (in rus).
84. Lebedev A.A., Uralov N.S. Patterns of formation of significant ice cover anomalies in the Greenland and Barents Seas // Research report. - AARI funds. – L. – 1972. – 184 p. (in rus).
85. Lipatov M. A., Volkov V. A., Mai R. I. Linear trends in the drift field of the ice cover in the Arctic Ocean //Oceanology. – 2021. – T. 61. – №. 3. – pp. 341-349 (in rus).
86. Lis N. A., Egorova E. S. Climatic variability of the ice coverage of the Barents Sea and its individual regions //Problems of the Arctic and Antarctic. – 2022. – T. 68. – №. 3. – pp. 234-247 (in rus).
87. Loginov V.F. Cosmic factors of climatic changes. – Minsk: Belarus. science. – 2020. – 168 p. (in rus).
88. Maksimov I. V., Geophysical Forces and Waters of the Ocean. - L .: Gidrometeoizdat. – 1970. – 447 p. (in rus).
89. Maksimov I.V. et al. Nutational migration of the Icelandic minimum of atmospheric pressure //Reports of the Academy of Sciences. - The Russian Academy of Sciences, 1967. – T. 177. – №. 1. – pp. 88-91 (in rus).
90. Malinin V. N., Gordeeva S. M. Physico-statistical method for forecasting oceanological characteristics (on the example of the North European basin). – Murmansk: PINRO Publishing House. – 2003. – 164 p. (in rus).
91. Malinin V. N., Shmakova V. Yu. Variability of energy-active zones of the ocean in the North Atlantic //Fundamental and applied climatology. – 2018. – T. 4. – pp. 55-70 (in rus).

92. Medvedev I. P., Kulikov E. A., Rabinovich A. B., Lapshin V. B. Chandler beats and pole tide in the North and Baltic Seas //Heliogeophysical Research. – 2018. – Release 18. – pp. 9-17 (in rus).

93. Guidelines for forecasting water temperature in the Northern Fishing Basin. – Murmansk: PINRO. – 1979. – Release 1. – 172 p. (in rus).

94. Mironov E. U. Ice conditions in the Greenland and Barents seas and their long-term forecast. - St. Petersburg: AARI. – 2004. – 320 p. (in rus).

95. Mironov E.U. Variability of ice conditions near the southwestern coast of Greenland due to hydrometeorological processes of various scales //Proceedings AARI. – 1979. – T. 363. – pp. 47-62 (in rus).

96. Mironov E.U. On the Possibility of Predicting Major Anomalies in the Greenland Sea //Proceedings AARI. – 1994. – T. 432. – pp. 96-106 (in rus).

97. Mironov E.U., Babko O.I., Tyuryakov A.B. Homogeneous ice regions of the Greenland and Barents Seas //Proceedings AARI. – 1997. – T. 437. – pp. 45-60 (in rus).

98. Mironov E.U., Lebedev A.A., Babko O.I. Patterns of formation of ice conditions in the Barents Sea and their long-term forecasting //Proceedings AARI. – 1998. – T. 438. – pp. 26-40 (in rus).

99. Mironov E.U., Tyuryakov A.B. The main patterns of formation of ice conditions in the Pechora Sea and their long-term forecast // Proceedings AARI. – 1998. – T. 438. – pp. 41-50 (in rus).

100. Mikhailova N. V., Bayankina T. M., Sizov A. A. Two regimes of interaction between the atmosphere and the ocean in the Atlantic sector of the Arctic basin // Oceanology. – 2021. – T. 61. – №. 4. – pp. 509-516 (in rus).

101. Forecast service guide. Section 3, Part III Marine Hydrological Forecast Service. GD 52.27.759-2011. (in rus).

102. Nesterov E. S. Polar cyclones: observations, reanalysis, modeling // Hydrometeorological research and forecasts. – 2020. – №. 1. – pp. 65-82 (in rus).

103. Nesterov E. S., North Atlantic Oscillation: Atmosphere and Ocean. M. Publishing house Triada. – 2013 – 144 p. (in rus).
104. Nikiforov E. G., Stereodynamic System of the Arctic Ocean. – AARI – 2006. – 176 p. (in rus).
105. Nikiforov E.G., Shpeikher A.O. Regularities of the formation of large-scale fluctuations in the hydrological regime of the Arctic Ocean. - Gidrometeoizdat - 1980. – 270 p. (in rus).
106. Petrukovich A. A., Dmitriev A. V., Struminsky A. B. Solar-terrestrial communications and space weather // Plasma heliophysics. – 2008. – T. 1. – pp. 175-257 (in rus).
107. Potanin V.A. About Possibilities of long-term forecast of the ice cover in the Barents Sea//Proceedings of the AARI. – 1987. –T.410. – 117-124 pp. (in rus).
108. Prokofiev O. M., Tregubova M. V., Chernichenko A. V. Long-term dynamics of the ice cover of the Barents Sea under the conditions of modern climate change // International scientific journal "Symbol of Science". – 2015. – T. 5. – pp. 262-264 (in rus).
109. Pudovkin M. I., Raspopov O. M. Mechanism of the impact of solar activity on the state of the lower atmosphere and meteorological parameters // Geomagnetism and aeronomy. – 1992. – T. 32. – №. 5. – pp. 1-22 (in rus).
110. Pudovkin M.I. Influence of solar activity on the state of the lower atmosphere and weather //Soros Educational Journal. – 1996. – № 10. – 106-112 pp. (in rus).
111. Rubashev B.M. Problems of solar activity. //M.-L.: Science. – 1964. – 362 p. (in rus).
112. Santsevich T.I., Khromtsova M.S., Moskal G.I. Fluctuations in the ice cover of the Barents Sea. // L.: Sea transport. – 1980. – 120 p. (in rus).
113. Sentyabov E.V., Bochkov Yu.A., Karsakov A.L. Coupling of large-scale changes in the thermals of the waters of the Norwegian and Barents Seas and its use in long-term forecasting of water temperature in the Barents Sea//Abstract

report X International Conf. on commercial oceanology. – M.: VNIRO. – 1997. – 114 p. (in rus).

114. Seryakov E. I. Long-term forecasts of the thermal state in the North Atlantic. //L.: Gidrometeoizdat. – 1979. – 165p. (in rus).
115. Sizov A.A. et al. Processes that determine the synchronous interdecadal variability of the surface temperature of the Barents and Black Seas // Marine Hydrophysical Journal. – 2022. – T. 38. – №. 3 (225). – pp. 276-290 (in rus).
116. Sleptsov-Shevlevich B.A., Boyarinov A.M. Solar wind, Earth's rotation and climate //St. Petersburg: Typography Blank Publishing House. – 2002. –159 p. (in rus).
117. Smirnov N.P., Vainovsky P.A., Titov Yu.E. Statistical analysis and forecast of oceanological processes. //St. Petersburg: Gidrometeoizdat. – 1992. – 198 p. (in rus).
118. Smirnova Yu. E. et al. Statistical characteristics of polar cyclones in the seas of the North European basin according to data from satellite microwave radiometers. – 2016. – №. 3. – pp. 27-36 (in rus).
119. Sustavov Yu.V. Physico-statistical model of water temperature variability in the Barents Sea and a method for calculating and predicting its components // Proceedings of the State Institute of Industries. – 1978. – Release 147. – pp. 34-44 (in rus).
120. Sustavov Yu.V. Physico-statistical method for predicting water temperature in the Barents Sea // Proceedings of LSMU. – 1985. – Release 91. – pp. 52-76 (in rus).
121. Timokhov L. A. et al. Dynamic ocean topography and surface geostrophic circulation in the Arctic basin in 2007–2011. //Problems of the Arctic and Antarctic. – 2012. – №. 3. – pp. 75-86 (in rus).
122. Timokhov L.A., Vyazigina N.A., Mironov E.U., Popov A.V. Peculiarities of seasonal and interannual variability of the Greenland Sea ice cover // Ice and Snow. – 2018. – T. 58. – №. 1. – pp. 127-134 (in rus).

123. Timokhov L.A., Borodachev V.E., Borodachev I.V., Vyazigina N.A., Mironov E.U., Janout M. Role of hydrometeorological factors and solar activity in interannual variability of ice coverage in the East Siberian Sea //Ice and Snow. – 2019a. – T.59. – №2. – C.222-232. (In Russian).

124. Timokhov L.A., Vyazigina N.A., Mironov E.U., Yulin A.V. Climatic changes in seasonal and long-term fluctuations in the ice cover of the Greenland and Barents Seas. //Problems of the Arctic and Antarctic. – 2019b – T.65. – №2. – pp. 148-168 (in rus).

125. Titkova T. B., Mikhailov A. Yu., Vinogradova V. V. Arctic front and ice cover of the Barents Sea in winter // Modern problems of remote sensing of the Earth from space. – 2014. – T. 11. – №. 3. – pp. 117-125 (in rus).

126. Tregubova M. V., Prokofiev O. M., and Mukhina A. V., "Long–term dynamics of ice cover in the Greenland Sea under conditions of modern climate change," Symbol of Science. – 2015. – №. 5. – pp. 265-267 (in rus).

127. Treshnikov A. F. et al. Geographical names of the main parts of the relief of the bottom of the Arctic basin // Problems of the Arctic and Antarctic. – 1967. – №. 27. – p. 5. (in rus).

128. Ugryumov A.I. Thermal regime of the ocean and long–range weather forecasts. – L .: Gidrometeoizdat. – 1981. – p. 17 (in rus).

129. Uralov N. S. Some features of seasonal and long–term variability of the position of the outer boundary of the ice in the Barents Sea. – 1961a. – №. 64. – pp. 39-77. (in rus).

130. Uralov N.S. The role of Atlantic waters in the variability of the ice cover in the Barents Sea. Dissert. cand. geogr. Sciences. – L: LSU. – 1961b. – 305 p. (in rus).

131. Fedorov V. M. Variations in the Earth's insolation and features of their accounting in physical and mathematical models of climate //Uspekhi fizicheskikh nauk. – 2019. – T. 189. – №. 1. – pp. 33-46 (in rus).

132. Fedorov V. M. Insolation of the Earth and modern climate changes. M.: Fismalit. – 2018. – 232 p. (in rus).

133. Fedorov V.M., Bukharov O.E., Bogolyubov D.P., Grebennikov P.B. Experience in medium–term forecasting of changes in the area of sea ice in the Northern Hemisphere based on calculations of incoming solar radiation and neural network modeling //Cryosphere of the Earth. – 2016. – T. 20. – №. 3. – pp. 43-50 (in rus).

134. Fedorova A. D., Popov A. V., Rubchenya A. V. Peculiarities of long–term variability of thermohaline characteristics of waters in the North Atlantic and the Greenland Sea in 1950–2012. //Meteorology and hydrology. – 2015. – №. 9. – pp. 49-58 (in rus).

135. Frolov I.E., Gudkovich Z.M., Karklin V.P., Kovalev E.G., Smolyanitsky V.M. Scientific research in the Arctic. V. 2. Climatic changes in the ice cover of the seas of the Eurasian shelf. – St. Petersburg: "Science". – 2007. – 136 p. (in rus).

136. Fuchs Yu.A. Forecast of monthly average anomalies of water temperature in the secular sections of the Barents Sea //Proceedings of the Hydrometeorological Center of the USSR. – 1980. – Release.221. – pp. 20-26 (in rus).

137. Chernyavskaya E. A. et al. Interannual variability of the characteristics of the surface layer and halocline of the Arctic basin //Problems of the Arctic and Antarctic. – 2020. – T. 66. – №. 4. – pp. 404-426 (in rus).

138. Shapkin B. S. et al. Long–term changes in ice cover in the area of the Spitsbergen and Franz Josef Land archipelagos // Ice and Snow. – 2021. – T. 61. – №. 1. – pp. 128-136 (in rus).

139. Shuleikin V.V. Physics of the sea. – M.: Nauka. – 1968. – 1090P. (in rus).

140. Eigenson M.S. Sun, weather and climate. - L .: Gidrometeoizdat. – 1963. – 276 p. (in rus).

141. Ecological Atlas. Barenc Sea. – M.: «NIR» Foundation. – 2020. – 447 p. (in rus).

142. Yulin A. V. et al. Interannual and seasonal variability of the ice coverage of the Russian Arctic seas in the modern climatic period // Proceedings of the State Oceanographic Institute. – 2019. – №. 220. – pp. 44-60 (in rus).

143. Aksenov Y. et al. On the future navigability of Arctic sea routes: High-resolution projections of the Arctic Ocean and sea ice //Marine Policy. – 2017. – T. 75. – pp. 300-317. (in rus).
144. Yulin A.V., Vyazigina N.A., Egorova E.S. Interannual and seasonal variability of Arctic sea ice extent according to satellite observations //Russian Arctic. – 2019. – №7. – pp. 28-40.
145. Asbjørnsen H. et al. Mechanisms Underlying Recent Arctic Atlantification //Geophysical Research Letters. – 2020. – T. 47. – №. 15. – p. e2020GL088036.
146. Barnston A. G., Livezey R. E. Classification, seasonality and persistence of low-frequency atmospheric circulation patterns //Monthly weather review. – 1987. – T. 115. – №. 6. – pp. 1083-1126.
147. Barton B. I., Lenn Y. D., Lique C. Observed Atlantification of the Barents Sea causes the polar front to limit the expansion of winter sea ice //Journal of Physical Oceanography. – 2018. – T. 48. – №. 8. – pp. 1849-1866.
148. Blindheim J., Osterhus S. The Nordic Seas, main oceanographic features //Geophysical Monograph-American Geophysical Union. – 2005. – T. 158. – p. 11.
149. Britannica E. et al. Britannica Book of the Year 2013. – Encyclopaedia Britannica, Inc., 2013.
150. Darwin G. H. IV. On the dynamical theory of the tides of long period //Proceedings of the Royal Society of London. – 1887. – T. 41. – №. 246-250. – pp. 337-342.
151. Deser C., Teng H. Evolution of Arctic sea ice concentration trends and the role of atmospheric circulation forcing, 1979–2007 //Geophysical Research Letters. – 2008. – T. 35. – №. 2.
152. Frolov I. Ye., Borodachev V. Ye., Mironov Ye. U. Ice regime of tie Barents and the Kara Seas, state and perspectives of studies //Norsk Polarinstitutt. – Oslo. – Rapport Nr. 97. – 1997. – pp. 23-26.
153. Furevik T. Annual and interannual variability of Atlantic Water temperatures in the Norwegian and Barents Seas: 1980–1996 //Deep Sea Research Part I: Oceanographic Research Papers. – 2001. – T. 48. – №. 2. – pp. 383-404.

154. Fyfe J.C. et al. Variability and trends of air temperature and pressure in the maritime Arctic //Scientific Reports. – 2013. – T. 3. – 2645 p.

155. Helland-Hansen B., Nansen F. The Norwegian Sea: its physical oceanography based upon the Norwegian researches 1900-1904. – Det Mallingske bogtrykkeri, 1909. – T. 2. – №. 2.

156. Ivanov V. V., Frolov I. E., Filchuk K. V. Transformation of Atlantic Water in the north–eastern Barents Sea in winter //Arctic and Antarctic Research. – 2020. – T. 66. – №. 3. – pp. 246-266.

157. Jakobsson M. et al. An improved bathymetric portrayal of the Arctic Ocean: Implications for ocean modeling and geological, geophysical and oceano graphic analyses //Geophysical Research Letters. – 2008. – T. 35. – №. 7.

158. Janout M. A. et al. Circulation in the northwest Laptev Sea in the eastern Arctic Ocean: Crossroads between Siberian River water, Atlantic water and polynya-formed dense water //Journal of Geophysical Research: Oceans. – 2017. – T. 122. – №. 8. – pp. 6630-6647.

159. Kay J. E., Holland M. M., Jahn A. Inter-annual to multi-decadal Arctic sea ice extent trends in a warming world //Geophysical Research Letters. – 2011. – T. 38. – №. 15.

160. Levitus S. et al. Global ocean heat content 1955–2008 in light of recently revealed instrumentation problems //Geophysical Research Letters. – 2009a. – T. 36. – №. 7.

161. Levitus S. et al. Barents Sea multidecadal variability //Geophysical Research Letters. – 2009b. – T. 36. – №19.

162. Lind S., Ingvaldsen R. B., Furevik T. Arctic warming hotspot in the northern Barents Sea linked to declining sea-ice import //Nature climate change. – 2018. – T. 8. – №. 7. – pp. 634-639.

163. Minobe S. A 50–70 year climatic oscillation over the North Pacific and North America //Geophysical Research Letters. – 1997. – T. 24. – №. 6. – pp. 683-686.

164. Mironov Ye. U., Babko O.I. Features of the ice conditions in the Barents Sea in the spring-summer of 1993-1994 and tendencies toward their changes in the last decade //Norsk Polarinstitutt, Oslo. – 1997. – Rapport Nr. 97 – pp. 290-292.

165. Morison J., Aagaard K., Steele M. Recent environmental changes in the Arctic: A review //Arctic. – 2000. – pp. 359-371

166. Munshi J. Trends in Polar Sea Ice Extent 1979-2015 //Available at SSRN 2598152. – 2015.

167. Mysak L. A., Manak D. K. Arctic sea-ice extent and anomalies, 1953–1984 //Atmosphere-Ocean. – 1989. – T. 27. – №. 2. – pp. 376-405.

168. Onarheim I. H. et al. Skillful prediction of Barents Sea ice cover //Geophysical Research Letters. – 2015. – T. 42. – №. 13. – pp. 5364-5371.

169. Ottersen G., Adlandsvik B., Loeng H.//Statistical modelling of temperature variability in the Barents Sea. – ICES CM 1994. – 16 p.

170. Parkinson C. L. et al. Arctic sea ice extents, areas, and trends, 1978–1996 //Journal of Geophysical Research: Oceans. – 1999. – T. 104. – №. C9. – pp. 20837-20856.

171. Polyakov I. V. et al. Greater role for Atlantic inflows on sea-ice loss in the Eurasian Basin of the Arctic Ocean //Science. – 2017. – T. 356. – №. 6335. – pp. 285-291.

172. Polyakov I. V., Johnson M. A. Arctic decadal and interdecadal variability //Geophysical Research Letters. – 2000. – T. 27. – №. 24. – pp. 4097-4100.

173. Polyakov I.V., Timokhov L.A., Alexeev V.A., Bacon S., Dmitrenko I.A., Fortier L., Frolov I.E., Gascard J.-C., Hansen E., Ivanov V.V., Laxon S., Mauritzen C., Perovich D., Shimada K., Simmons H.L., Sokolov V.T., Steele M., Toole J. Arctic Ocean warming contributes to reduced polar ice cap //Journal of Physical Oceanography. – 2010. – T. 40. – №. 12. – pp. 2743–2756.

174. Pope J. O. et al. The impact of wintertime sea-ice anomalies on high surface heat flux events in the Iceland and Greenland Seas //Climate Dynamics. – 2020. – T. 54. – №. 3. – pp. 1937-1952.

175. Rigor I. G., Wallace J. M., Colony R. L. Response of sea ice to the Arctic Oscillation //Journal of Climate. – 2002. – T. 15. – №. 18. – pp. 2648-2663.

176. Sandø A.B., Gao Y., Langehaug H.R. Poleward ocean heat transports, sea ice processes, and Arctic sea ice variability in NorESM1-M simulations //Journ. of Geophysical Research: Oceans. – 2014. – V. 119. – № 3. – pp. 2095–2108.

177. Selyuzhenok V. et al. Sea ice volume variability and water temperature in the Greenland Sea //The Cryosphere. – 2020. – T. 14. – №. 2. – pp. 477-495.
178. Skagseth Ø. et al. Volume and heat transports to the Arctic Ocean via the Norwegian and Barents Seas //Arctic–Subarctic Ocean Fluxes. – Springer, Dordrecht. – 2008. – pp. 45-64.
179. Sorteber A., Kvingedal B. Atmospheric forcing on the Barents Sea winter ice cover. //Journal of Climate. – 2006. – V. 19. – pp. 4772–4784.
180. Vinje T. Anomalies and trends of sea-ice extent and atmospheric circulation in the Nordic Seas during the period 1864–1998 //Journal of Climate. – 2001. – T. 14. – №. 3. – pp. 255–267.
181. Vinje T. Frequency distribution of sea ice, ridges and water openings in the Greenland and Barents Seas //Norsk Polarinstitutt, Rapportserie. Oslo. – Nr. 15. –1984. – 27 p.
182. Vinje T. E. On the extreme sea ice conditions observed in the Greenland and Barents Seas in 1979 //Norsk Polarinstitutt Arbok. – 1980.
183. Walczowski W. Atlantic water in the Nordic seas. Properties, variability, climatic importance // GeoPlanet: Earth Planet Science. – Springer – 2014 – 172 p.
184. Wallace J. M., Gutzler D. S. Teleconnections in the geopotential height field during the Northern Hemisphere winter //Monthly weather review. – 1981. – T. 109. – №. 4. – pp. 784–812.
185. Walsh J. E., Johnson C. M. An analysis of Arctic sea ice fluctuations, 1953–77 //Journal of Physical Oceanography. – 1979. – T. 9. – №. 3. – pp. 580–591.
186. Wang J. et al. Is the Dipole Anomaly a major driver to record lows in Arctic summer sea ice extent? //Geophysical Research Letters. – 2009. – T. 36. – №. 5.
187. Wang J., Ikeda M. Arctic oscillation and Arctic sea-ice oscillation //Geophysical Research Letters. – 2000. – T. 27. – №. 9. – pp. 1287-1290.
188. Watanabe E. et al. Arctic dipole anomaly and its contribution to sea ice export from the Arctic Ocean in the 20th century //Geophysical research letters. – 2006. – T. 33. – №. 23.

189. World Meteorological Organization. WMO sea-ice nomenclature, terminology, codes and illustrated glossary // WMO/OMM/BMO. Geneva. – 2017. –№259. – 147 p.

190. Wu B., Wang J., Walsh J. Possible feedback of winter sea ice in the Greenland and Barents Seas on the local atmosphere //Monthly weather review. – 2004. – T. 132. – №. 7. – pp. 1868-1876.

191. Yashayaev I., Seidov D. The role of the Atlantic Water in multidecadal ocean variability in the Nordic and Barents Seas //Progress in Oceanography. – 2015. – T. 132. – pp. 68-127.

192. Zhang X. et al. Recent radical shifts of atmospheric circulations and rapid changes in Arctic climate system //Geophysical Research Letters. – 2008. – T. 35. – №. 22.

## LIST OF ABBREVIATIONS

**AARI** – Arctic and Antarctic Research Institute;

**NEB**– North European Basin;

**GS** – Greenland Sea;

**BS** – Barents Sea;

**NS** – Norwegian Sea;

**KM** – Kola meridian;

**SST** – sea surface temperature;

**TA** – atmospheric temperature at the surface of the water;

**SD** – standard deviation;

**CV** – the coefficient of variation;

**CC** – correlation coefficient;

**AO** – Arctic Oscillation;

**AMO** – Atlantic Multi-Decade Oscillation;

**NAO** – North Atlantic Oscillation;

**AD** –Arctic Dipole Oscillation;

**PNA** – Pacific North American Oscillation;

**EOF** – empirical orthogonal function;

**MC** – main component;

**R** – radiation balance;

**P** – turbulent heat transfer between the ocean surface and the atmosphere;

**LE** – heat consumption for evaporation;

**B** – surface heat balance;

**ACF** – autocorrelation function;

**MRA** – multi regression analysis;

**X and Y** – latitude and longitude coordinates of the position of the Earth's pole (short-period nutation terms in longitude and inclination), respectively;

**$\Delta\varepsilon$ and $\Delta\psi$** – longitude and latitude coordinates of the Celestial ephemeris pole relative to the Conditional earth pole;

**lod** – fluctuation length of the day;

**Wolf** – Wolf numbers, indicator of solar activity;

**$C_W$ and $C_S$** – distance anomalies between the Earth and the Sun for the winter W (October-March) and summer W (April-September) half-years.

# APPENDIX A

Table A.1. Correlation coefficients between predictors in the developed equations 4.5.1–4.8.6

| Predictors | R | Predictors | R | Predictors | R |
|---|---|---|---|---|---|
| $AMO_{-2}$, X | 0,42 | X, $C_W$ | –0,55 | Δε, $PNA_W$ | –0,25 |
| $AMO_{-2}$, $C_W$ | –0,17 | X, $PNA_W$ | 0,11 | Wolf, X | –0,09 |
| $AMO_{-2}$, $PNA_W$ | –0,02 | X, $AO_S$ | 0,05 | Wolf, $AD_W$ | –0,17 |
| $AMO_{-2}$, $PNA_S$ | 0,32 | X, Δε | –0,61 | $Wolf_{-1}$, $PNA_{W-1}$ | –0,03 |
| $AMO_{-2}$, $AO_S$ | 0,10 | X, Δψ | –0,60 | Wolf, $AO_S$ | 0,07 |
| $AMO_{-2}$, $AD_W$ | –0,10 | X, $NAO_{W-1}$ | 0,48 | $Wolf_{-1}$, $T_W$ (GS) | 0,02 |
| $AMO_{-2}$, Wolf | –0,02 | X, $PNA_S$ | 0,38 | $Wolf_{-1}$, $X_{-1}$ | –0,07 |
| $AMO_{-2}$, $NAO_{W-}$ | 0,08 | X, $AD_W$ | –0,18 | $Wolf_{-1}$, $L_{AUT-1}$(GS) | –0,03 |
| $AMO_{-2}$, Δε | –0,21 | $X_{-1,}$ $L_{SP}$ | –0,35 | $Wolf_{-1}$, $AD_W$ | –0,21 |
| $AMO_{-2}$, Δψ | –0,26 | $X_{-1,}$ $AO_{W-1}$ | 0,38 | $T_S$ (GS), $AD_W$ | –0,11 |
| $AMO_{-3}$, $AO_{W-1}$ | 0,02 | $X_{-1}$, $AD_W$ | –0,24 | $T_W$ (GS), $L_{AUT-1}$(GS) | –0,42 |
| $AMO_{-3}$, $X_{-1}$ | 0,41 | $X_{-1}$, $T_S$ (GS) | 0,64 | $T_W$ (GS), $PNA_W$ | 0,27 |
| $AMO_{-3}$, $T_S$ (GS) | 0,39 | $X_{-1}$, Δε | –0,58 | $T_S$ (GS), $L_{SP}$ (GS) | –0,56 |
| $AMO_{-3}$, $L_{SP}$(GS) | –0,14 | $X_{-1}$, $PNA_{W-1}$ | 0,11 | $PNA_{W-1,}$ $AD_W$ | –0,40 |
| $AMO_{-3}$, Δε | –0,18 | Δε, $AO_S$ | –0,11 | $PNA_{S,}$ $NAO_{W-1}$ | 0,02 |
| $AMO_{-3}$, $AD_W$ | –0,03 | Δε, $AD_W$ | 0,32 | $AD_{W,}$ $L_{SP}$(GS) | 0,13 |
| $AMO_{-3}$, $Wolf_{-1}$ | –0,02 | Δε, Wolf | 0,06 | $AD_{W,}$ $AO_{W-1}$ | 0,21 |
| $AMO_{-3}$, $PNA_{W-1}$ | –0,09 | Δε, $Wolf_{-1}$ | 0,05 | $AD_{W,}$ $AO_S$ | –0,15 |
| $AMO_{-3}$, $X_{-1}$ | 0,41 | Δε, $PNA_{W-1}$ | –0,25 | $AD_{W-1,}$ $T_W$ (GS) | –0,26 |
| $AMO_{-4}$, $T_W$ (GS) | 0,27 | Δε, $T_S$ (GS) | –0,74 | $AD_{W-1,}$ $PNA_W$ | –0,07 |
| $AMO_{-4}$, $W_{-1}$ | –0,09 | Δε, $T_W$ (GS) | –0,74 | $AO_{W-1,}$ $T_S$ (GS) | 0,34 |
| $AMO_{-4}$, Δε | –0,17 | Δε, $L_{AUT-1}$(GS) | 0,57 | $AO_{W-1,}$ $L_{SP(GS)}$ | –0,32 |
| $AMO_{-4}$, $PNA_W$ | 0,11 | Δψ, $NAO_{W-1}$ | –0,52 | $C_{S,}$ $NAO_{W-1}$ | –0,47 |
| $AMO_{-4}$, $AD_{W-1}$ | –0,04 | Δψ, $PNA_S$ | –0,29 | $C_{S,}$ $PNA_S$ | –0,24 |
| $C_W$, $PNA_W$ | –0,28 | $C_W$, $AO_S$ | –0,06 | $C_W$, $AD_W$ | 0,28 |